

Investigating both sides of the Arabidopsis-Pst interaction

INVESTIGATING BACTERIAL GROWTH/BIOFILM  
FORMATION AND THE PLANT TRANSCRIPTIONAL  
LANDSCAPE IN THE *Arabidopsis-Pseudomonas syringae*  
*pv tomato* INTERACTION

By Garrett M. NUNN, B.Sc.

*A Thesis Submitted to the School of Graduate Studies in the Partial  
Fulfillment of the Requirements for the Degree Master of Science*

McMaster University © Copyright by Garrett M. NUNN May 12,  
2020

McMaster University

Master of Science (2020)

Hamilton, Ontario (Department of Biology)

TITLE: Investigating bacterial growth/biofilm formation and the plant transcriptional landscape in the *Arabidopsis-Pseudomonas syringae pv tomato* interaction

AUTHOR: Garrett M. NUNN (McMaster University)

SUPERVISOR: Dr. Robin K. CAMERON

NUMBER OF PAGES: xvii, 132

# Abstract

*Arabidopsis thaliana* exhibits a developmentally regulated disease resistance response known as Age-Related Resistance (ARR), a process that requires intercellular accumulation of salicylic acid (SA), which is thought to act as an intercellular antimicrobial and antibiofilm agent against the phytopathogen *Pseudomonas syringae* during infection of *Arabidopsis* leaves. During infection, *P. syringae* forms aggregates thought to consist of bacterial cells and extracellular polymers, such as alginate, extracellular DNA, lipids, and proteins. In this thesis the *Arabidopsis thaliana*-*Pseudomonas syringae* pv *tomato* (*Pst*) pathosystem was used to explore i) the contribution of alginate in protecting *Pst* during growth in vitro against the antimicrobial and antibiofilm effects of SA, and ii) various aspects of ARR including global gene expression analysis. At moderate SA concentrations, planktonic free-swimming bacterial cells of *Pst*  $\Delta algU$  *mucAB*  $\Delta algD$ , a mutant with reduced virulence, grew to lower densities than wild-type *Pst* and the alginate biosynthesis mutant *Pst*  $\Delta algD$  in apoplast-mimicking minimal media, leading to the idea that AlgU regulates the T3SS and iron storage and uptake genes. This study also provides evidence that the *Arabidopsis* PAMP recognition mutants *efr-1* and *fls2* are partially ARR-defective and may contribute to ARR and the *bak1-3* mutant may be required for ARR, suggesting PTI-related responses contribute to ARR. Lastly, comparative transcriptome analyses of susceptible young and ARR-competent mature plants responding to *Pst*, suggests that JA pathway genes are expressed in young but not mature plants. This work highlights the complex interaction between *Arabidopsis thaliana* and *Pseudomonas syringae* pv. *tomato*.



# *Acknowledgements*

While many people will support me throughout my career. Only one can start it. Thanks Robin, for believing in me and being an impressive model species of a supervisor. To my lab mates, former and current I have loved our little lab family. Angela, from my first week in lab to your last, you were a great mentor and friend. Thanks for all the emotional support and helping me grow from a helpless seedling to a researcher. Thanks to Noah and Natalie, for making the lab feel like a family for the last year.

Thanks to my committee members, Dr. G. Brian Golding and Dr. Elizabeth Weretilnyk. I have often said my favourite part of research is the challenge in defending it. Thank you for making this challenge fun and broadening my view.

To my family, it has been a wild ride. Who would've thought my high school dream would become a reality? It has gone better than I could have ever hoped. From Aurora to Banff to Hamilton you have always been there for me. You have been there during my best and worst moments. Mom, thanks for being there for me whenever I was over-stressed and needed a break. I could always rely on home for a good nap (well not so much recently). Dad, thanks for always tickling my brain and nurturing my curiosity (as persistent as it could be at times). Neither of you ever doubted me for a second and that meant the world. To my little sister, Bridget, you are a bright light for all those around you and every time you come back from globe-trotting, you have made my world a little brighter.

As for my girlfriend, while you've only been in my life for a year and a half, it has been amazing and meant more to me than I can express, thanks sweet pea.

Maybe, I'll win a squash game this year (as of current writing, 2W-14L, so doing pretty good!).

If you are lucky, you only get two opportunities to write your acknowledgements, and I don't want this to seem harder than it was. It was hard, but when you are lucky enough to do something you love, as I have been, everything is a little easier. The old idiom "work hard, play hard" comes to mind and for me research will always be both.

# Contents

<b>Abstract</b>	<b>iii</b>
<b>Acknowledgements</b>	<b>v</b>
<b>Acronyms</b>	<b>xiv</b>
<b>Declaration of Authorship</b>	<b>xvii</b>
<b>1 Introduction</b>	<b>1</b>
1.1 Introduction . . . . .	1
1.2 Plant responses to infection . . . . .	2
1.3 The <i>Arabidopsis-Pseudomonas syringae</i> pathosystem . . . . .	2
1.4 Development of <i>P. syringae</i> infection . . . . .	3
1.4.1 Coronatine . . . . .	3
1.4.2 The role of biofilm formation during <i>Pseudomonas</i> infections	4
Levan . . . . .	8
Cellulose . . . . .	9
Alginate . . . . .	10
1.4.3 Type 3 secretion systems and effector proteins . . . . .	13
1.5 PAMP-triggered immunity (PTI) . . . . .	16
1.6 Effector-triggered immunity (ETI) . . . . .	18
1.7 Salicylic acid . . . . .	20
1.8 Age-Related Resistance (ARR) . . . . .	22
1.8.1 The role of SA during ARR . . . . .	23
1.8.2 The role of CYP71A12 and CYP71A13 during ARR . . . . .	25

1.8.3	SA transport . . . . .	26
1.8.4	ARR signaling pathway . . . . .	29
1.9	Hypotheses and objectives . . . . .	30
1.10	Cameron lab contributions not presented in this thesis . . . . .	31
<b>2</b>	<b>Materials &amp; Methods</b>	<b>33</b>
2.1	Plant growth conditions . . . . .	33
2.2	Bacterial growth and inoculations . . . . .	34
2.3	RNA isolation . . . . .	36
2.4	Library preparation and sequencing . . . . .	36
2.5	Antibacterial growth curve assays . . . . .	37
2.6	Biofilm formation assays . . . . .	38
2.7	Statistical analysis . . . . .	39
<b>3</b>	<b>Investigating the role of alginate in protecting <i>Pst</i> from the antimicrobial effects of salicylic acid</b>	<b>41</b>
3.1	<i>In vitro</i> growth of <i>Pseudomonas syringae</i> pv. <i>tomato</i> ( <i>Pst</i> ) alginate mutants . . . . .	42
3.2	Effect of salicylic acid on growth of <i>Pst</i> $\Delta$ <i>algD</i> and <i>Pst</i> $\Delta$ <i>algU mucAB</i> $\Delta$ <i>algD</i> . . . . .	44
3.3	Effect of salicylic acid on biofilm formation by <i>Pst</i> $\Delta$ <i>algD</i> and <i>Pst</i> $\Delta$ <i>algU mucAB</i> $\Delta$ <i>algD</i> . . . . .	46
3.4	The effect of bacterial strain and temperature on biofilm formation	49
<b>4</b>	<b>Elucidating the ARR signaling pathway</b>	<b>57</b>
4.1	Do PTI signaling components contribute to ARR? . . . . .	58
4.2	RNA-sequencing to identify differentially expressed genes during ARR	60
4.2.1	Quality checking before sequencing . . . . .	62
4.2.2	Sample dispersion of young and mature plants responding to <i>Pst</i> . . . . .	68
4.2.3	Modeling and differential gene expression analysis during Age-Related Resistance . . . . .	70
4.2.4	Functional analysis of genes expressed or suppressed during Age-Related Resistance . . . . .	73
<b>5</b>	<b>Discussion</b>	<b>77</b>
5.1	The role of AlgU during <i>Pst</i> growth in the leaf intercellular space-mimicking environment . . . . .	77
5.2	The role of alginate in protecting <i>Pst</i> against the growth inhibitory effects of SA . . . . .	81
5.3	Exploring conditions that effect <i>Pst</i> biofilm formation . . . . .	83
5.3.1	SA as an antibiofilm agent . . . . .	87

5.3.2	Exploring EPS composition of <i>Pst</i> biofilms . . . . .	88
5.4	ARR . . . . .	90
5.4.1	Contribution of PTI components to ARR . . . . .	90
5.4.2	RNA-sequencing . . . . .	91
5.5	Conclusions . . . . .	92
<b>A</b>	<b>Appendix</b>	<b>93</b>
A3	Chapter 3 Appendix . . . . .	93
A4	Chapter 4 Appendix . . . . .	96
	<b>Bibliography</b>	<b>101</b>



# List of Figures

1.1	The proposed life-cycle of biofilm formation in <i>Pseudomonas aeruginosa</i> ( <i>P. aeruginosa</i> ) . . . . .	6
1.2	Chemical structure of <i>Pseudomonas syringae</i> pv. <i>tomato</i> ( <i>Pst</i> ) extracellular polysaccharides. . . . .	8
1.3	Model of proposed cellular effects of increased AlgU expression . . .	14
1.4	Model of flg22-initiated PTI . . . . .	17
3.1	Growth of <i>Pst</i> <sub>165K</sub> $\Delta$ <i>algU mucAB <math>\Delta</math>algD</i> and <i>Pst</i> <sub>165K</sub> $\Delta$ <i>algD</i> in rich and minimal media . . . . .	43
3.2	Antibacterial activity of SA on <i>Pst</i> <sub>165K</sub> $\Delta$ <i>algU mucAB <math>\Delta</math>algD</i> and <i>Pst</i> <sub>165K</sub> $\Delta$ <i>algD</i> compared to wild-type <i>Pst</i> <sub>165K</sub> . . . . .	45
3.3	Antibiofilm activity of SA on <i>Pst</i> <sub>165K</sub> , <i>Pst</i> <sub>165K</sub> $\Delta$ <i>algD</i> , and <i>Pst</i> <sub>165K</sub> $\Delta$ <i>algU mucAB <math>\Delta</math>algD</i> . . . . .	48
3.4	Variability of biofilm formation among <i>Pst</i> strains. . . . .	50
3.5	Temperature-dependent growth and biofilm formation in <i>Pst</i> pVSP1 and <i>Pst</i> <sub>165K</sub> . . . . .	52
3.6	Growth to biofilm formation correlation by strain . . . . .	54
3.7	Biofilm formation over time at various concentrations of SA . . . . .	55
4.1	ARR assay of various PTI mutants . . . . .	59
4.2	RNA-sequencing experimental timeline . . . . .	60
4.3	Age-Related Resistance response for RNA-sequencing experiment . . .	62
4.4	RNA sample quality for RNA-sequencing . . . . .	64
4.5	RNA-seq quality checks . . . . .	67

4.6	RNA-sequencing sample dispersion plots . . . . .	69
4.7	Differential gene expression during infection of young and mature plants . . . . .	72
4.8	Functional analysis of defense-related genes in response to <i>Pst</i> in young and mature plants . . . . .	76
A3.1	Bactericidal activity of SA on wild type <i>Pst</i> pDSK-GFPuv and <i>Pst</i> <sub>165K</sub> $\Delta$ <i>algD</i> . . . . .	94
A3.2	Summary of growth of various <i>Pst</i> isolates without agitation . . . . .	95
A4.1	Preliminary data on bacterial growth in mature plants of PTI mutants . . . . .	97
A4.2	Comparison of rRNA banding in intact and degraded total RNA samples from leafy tissue . . . . .	97

# List of Tables

2.1	<i>Arabidopsis thaliana</i> ( <i>Arabidopsis</i> ) plant lines used in this study . . .	34
2.2	Bacterial strains and plasmids used in this study . . . . .	35
A3.1	Minimum inhibitory and bactericidal activities of SA . . . . .	94
A4.1	RNA sample quality for RNA-sequencing of ARR . . . . .	96
A4.2	The top up-regulated genes in <i>Pst</i> compared to mock-inoculated mature plants at 24 hpi . . . . .	98
A4.3	The top down-regulated genes in <i>Pst</i> compared to mock-inoculated mature plants at 24 hpi . . . . .	99

# Acronyms

**ABC** ATP-binding cassette

***Arabidopsis*** *Arabidopsis thaliana*

**ARR** Age-related resistance

**BAK1** BRASSINOSTEROID INSENSITIVE1-ASSOCIATED RECEPTOR KINASE1

**CERK1** CHITIN ELICITOR RECEPTOR KINASE1

**CFW** calcofluor white

**COI1** CORONATINE INSENSITIVE PROTEIN1

**ConA** concanavalin A

**DHCA** Dihydrocamalexamic acid

**EFR** EF-TU RECEPTOR

**EPS** extracellular polysaccharides

**EPS1** ENHANCED PSEUDOMONAS SUSCEPTIBILITY1

**ETI** Effector-triggered immunity

**FLC** FLOWERING LOCUS C

**FLS2** FLAGELLIN-SENSITIVE2

**GO** gene ontology

**HIM** *hrp*-inducing minimal media

**hpi** hours post-inoculation

**HR** Hypersensitive response

***Hrp*** Hypersensitive response and pathogenicity

**ICS** isochorismate

**ICS1** ISOCHORISMATE SYNTHASE1

**IWFs** Intercellular washing fluids

**JA** jasmonic acid

**JAZ10** JASMONATE-ZIM-DOMAIN PROTEIN10

**LYK5** LYSM-CONTAINING RECEPTOR-LIKE KINASE5

**MATE** multidrug-and-toxin extrusion

**MEX** multi-drug efflux

***N. benthamiana*** *Nicotiana benthamiana*

**NPR** NON-EXPRESSOR OF PATHOGENESIS-RELATED GENES

***P. aeruginosa*** *Pseudomonas aeruginosa*

**PAL** phenylalanine

**PAMP** pathogen-Associated Molecular Pattern

**PBS3** AVRPPHB SUSCEPTIBLE3

**PCA** principal component analysis

**PDR** pleiotropic drug resistance

**PR** Pathogenesis-related

**PRR** pattern recognition receptor

***Psg*** *Pseudomonas syringae* *pv. glycinea*

***Psm*** *Pseudomonas syringae* *pv. maculicola*

***Pss*** *Pseudomonas syringae* *pv. syringae*

*Pst* *Pseudomonas syringae* pv. *tomato*

*P. syringae* *Pseudomonas syringae*

**PTI** PAMP-triggered immunity

**RIN** RNA integrity number

**RIN4** RPM1-INTERACTING PROTEIN4

**RINe** RNA integrity number equivalent

**ROS** Reactive Oxygen Species

**RPM1** RESISTANCE TO *P. SYRINGAE* PV *MACULICOLA*1

**SA** Salicylic acid

**SAG** Salicylic acid glucose

**SAR** Systemic-acquired resistance

**SARD1** SAR-DEFICIENT1

**SID2** SALICYLIC ACID INDUCTION DEFICIENT2

**SOC1** SUPPRESSOR OF CONSTANS1

**SVP** SHORT VEGETATIVE PHASE

**T3SS** type 3 secretion system

**WHY1** WHIRLY1

# Declaration of Authorship

I, Garrett M. NUNN, declare that this thesis titled, “Investigating bacterial growth/biofilm formation and the plant transcriptional landscape in the *Arabidopsis-Pseudomonas syringae pv tomato* interaction” and the work presented in it are my own.



# Chapter 1

## Introduction

### 1.1 Introduction

Plants perceive and respond to indicators of danger, allowing them to thrive in hostile conditions, including seasonal changes, salt-stress, nutrient deficiency, herbivory, and microbial infection (Simpson and Dean, 2002; Appel et al., 2014; Carella et al., 2016; Velasco et al., 2016; Kazachkova et al., 2018).

The study of how plants respond to their environment is globally important as failure to adequately respond to abiotic or biotic stress can negatively affect the food security of those in need as well as negatively impact the economic output from farms (Oerke, 2006). From 2010 to 2014, all crop pests (pathogens, arthropods, and weeds) caused a preharvest loss of at least 17.2% among major food crops such as wheat, rice, maize, potato and soybean (Savary et al., 2019).

## 1.2 Plant responses to infection

Pathogens have evolved various pathogenic weapons to evade plant defence responses and plants have evolved molecular mechanisms to resist pathogen infection (Gilbert and Parker, 2010). The plant innate immune system provides protection against a wide variety of infections. Three modes of infection common in plant-pathogen interactions are necrotrophy, biotrophy and hemibiotrophy (Xin and He, 2013). During necrotrophy, some fungal and bacterial pathogens make use of plant cell wall-degrading enzymes to kill host cells and feed on dead cells (Choi et al., 2013; Kubicek et al., 2014). In contrast, biotrophic leaf pathogens access the leaf apoplast through the stomata, where they suppress plant defence and manipulate plant metabolism in living plant cells to obtain nutrients to grow and multiply in the plant (Spanu and Panstruga, 2017). Hemibiotrophic pathogens, like *Pseudomonas syringae* (*P. syringae*), combine biotrophy and necrotrophy (Xin and He, 2013). These pathogens begin infection as biotrophs within the host and then switch to necrotrophy to kill plant cells and access the leaf surface for dispersal (Xin and He, 2013).

## 1.3 The *Arabidopsis-Pseudomonas syringae* pathosystem

Bacterial speck is a disease of both foliar and fruit tissue in tomato caused by the hemibiotrophic phytopathogen *Pseudomonas syringae* *pv.* *tomato* (*Pst*). In ideal

growth conditions, bacterial speck can cause a severe reduction in fruit yield and quality (Cai et al., 2011). The strain most frequently studied, *Pst* DC3000, was originally isolated from tomato (Cuppels, 1986). This strain of *Pst* was discovered to be highly virulent in the apoplast of foliar tissue of the model flowering plant, *Arabidopsis* (Whalen et al., 1991). The *Arabidopsis-Pseudomonas* interaction is an important pathosystem with a wide variety of genetic tools available for both the plant and pathogen (Bevan and Walsh, 2005; Xin et al., 2018).

## 1.4 Development of *P. syringae* infection

*P. syringae* has a number of pathogenic weapons that contribute to the successful infection of *Arabidopsis*. These weapons include type-3-secretion systems that secrete effector proteins into plant cells, coronatine production and may include biofilm formation (Osman et al., 1986; Mann and Wozniak, 2012; Geng et al., 2014; Lam et al., 2014), all of which either contribute to suppression of plant defence or manipulation of plant metabolism to create a favourable environment for growth (Truman et al., 2006). Several of these weapons are used by *Pst* and are described below.

### 1.4.1 Coronatine

One pathogenic weapon used by *Pst* during infection is the phytotoxin coronatine. Coronatine is thought to function during infection by promoting invasion of the apoplast (Mittal and Davis, 1995) by re-opening stomata (Panchal et al., 2016)

after plant-initiated closure of stomata in response to bacterial infection. Re-opening of stomata results in enhanced movement of *Pst* into intercellular spaces from the leaf surface. Coronatine is also thought to support *Pst* growth in leaf intercellular spaces, since *Pst* coronatine biosynthesis mutants consistently displayed lower bacterial density compared to wild type in leaf intercellular spaces (Ma et al., 1991; Brooks et al., 2004). Recently, RNA-sequencing demonstrated that *Pst* up-regulates the coronatine biosynthesis gene cluster upon inoculation into the apoplast (Zheng et al., 2012; Nobori et al., 2018) providing additional evidence of the importance of coronatine during infection. In support of this, coronatine acts to promote *Pst* growth through activation of plant jasmonic acid (JA) responses as coronatine is very similar to JA-Ile in chemical structure (reviewed in Geng et al., 2014). Once in the plant cytoplasm coronatine can bind to CORONATINE INSENSITIVE PROTEIN1 (COI1), the JA receptor, leading to activation of JA responses and inhibition of SA-mediated defense (reviewed in Geng et al., 2014). Negative feedback of JA responses is regulated by alternative splicing of JASMONATE-ZIM-DOMAIN PROTEIN10 (JAZ10), thus preventing constitutive expression of JA defense responses (Moreno et al., 2013).

#### **1.4.2 The role of biofilm formation during *Pseudomonas* infections**

Bacteria exist as individual cells but many species form large communities of individuals, called biofilms (Mann and Wozniak, 2012). Biofilms consist of bacterial

cells surrounded by a matrix of lipids, proteins, extracellular (e)DNA, and extracellular polysaccharides (EPS) (Mann and Wozniak, 2012). Lipids, eDNA, and EPS are structural components of biofilm, while many proteins are embedded within the matrix. Some of these proteins aid in dispersal by degrading components of the biofilm, such as the alginate lyase AlgL (reviewed in Flemming et al., 2007).

Biofilm formation by *P. syringae* has not been extensively studied, however biofilm formation in the related human pathogen, *Pseudomonas aeruginosa* has been extensively studied (O’Toole, 2010; Gomila et al., 2015). Based on *in vitro* studies, *P. aeruginosa* biofilm formation is thought to be divided into four distinct stages: attachment, development, maturation and dispersal (Kaplan, 2010). Attachment begins with a reversible surface-attachment of free-swimming planktonic bacteria via adhesins and electrostatic forces (Kaplan, 2010). Shortly after surface attachment, the bacteria lose their flagella as they switch from planktonic to sessile growth, and begin production of EPS, forming an immature biofilm (Waite et al., 2005). The immature biofilm continues to thicken due to bacterial reproduction and production of matrix components until maturity (Sharma et al., 2019). The matrix of a mature biofilm is thought to contribute to antimicrobial resistance, by preventing antimicrobial diffusion, generating antibiotic resistant persister cells and promoting efflux of antibiotics out of the bacterial cytoplasm (Gilbert et al., 1997; Pearson et al., 1999; Waite et al., 2005; Sharma et al., 2019). Once mature, dispersal of bacterial cells from the biofilm can occur through physical disruption of the matrix or enzymatic degradation of the extracellular biofilm matrix (Flemming et al., 2007). Dispersed bacterial cells are thought to make flagella, as *P. aeruginosa* cells have been observed to swim away from biofilms during the later

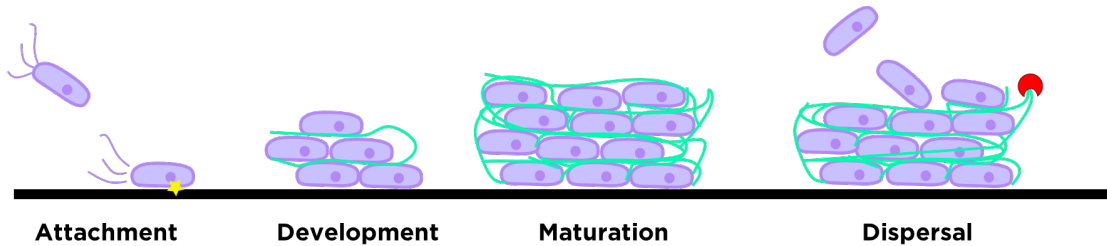


FIGURE 1.1: **The proposed life-cycle of biofilm formation in *P. aeruginosa*.** This figure is based on the information presented in (Kaplan, 2010). Briefly, there are four distinct stages of biofilm formation (i) attachment, (ii) development, (iii) maturation and (iv) dispersal. During attachment, bacteria irreversibly attach to a surface, lose flagella and begin to produce biofilm matrix components (Waite et al., 2005; Kaplan, 2010). Production of matrix components and replication continues throughout development (Sharma et al., 2019). Biofilm maturation is characterised by the manifestation of resistance to environmental stressors and antibiotics (Flemming, 1993; Gilbert et al., 1997; Díaz-Salazar et al., 2017). After maturation, dispersal can occur by physical or enzyme-mediated separation from the underlying surface, thereby starting the cycle anew (Kaplan, 2010).

stages of development (Sauer et al., 2002; Davies and Marques, 2009). Dispersal is thought to promote infection by allowing bacterial cells to move to new areas in the host to begin biofilm formation at new sites (Flemming et al., 2007). It is possible that *P. syringae* biofilm formation progresses in a similar manner as *Pst* and *P. aeruginosa* PAO1 share an average nucleotide identity of 74% while identity of PAO1 to *Cellvibrio japonicus* was only 66% (calculated using blast ANIb) (Mulet et al., 2010). Furthermore, 53% of *P. aeruginosa* genes have *Pst* homologs (>80% identity at the nucleotide level) (Jensen et al., 2004).

During infection of *Arabidopsis* by *Pst*, biofilm formation may contribute to protecting *Pst* cells against environmental stress experienced during infection of

the leaf intercellular space. Leaf intercellular stress includes desiccation, salt-stress, starvation and antimicrobial activity (Flemming, 1993; Gilbert et al., 1997; Díaz-Salazar et al., 2017). More specifically, some EPS produced by *Pseudomonas syringae* *pv.* *syringae* (*Pss*) was associated with epiphytic growth on host (bean) and non-host plants (tomato), suggesting that EPS production is important for infection (Yu et al., 1999). In terms of EPS production, *Pst* DC3000 contains the genomic loci for synthesis of polysaccharide single locus (*psl*), levan, cellulose and alginate (Buell et al., 2003). Only production of levan, cellulose and alginate have been observed in *P. syringae* during *in vitro* studies of *Pseudomonas syringae* *pv.* *glycinea* (*Psg*) and *Pst* (Osman et al., 1986; Prada-Ramírez et al., 2016).

EPS of biofilms are often visualised using concanavalin A (ConA), a fluorescently labelled lectin that binds to mannose (Goldstein and Poretz, 1986). concanavalin A (ConA) is thought to bind the mannuronic acid subunits of alginate (Strathmann et al., 2002) and was found to bind alginate isolated from *P. aeruginosa* biofilms, but was unable to bind *Psg* biofilms (Strathmann et al., 2002; Laue et al., 2006). Therefore Laue et al. (2006) suggest ConA might not bind alginate in *Psg* due to a lower ratio of mannuronic acid subunits compared to *P. aeruginosa*. ConA also binds levan, another EPS produced by *Pst* suggesting that levan may be an important component of *Pst* biofilms (Fig. 1.2; Goldstein and Poretz, 1986; Osman et al., 1986)

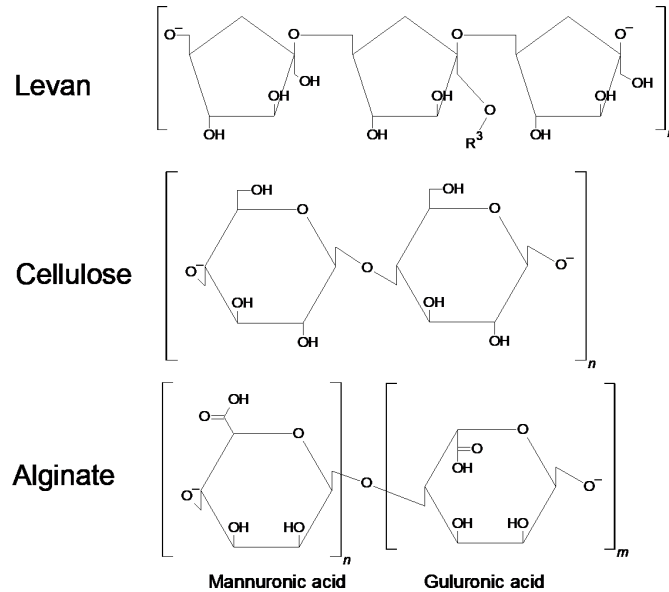


FIGURE 1.2: Chemical structure of *Pst* extracellular polysaccharides.

## Levan

Levan is a  $\beta$ -branched polyfructan (Fig. 1.2) synthesized from sucrose by the extracellular enzyme levansucrase in *Psg* (Osman et al., 1986; Li and Ullrich, 2001; Laue et al., 2006). The function of levan is poorly understood because the biofilm model species *P. aeruginosa* lacks the genes that encode levansucrase (Loper et al., 2012) and the role of *Pst*-produced levan during infection remains uncharacterised. However, several *in vitro* studies are helping to reveal the function of levan in *Psg* biofilms (Osman et al., 1986; Li and Ullrich, 2001; Laue et al., 2006). To facilitate the development of large mature biofilms, *Psg* was grown using a continuous flow cell, thereby providing a constant supply of fresh nutrients to the growing biofilm (Laue et al., 2006). Laue et al. (2006) found that ConA localised to the spaces between bacterial cells in developing biofilms of alginate-deficient levan-producing

*Psg*. For this reason, it was speculated that levan may function in carbohydrate nutrient storage rather than playing a structural role in biofilm development (Laue et al., 2006).

Given that ConA was found to bind alginate in *P. aeruginosa*, which lacks the genes required for levan production (Strathmann et al., 2002) and *Psg* produces both alginate and levan, Laue et al. (2006) examined the alginate and levan binding specificity of ConA in *Psg* biofilms. They found that ConA stained mature wild-type *Psg* biofilms but not mature biofilms of levansucrase mutants grown in continuous flow cultures suggesting that *Psg* biofilms contain the EPS levan (Laue et al., 2006). To confirm that ConA was binding specifically to levan, *Psg* biofilms were treated with a levan-degrading enzyme and this treatment was found to reduce ConA binding to background levels (Laue et al., 2006). These results suggest that levan, but not alginate, is a major EPS component of *Psg* biofilms. Given that *Psg* and *Pst* are different pathovars of the same species, it is possible to speculate that levan is an EPS component of *Pst* biofilms.

## Cellulose

Cellulose is a polysaccharide composed of  $\beta(1,4)$ -linked glucose subunits (Fig. 1.2) found in plant cell walls (Mitra and Loqué, 2014). The  $\beta(1,4)$  glucose linkages of cellulose are ideal binding substrates for the fluorescent dye calcofluor white (CFW) (Mitra and Loqué, 2014). When many *P. syringae* isolates, including *Pst*, were selectively grown in static king's B cultures, a wrinkly biofilm-like structure formed at the air-liquid interface (Ude et al., 2006). The structure of air-liquid

biofilms is unlike archetypal biofilms which form at surface-liquid interfaces (Ude et al., 2006). To determine the composition of the air-liquid biofilm structure the cellulose-specific dye CFW was used. The air-liquid biofilms of *Pst* were found to bind CFW, suggesting that *Pst* produces cellulose (Ude et al., 2006). A follow-up study determined that CFW did not stain biofilms of the proposed cellulose synthase mutant *Pst*  $\Delta wssBC$  at the air-liquid boundary, suggesting that cellulose is a component of *Pst* biofilms (Farias et al., 2019). Additionally, air-liquid biofilms of wild-type *Pst*, but not the cellulose synthase mutant (*Pst*  $\Delta wssBC$ ), were observed to contain a matrix-like structure, suggesting that cellulose could be a major structural component of *Pst* biofilms (Farias et al., 2019). The *Pst*  $\Delta wssBC$  mutant grew like wild-type *Pst* in tomato, suggesting that cellulose is not important for successful infection of tomato (Prada-Ramírez et al., 2016). In contrast, the *Pst* cellulose synthase (WssBC) operon was highly expressed when *Pst* interacted with resistant compared to susceptible *Arabidopsis*, suggesting cellulose could be important for growth in resistant but not susceptible plants (Nobori et al., 2018). Recently, our lab observed co-localization of CFW staining and *Pst* biofilm-like aggregates in infected *Arabidopsis* leaves suggesting that cellulose may be a component of *Pst* biofilms (Fufeng et al., 2020).

## Alginate

Alginate is the most widely studied EPS in *Pseudomonad* species (Doggett, 1969). Alginate is an EPS made up of homopolymeric blocks of  $\beta(1,4)$ -mannuronic acid and  $\alpha(1,4)$ -guluronic acid (Fig. 1.2; Grasdalen, 1983). Alginate production by *Psg* was directly confirmed using NMR (Bruegger and Keen, 1979; Osman et

al., 1986). The lectin binding protein ConA binds  $\beta(1,4)$ -mannuronic linkages found in alginate (Goldstein and Poretz, 1986). Experiments with wild-type and alginate-deficient *Psg* demonstrated that ConA stained both wild-type and alginate-deficient *Psg* biofilms suggesting that ConA is interacting with a different EPS rather than alginate (Laue et al., 2006). As the ratio of mannuronic to guluronic acid varies among isolates of *P. aeruginosa* (Evans and Linker, 1973), it is possible that this ratio is highly variable in other *Pseudomonas* species. Therefore *Psg* alginate may also contain low mannuronic acid content and may not be detected by ConA (Laue et al., 2006). As mannuronic and guluronic acid are both uronic acids, the concentration of uronic acid gives a reasonable estimate of alginate concentration (Osman et al., 1986). To determine if alginate production was regulated by AlgU, Markel et al. (2016) measured the concentration of uronic acid in various strains of *Pst*. Uronic acid production was higher in wild type, than  $\Delta algD$  or  $\Delta algU mucAB$  lines of *Pst* (Markel et al., 2016). Overexpression of AlgU rescued wild-type levels of uronic acid production in *Pst*  $\Delta algU mucAB$  but not *Pst*  $\Delta algD$  (Markel et al., 2016) suggesting that alginate production is controlled by the regulatory protein, AlgU and requires the biosynthetic enzyme AlgD. AlgD is a GDP-mannose-dehydrogenase which in *P. aeruginosa* produces the mannuronic acid present in alginate polymers (Tatnell et al., 1994; Hay et al., 2013). While this has never been experimentally proven in *P. syringae*, the coding sequence of AlgD in *Pss* FF5, shares 80-90% nucleotide identity with the putative ortholog in *P. aeruginosa* cystic fibrosis isolates suggesting functional similarity between these proteins (Tatnell et al., 1994; Fakhr et al., 1999).

In several *Pseudomonas* species the regulation of alginate production is controlled by the AlgU MucAB operon (Martin et al., 1994; Markel et al., 2016). AlgU (also known as RpoE, AlgT,  $\sigma^E$ , or  $\sigma^{22}$ ) is an ECF sigma factor which localises to the cytoplasm at the inner plasma membrane. ECFs are a family of proteins that perceive stress signals from outside the membrane via binding to a transmembrane protein. The transmembrane protein for AlgU is the anti-sigma factor MucA, which in the absence of external stimuli, binds and sequesters *P. aeruginosa* AlgU (Xie et al., 1996; Mathee et al., 1997). MucA is protected from proteolytic cleavage by the periplasmic localising protein MucB (Mathee et al., 1997; Cezairliyan and Sauer, 2009). However in response to external stimuli MucA is degraded through AlgW-mediated proteolytic cleavage which frees AlgU to induce expression of the alginate biosynthetic operon including AlgD, thereby initiating alginate production (Qiu et al., 2007; Cezairliyan and Sauer, 2009; Markel et al., 2016). In *P. aeruginosa*, but not *P. syringae*, another regulator, AlgR is required for activation of the AlgD operon (Mohr et al., 1991; Fakhr et al., 1999). Therefore it is possible that *Pst* AlgU directly binds the AlgD promoter sequence, which contains the AlgU consensus binding sequence (Fakhr et al., 1999).

Currently, only a handful of studies have investigated the function of *P. syringae* alginate in plant-pathogen interactions. Yu et al. (1999) found that alginate production was important for the epiphytic growth of *Pss* on bean leaves, indicating that alginate could be important for infection. This has been supported more recently when the alginate biosynthesis cluster, including AlgD was found to be expressed at higher levels by *Pst* in *Arabidopsis* compared to *in vitro* (Nobori et al., 2018). Additionally, studies in tomato demonstrated that the *Pst*  $\Delta algU mucAB$

mutant grew less well ( 3.5-fold lower levels of bacteria) compared to wild-type *Pst* (Markel et al., 2016). Wild-type *Pst* bacterial levels in tomato were restored in cells complemented with AlgU, suggesting that AlgU is a regulator required for successful infection by *Pst* of tomato (Markel et al., 2016).

The sigma factor AlgU is involved in many other cellular processes besides alginate production (Fig. 1.3). For example, RNA sequencing analysis of *Pst*  $\Delta algU$  *mucAB*  $\Delta algD$  growing in culture with or without a functional copy of AlgU, revealed that expression of AlgU coincided with expression of genes involved in T3SS pilus formation, production of effector proteins, and iron mobilisation, while expression of genes involved in motility and iron storage were repressed (Markel et al., 2016). Studies in wild-type and *Pss*  $\Delta algU$  revealed that AlgU function was associated with greater tolerance to heat and H<sub>2</sub>O<sub>2</sub> treatments (Keith and Bender, 1999). Osmotic stressors, NaCl and sorbitol treatments strongly induced GUS activity in an AlgU promoter:GUS transgenic *Pss* suggesting that AlgU may regulate the response to osmotic stress (Keith and Bender, 1999). The data from these studies suggests AlgU is a regulator of numerous cellular processes and several of these processes are known to be important for successful infection of plants (Fig. 1.3; Keith and Bender, 1999; Markel et al., 2016).

### 1.4.3 Type 3 secretion systems and effector proteins

To evade plant defence responses many bacterial pathogens secrete effector proteins into the plant cytoplasm using the type 3 secretion system (T3SS) (Jin et al., 2001; Li et al., 2002). The *P. syringae* T3SS pilus and many effector proteins

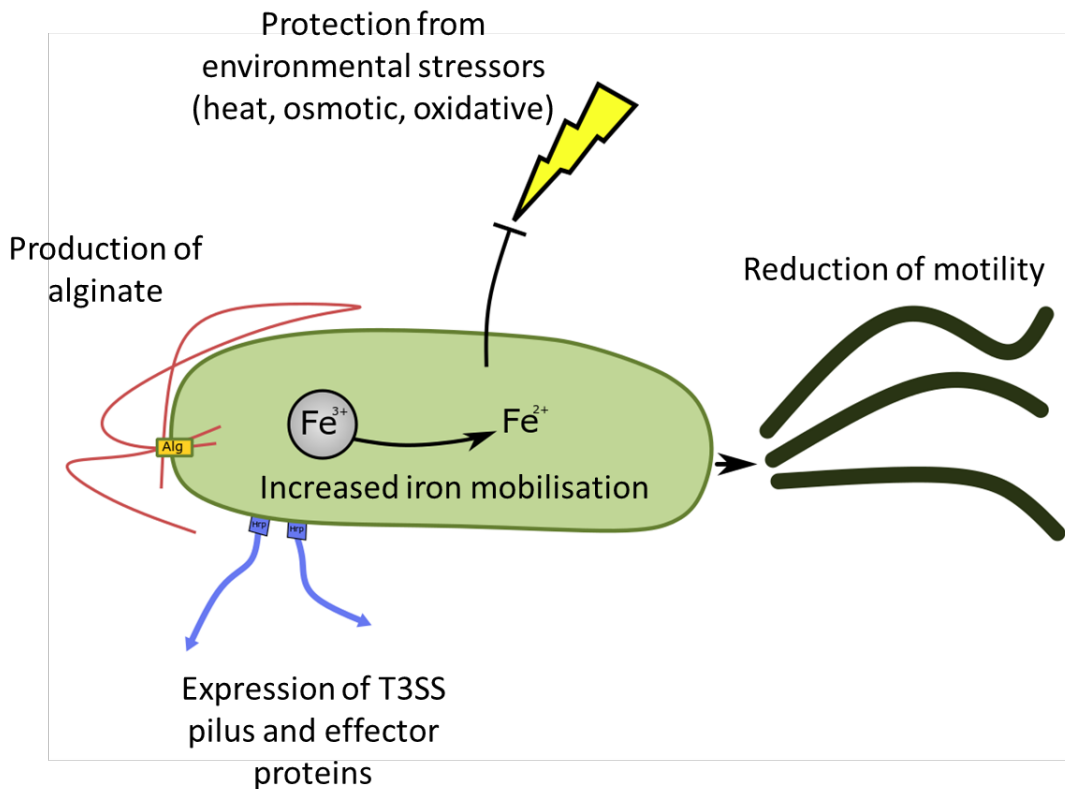


**FIGURE 1.3: Model of proposed cellular effects of increased AlgU expression.** Functional AlgU in *P. syringae* is associated with tolerance to environmental stressors, including heat, osmotic and oxidative stress (Keith and Bender, 1999). Another study determined that overexpression of AlgU caused differential expression of genes involved in many biological processes (Markel et al., 2016). These results suggest that up-regulation of AlgU could cause concurrent production of alginate, mobilisation of iron, reduction in motility, and induction of the T3SS-gene cluster (involved in effector protein and T3SS pilus formation) (Markel et al., 2016).

are encoded in the Hypersensitive response and pathogenicity (*Hrp*) gene cluster (Buell et al., 2003). As many of these genes contribute to infection, this gene cluster is a genomic region of great importance for infection. Regulation of the *Hrp* gene cluster is thought to be controlled mainly by the *Pst* ECF sigma factor HrpL (Lam et al., 2014). The expression of HrpL and therefore the *Hrp* gene

cluster is regulated by the transcriptional activator HrpRS (Jovanovic et al., 2014). A recent study used a combined approach of Chip-Seq and RNA-sequencing to explore the regulatory effects of AlgU in *Pst*. This study revealed that AlgU bound the promoter region of HrpRS and expression of AlgU induced HrpRS expression (Markel et al., 2016). This suggests that AlgU directly regulates expression of the *Hrp* gene cluster through positive regulation of HrpRS, thus AlgU could be important for infection through activation of the *Hrp* pilus and effector proteins (Markel et al., 2016).

Investigating the environmental cues which facilitate the perception of the plant apoplast (leaf intercellular spaces) is important for understanding how bacteria regulate pathogenesis genes to begin infection in leaves. For example, growth of *Pst* in apoplast mimicking *hrp*-inducing minimal media (HIM) media stimulated expression of the Hrp transcriptional activators HrpL and HrpRS (Kim et al., 2009; Stauber et al., 2012). Furthermore, changing the carbon source present in HIM media differentially affected the expression of the *Pst* transcriptional activators HrpL and HrpRS as well as the downstream virulence effector AvrPto (Stauber et al., 2012). Changing the carbon source in HIM from fructose to citric acid or succinate reduced expression of HrpRS, HrpL and AvrPto (Stauber et al., 2012). This suggests that certain carbon sources facilitate bacterial recognition of the leaf apoplastic space. Moreover, another virulence effector HopA1 was expressed when cultured in HIM supplemented with iron, suggesting iron availability could also be a signal to alert bacteria that they are in the leaf apoplast (Kim et al., 2009). These studies provide novel insights into bacterial perception of plant metabolites that stimulate the infection process.

## 1.5 PAMP-triggered immunity (PTI)

One of the first responses that plants employ to resist pathogens is PTI (Boller and Felix, 2009). pathogen-Associated Molecular Patterns (PAMPs) are general features common to a wide variety of pathogens, such as chitin, a constituent of fungal cell walls, elongation factor (EF)-Tu, a component of the translation machinery of bacteria, and flagellin, the major protein of bacterial flagella (Kunze et al., 2004; Zipfel et al., 2004; Cao et al., 2014). Plants recognise PAMPs using cell surface pattern recognition receptors (PRRs) (Chinchilla et al., 2006). These PRRs include CHITIN ELICITOR RECEPTOR KINASE1 (CERK1), EF-TU RECEPTOR (EFR) and FLAGELLIN-SENSITIVE2 (FLS2), that can bind chitin, EF-Tu, and flagellin, respectively (Chinchilla et al., 2006; Nekrasov et al., 2009; Cao et al., 2014). The recognition of flagellin and EF-Tu requires not only the corresponding PRRs, but BRASSINOSTEROID INSENSITIVE1-ASSOCIATED RECEPTOR KINASE1 (BAK1), a leucine-rich receptor kinase (Heese et al., 2007; Roux et al., 2011). Research suggests that upon PAMP binding, FLS2 and EFR undergo a conformational change and heterodimerize with BAK1 (Fig. 1.4; Chinchilla et al., 2007). BAK1 is then thought to activate BIK1, since BAK1 can heterodimerize and phosphorylate BIK1 *in vitro* (Lin et al., 2014).

In addition to interacting with BAK1, BIK1 is thought to act at the convergence of several PAMP-PRR pathways to induce WRKY signaling (Zhang et al., 2010; Lal et al., 2018). For example, BIK1 activation also occurs when chitin is perceived by the LYSM-CONTAINING RECEPTOR-LIKE KINASE5 (LYK5)-CERK1 complex (Liu et al., 2018). In this complex, CERK1 activation is thought

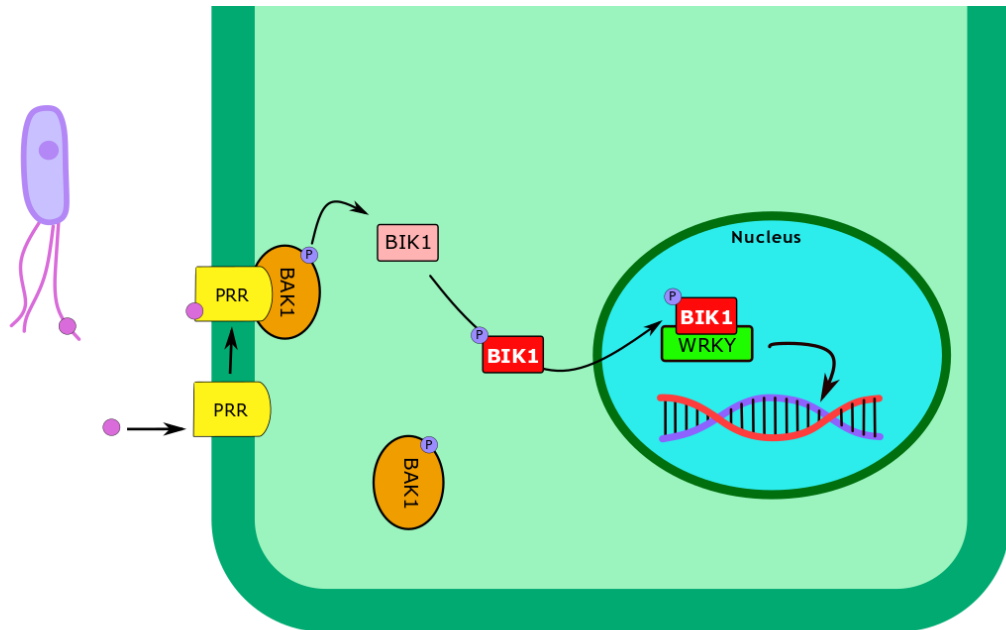


FIGURE 1.4: **Model of flg22-initiated PTI.** The initiation of PTI begins with the binding of the bacterial flg22 epitope to the PRR, FLS2 (Chinchilla et al., 2006). BAK1 recognizes the flg22-FLS2 PAMP-PRR complex and phosphorylates BIK1 (Lin et al., 2014). Upon phosphorylation BIK1 binds WRKY transcription factors to activate downstream PTI defense genes (Tsuda and Somssich, 2015; Lal et al., 2018; Liu et al., 2018)

to require heterodimerization with the chitin receptor LYK5, thereby activating BIK1 (Cao et al., 2014). BIK1 localises to both the plasma membrane and the nucleus, where it was shown to interact with Salicylic acid (SA)- and JA-related WRKY factors in *Nicotiana benthamiana* using a bimolecular fluorescent complementation assay (Lal et al., 2018). The kinase activity of BIK1 is required for positively regulating downstream PTI signaling in response to flg22, elf18 (a derivative of EF-Tu) and chitin (Zhang et al., 2010; Lal et al., 2018). This data

demonstrates that upon phosphorylation, BIK1 induces PTI downstream signaling via the WRKY transcription factors (Fig. 1.4; Tsuda and Somssich, 2015; Lal et al., 2018; Liu et al., 2018).

PTI signaling initiates several defense responses including stomatal closure, callose deposition in the cell wall, and accumulation of several defence related molecules, including phytoalexins and Pathogenesis-related (PR) proteins (Henry et al., 2013). The PTI response is thought to produce an inhospitable environment for invading pathogens (Laluk and Mengiste, 2010) and pathogens are thought to have evolved mechanisms to suppress PTI (Zvereva and Pooggin, 2012).

Several *Pst* virulence effectors have been implicated in suppression of these defense responses. For example, AvrPto is a member of the HrpL regulon and is up-regulated by AlgU (Ferreira et al., 2006; Markel et al., 2016). *In vitro* and *in vivo* studies demonstrated that AvrPto binds the PRRs, FLS2 and EFR (Xiang et al., 2008) and binding of AvrPto to FLS2 and EFR inhibited the autophosphorylation of these PRRs and was required for maximal suppression of PTI by AvrPto (Xiang et al., 2008).

## 1.6 Effector-triggered immunity (ETI)

As pathogens evolved effectors to suppress plant defence responses, plants evolved mechanisms to detect these effectors and initiate Effector-triggered immunity (ETI) (Zvereva and Pooggin, 2012). Pathogen effectors are detected by Resistance (R) receptors either directly or indirectly (Hurley et al., 2014). One example of

an indirect interaction occurs when the R receptor RESISTANCE TO *P. SYRINGAE PV MACULICOLA1* (RPM1) perceives that the plant protein, RPM1-INTERACTING PROTEIN4 (RIN4), has been proteolytically degraded by the *Pst* effector AvrRpt2. This recognition of RIN4 degradation leads to activation of the ETI response (Mackey et al., 2002; Axtell and Staskawicz, 2003; Kim et al., 2005).

Even though ETI and PTI employ similar signaling networks to induce defence, there are differences between these responses (Tsuda and Katagiri, 2010). The current theory is that the main difference PTI and ETI is length of the response, PTI is considered to be transient, while ETI is a prolonged response (Tsuda and Katagiri, 2010). This is consistent with recent findings that during ETI but not other defence responses there is a prolonged activation of the MAPK signaling cascade, which leads to the activation of defense responses (Tsuda et al., 2013). However, the PTI and ETI pathways share signaling components such as Ca<sup>2+</sup>, Reactive Oxygen Species (ROS) bursts and transcriptional reprogramming (Tsuda and Katagiri, 2010). The Hypersensitive response (HR), a form of programmed cell death is associated with ETI and is thought to limit the spread of biotrophic pathogens (reviewed in Cui et al., 2015). Finally, SA accumulates in *Arabidopsis* both within the cell and in the intercellular space during ETI (Carviel et al., 2014). During ETI, SA acts as a signaling molecule and initiates downstream defence pathways (Vlot et al., 2009).

## 1.7 Salicylic acid

Many studies support the idea that the phenolic compound, salicylic acid is a signaling molecule in plant defence responses (reviewed in Vlot et al., 2009). In *Arabidopsis*, biosynthesis of SA occurs in one of two pathways, the isochorismate (ICS) or phenylalanine (PAL) pathways. ISOCHORISMATE SYNTHASE1 (ICS1) catalyzes the production of isochorismate from chorismate (Dempsey et al., 2011). A recent study provides evidence that the conversion of isochorismate to SA is completed by ENHANCED PSEUDOMONAS SUSCEPTIBILITY1 (EPS1) and AVRPPHB SUSCEPTIBLE3 (PBS3) (Torrens-Spence et al., 2019).

SA biosynthesis via the ICS pathway is an important part of disease resistance (Wildermuth et al., 2001). ICS1, also known as SALICYLIC ACID INDUCTION DEFICIENT2 (SID2), is expressed in response to infection by *P. syringae* and the ICS1 mutant *sid2-2* accumulates little SA in response to infection (Wildermuth et al., 2001). *Pseudomonas syringae* *pv. maculicola* (*Psm*) was found to grow more quickly in the *sid2-2* mutant compared to wild-type *Arabidopsis* (Wildermuth et al., 2001). SA is produced in chloroplasts and then exported to the cytoplasm via the plastid envelope localised transporter EDS5 (Serrano et al., 2013; Yamasaki et al., 2013). Plants that are defective in producing isochorismate-derived SA are defective in ETI, PTI, Systemic-acquired resistance (SAR), and Age-related resistance (ARR) (Kus et al., 2002; reviewed in Vlot et al., 2009). This demonstrates that SA is an important plant metabolite that governs a wide spectrum of plant defense responses.

The defence regulator NON-EXPRESSOR OF PATHOGENESIS-RELATED GENES (NPR)1 plays a central role in SA-mediated defence responses such as PTI, ETI and SAR. Upon SA accumulation, NPR1 becomes activated and translocates to the nucleus to activate expression of downstream defence genes such as PR1 (Kinkema et al., 2000). Whether SA activates NPR1 through direct binding is still an active area of research. Researchers at Duke University found that *in vitro* purified GST-tagged NPR3 and NPR4, but not NPR1 bound SA, suggesting that NPR1 is controlled through NPR3/4 (Fu et al., 2012). However several other studies support the idea that SA binds NPR1 directly (Wu et al., 2012; Manohar et al., 2015; Ding et al., 2018). Wu et al. (2012) and Ding et al. (2018) identified independent single amino acid mutations in NPR1 that caused conformational changes in NPR1 that inhibited SA binding *in vitro*. Another study used several high throughput methods developed to identify putative SA binding proteins and found that NPR1 bound SA (Manohar et al., 2015). Additionally, Wu et al. (2012) suggest that NPR1 requires copper to bind SA, however unpublished evidence suggests that copper did not induce GST-NPR1 to bind SA (Yan and Dong, 2014). It is possible that the large GST affinity tag used in this study could have negatively affected the biological function of the GST-NPR1 fusion protein and inhibited SA binding (Zhao et al., 2013).

Some think that NPR1-mediated activation of defense is mediated through control of NPR1 protein levels. The Cullin 3 (CUL3) E3 ligase adapters NPR3 and NPR4 have been implicated in NPR1-degradation activity (Fu et al., 2012). These SA-binding proteins were found to interact with NPR1 in an SA-dependent

manner and upon interaction, function as adapters for CUL3 ubiquitin E3 ligase, thereby mediating the degradation of NPR1 (Fu et al., 2012). The authors suggest that NPR4 prevents over activity of SA-mediated defences by degrading NPR1 at low SA concentrations, while at high SA concentrations NPR3 prevents prolonged activation of SA-mediated defences through degradation of NPR1 (Fu et al., 2012). Alternatively, NPR3/4 could function as defence responses regulators as they were found to redundantly repress the early defence genes WRKY70 and SAR-DEFICIENT1 (SARD1) (Ding et al., 2018). Interestingly, treatment with SA alleviated the NPR3/4-mediated repression of WRKY70 and SARD1, suggesting that these proteins could function independently of NPR1 (Ding et al., 2018).

## 1.8 Age-Related Resistance (ARR)

As many plants age they become resistant to infection, this phenomenon is called Age-Related Resistance (ARR). ARR has been observed in many crop plants such as maize, soybean, strawberry, cabbage, tobacco, pepper, and tomato (reviewed in Develey-Rivière and Galiana, 2007). ARR has been observed during the interaction of *Arabidopsis* with *Pst*, *Psm* and the oomycete, *Hyaloperonospora parasitica* (Kus et al., 2002; Rusterucci et al., 2005; Carviel et al., 2009).

In *Arabidopsis*, the onset of ARR corresponds with the transition from vegetative to reproductive growth, suggesting that one underlying mechanism could be controlling both flowering and ARR (Kus et al., 2002). To investigate if early initiation of flowering induces ARR, plants were grown in conditions that led to early or delayed flowering. Under short days, plants flower later at 5 to 6 weeks

and ARR onset in *Arabidopsis* typically occurs at 5 to 6 wpg (Kus et al., 2002). However, when grown under long days, *Arabidopsis* flowered earlier at 3 to 4 weeks and ARR onset occurred earlier at 3 to 4 wpg (Rusterucci et al., 2005). This supports the hypothesis that ARR and flowering are related. However, the reason plants flower faster under long days is probably due to faster development, therefore ARR could be induced by a related developmental pathway rather than a flowering pathway. To determine if the initiation of flowering is coupled with ARR onset, the ARR competence of several early and late flowering mutants of ARR was examined. Both early and late flowering mutants displayed ARR at 5 to 6 weeks, therefore the transition from vegetative to reproductive growth is probably not the cue for ARR onset (Wilson et al., 2013).

### 1.8.1 The role of SA during ARR

The ability to accumulate SA is important during ARR as several SA accumulation mutants, *NahG*, *sid2* and *eds5*, were shown to be ARR-defective (Kus et al., 2002). Since SA generally acts as a defence signaling compound in young plants, it is interesting that NPR1, a central regulator of defence, and WHIRLY1 (WHY1), another SA-dependent defence regulator, were not required for ARR (Kinkema et al., 2000; Kus et al., 2002; Desveaux et al., 2004; Carella et al., 2015). Additionally, young plants accumulate PR1 transcripts 12 to 24 hours after treatment with SA, while mature ARR-responding plants in which SA accumulates to high levels, express little PR1 (Cameron and Zaton, 2004; Uquillas et al., 2004). These data suggest that SA functions in a different way during ARR (Kus et al., 2002).

During infection *Pst* grows in the leaf apoplastic space (Whalen et al., 1991) and this gave rise to the idea that SA could act directly as an antimicrobial agent in the apoplast (Cameron and Zaton, 2004). To investigate this hypothesis, Intercellular washing fluids (IWFs) from the apoplast of mature and young leaves were collected during infection. IWFs from mature, but not young plants inhibited bacterial growth, suggesting something important to defence was present in the IWFs (Cameron and Zaton, 2004). Moreover, SA was shown to accumulate in IWFs collected from ARR-competent mature, but not IWFs collected from young plants inoculated with *Pst* (Cameron and Zaton, 2004). Taken together, these two experiments support the hypothesis that SA accumulates in the leaf intercellular space during ARR and could act as an antimicrobial agent.

To obtain evidence in support of the idea that SA acts as an antimicrobial agent, *Pst* were cultured in leaf intercellular space-mimicking HIM media, supplemented with various concentrations of SA. It was observed that high concentrations of SA (>1 mM) completely inhibited the growth of *Pst* bacteria (Wilson et al., 2017). At SA concentrations that were estimated in to be present in the leaf intercellular space during ARR, SA modestly inhibited growth of *Pst* in culture (Cameron and Zaton, 2004; Wilson et al., 2017). This could indicate that SA in the apoplast has an additional antimicrobial effect during infection (Wilson et al., 2017). To determine if SA could act as an antibiofilm agent during infection, *Pst* was grown in apoplastic mimicking minimal media supplemented with SA without agitation. The biofilm formation of *Pst* was completely inhibited at concentrations of SA (100  $\mu$ M) estimated to be present in the apoplast during infection (Wilson et al., 2017).

### 1.8.2 The role of CYP71A12 and CYP71A13 during ARR

ARR microarrays were employed to find genes that may be important for ARR by identifying transcripts that were up- or down-regulated in mature ARR-competent plants in response to *Pst*, compared to mock-inoculated plants (Carviel et al., 2009). The most highly up-regulated gene in mature plants was CYP71A13, a cytochrome P450 involved in camalexin biosynthesis (Carviel et al., 2009). CYP71A13 appears to function redundantly with CYP71A12 based on the fact that these genes share 89% amino acid sequence similarity and the biosynthesis of the downstream indolic compound, camalexin, requires only one of these genes (Müller et al., 2015). Interestingly, a *cyp71a12 cyp71a13* double mutant was partially ARR defective (Kempthorne, 2018). This combined with the ARR competence of the camalexin biosynthesis mutant *pad3-1*, suggests that an indole derivative other than camalexin is important for ARR (Kempthorne, 2018). To determine which indole derivative was important for ARR, ultra-performance liquid chromatography mass spectrometry was performed on intercellular washing fluids collected from mature and young plants (Kempthorne, 2018). Non-targeted metabolomic analysis identified Dihydrocamalexin acid (DHCA) as accumulating in IWFs of mature but not young plants (Kempthorne, 2018). Supporting the connection between DHCA and CYP71A12 and CYP71A13, the partial ARR defect observed in *cyp71a12 cyp71a13* could be complemented by infiltrating leaves with DHCA prior to inoculation with *Pst* (Kempthorne, 2018). These data support the hypothesis that CYP71A12 and CYP71A13 contribute to ARR by producing intercellular DHCA. However, DHCA does not appear to have *in vitro* antibiofilm activity (Kempthorne, 2018).

### **1.8.3 SA transport**

The current understanding of defence-related SA transport begins in chloroplasts, where ICS1 converts chorismate to isochorismate (Garcion et al., 2008; Fragniere et al., 2011) which is converted to SA by EPS1 and PBS3 (Torrens-Spence et al., 2019). Once SA is produced in the chloroplasts, EDS5 a multidrug-and-toxin extrusion (MATE) protein, is thought to transport SA into the cytoplasm (Nawrath et al., 2002; Serrano et al., 2013; Yamasaki et al., 2013). Once in the cytoplasm, SA is thought to be converted into Salicylic acid glucose (SAG) conjugates, which are more water-soluble and inactive (Dean et al., 2003; Dean and Mills, 2004; Dempsey et al., 2011; Maruri-López et al., 2019). Data from our lab demonstrates that SA is present in the intercellular space during ARR, ETI and PTI, suggesting that SA transport into the intercellular space could be widely conserved during immune responses (Cameron and Zaton, 2004; Carviel et al., 2014; Fufeng et al., 2020).

The SA cytoplasm-to-apoplast transport mechanism is still unknown, although there are a couple of mechanistic possibilities. One possibility is that the active form of SA is transported into the apoplast (Dempsey et al., 2011). As the only known plant SA transporter, EDS5, is a MATE protein, it is possible that another MATE protein is responsible for SA transport into the apoplast (Nawrath et al., 2002; Serrano et al., 2013).

Another possibility is that SAG, an inactive form of SA, is transported into the apoplast, whereupon the glucoside is removed. As treatment with an ATP-binding

cassette (ABC) transport inhibitor reduced SAG uptake by vacuolar membrane-enriched vesicles, an unidentified ABC transporter was implicated in transport of SAG into the vacuole (Vaca et al., 2017). The ABC subfamily G contains two types of transporters, the white-brown complex (WBC) transporters and pleiotropic drug resistance (PDR) transporters (Lefèvre and Boutry, 2018). Several members of the ABC transporter G subfamily have been implicated in secretion of defense-related compounds to plant surfaces (Campbell et al., 2003; Campe et al., 2016; Hwang et al., 2016; Khare et al., 2017; He et al., 2019; Matern et al., 2019). This leads to the idea that an ABC subfamily G transporter is responsible for secretion of either SA or its inactive form into the leaf apoplast.

The best current candidate for an apoplastic SA-transporter is probably the ABC subfamily G protein PDR8, also known as PEN3 or ABCG36. When transiently expressed in *N. benthamiana*, PDR8 localised to the cytoplasm-plasma membrane interface (Campe et al., 2016). Additionally, in *Arabidopsis* PDR8 and PDR12 were the only PDR proteins expressed upon fungal infection and a GUS reporter assay found that both of these PDR proteins localised to the site of infection (He et al., 2019). In response to fungal infection, PDR8 has been shown to play an active role in transport of many tryptophan-derived metabolites, including DHCA (Strader and Bartel, 2009; Lu et al., 2015; He et al., 2019; Matern et al., 2019). Additionally, PDR8 was found to act as cadmium extrusion pump during heavy metal toxicity demonstrating it has broad substrate specificity (Kim et al., 2009). The broad substrate specificity of PDR8 suggest that SA or SAG could be transported by this protein.

However, there is no direct evidence that PDR8 is an SA/SAG transporter,

although there is some circumstantial evidence suggesting it could act in this role. Hyperaccumulation of camalexin and 4OGlcI3F in *pen3* mutants was used as the basis for research that eventually led to PDR8 being described as a transporter of these trp-metabolites (Lu et al., 2015; He et al., 2019). In the same way, SA and SAG were determined to hyperaccumulate in the tissue of several *pen3* mutants in response to fungal infection, supporting the idea that PDR8 could be an SA/SAG transporter (Lu et al., 2015). Independently, Stein et al. (2006) found that in response to infection many SA pathway associated genes responded more strongly in *pen3-1* compared to wild-type *Arabidopsis*. Interestingly, PDR8 might act as an SA transporter during ETI, as infection with avirulent *Pst* results in accumulation of PDR8 and SA (Glombitza et al., 2004; Carviel et al., 2014). Taken together, these data suggest that PDR8 might transport SA into the apoplast during both fungal infection and ETI.

PDR8 and PDR12 may also function redundantly in SA/SAG and camalexin transport into the apoplast as evidence suggests these proteins both secrete camalexin in response to fungal infection (He et al., 2019). Furthermore, transcripts of PDR12, but not other PDR genes had higher expression levels upon fungal infection in *pen3-1* compared to wild type (Campbell et al., 2003). Additionally, PDR12 expression was induced 260-fold by treatment with salicylic acid, suggesting PDR8 and PDR12 could redundantly export SA into the apoplast (Campbell et al., 2003; Stein et al., 2006). This problem could be avoided by studying the *pdr8 pdr12* double mutant alongside the individual mutants (He et al., 2019).

#### 1.8.4 ARR signaling pathway

Although ARR competence can be uncoupled from flowering, a number of flowering time regulators have been found to be involved in the ARR response (Wilson et al., 2013; Wilson et al., 2017).

Wilson et al. (2013) provided evidence that FLOWERING LOCUS C (FLC), a negative regulator of flowering may contribute to ARR, however the mechanism for FLC involvement in ARR has not been investigated, whereas the role of SHORT VEGETATIVE PHASE (SVP) and SOC1 was investigated further. The two MADS-domain transcription factors, FLC and SVP can individually suppress several flowering time regulators (Deng et al., 2011; Gregis et al., 2013). SVP and FLC are thought to form a complex to enhance suppression of flowering (Mateos et al., 2015). Specifically, Chip-Seq and qRT-PCR revealed that SVP could bind to the promoter sequence and repress expression of SUPPRESSOR OF CONSTANS1 (SOC1) (Li et al., 2008). SOC1 is a positive regulator of LEAFY (LFY), which promotes reproductive growth (reviewed in Amasino, 2010). During ARR, the SVP mutants *svp-32* and *svp-41* were demonstrated to be ARR-defective and unable to repress flowering (Wilson et al., 2017). Crossing the ARR-defective plant line *svp-32* with the late flowering mutant *soc1-2* mutant rescued ARR, suggesting SVP represses SOC1 during ARR (Wilson et al., 2017). Characterising the ARR response in *soc1-101D* revealed that SOC1 overexpression repressed ICS1 and accumulation of intercellular SA (Wilson et al., 2017). This suggests that SOC1 acts downstream in the ARR signaling pathway to suppress accumulation of SA in the intercellular space until SVP becomes competent to repress SOC1 allowing SA to

accumulate in the intercellular space where it is thought to act as an antimicrobial and antibiofilm agent (Wilson et al., 2017).

## 1.9 Hypotheses and objectives

### CHAPTER 3: Investigating the role of alginate in protecting *Pst* from the antimicrobial effects of salicylic acid.

Hypothesis: The ability to produce alginate contributes to protecting *Pst* from the antimicrobial and antibiofilm effects of SA *in vitro*.

Objectives:

- i Examine if SA negatively impacts the *in vitro* growth of *Pst* mutants that produce little alginate (*Pst*  $\Delta$ *algD*, *Pst*  $\Delta$ *algU mucAB*  $\Delta$ *algD*) compared to wild-type *Pst*.
- ii Examine if SA negatively impacts *in vitro* biofilm formation in *Pst* mutants that produce little alginate (*Pst*  $\Delta$ *algD*, *Pst*  $\Delta$ *algU mucAB*  $\Delta$ *algD*).

### CHAPTER 4: Exploring global gene expression during ARR and the contribution of PTI to ARR

Hypothesis 1: Components of the PTI pathway contribute to ARR

Objective: Determine the ARR competency of the PTI mutants *bak1-3*, *bik1*, *efr*, and *fls2*.

Hypothesis 2: Many genes that are differentially expressed during ARR contribute to ARR.

Objective: Use RNA-Seq to identify differentially expressed genes in mature ARR-competent compared to young ARR-incompetent plants to identify candidate genes that may contribute to a successful ARR response.

## 1.10 Cameron lab contributions not presented in this thesis

### PAMP-triggered immunity and biofilm formation

Current research in our lab includes investigating if biofilm formation is an important component of *Pst* pathogenesis and virulence during infection of *Ara-bidopsis*. I contributed to this investigation by assisting with imaging and quantification of wild-type *Pst* and *Pst*  $\Delta algU mucAB \Delta algD$  biofilm-like aggregates and determining if these aggregates contain biofilm components. I also helped to investigate if SA acts as an antimicrobial and antibiofilm agent during PTI. I will be an author on a paper describing this work.

### PIP-induced defence in cucumber

Other research in the lab is focused on examining the resistance- inducing activity of pipecolic acid, a small naturally produced compound involved in SAR.

I contributed to a number of these pipelic acid induced resistance assays in cucumber. I will be an author on a paper describing this work.

# Chapter 2

## Materials & Methods

### 2.1 Plant growth conditions

Seed Sterilization: Seeds were placed in 1 ml of 70% ethanol for 2 minutes. After this, ethanol was discarded, and seeds were sterilised with a solution of 30% bleach and 0.1% Tween 20. This solution was left shaking for 10 minutes. Once sterile, solution was discarded, and seeds were rinsed 5 times with 1 ml sterile water to rinse out excess detergent and bleach. After the final rinse, seeds were suspended in 0.1% sterile phytoblend. They were left to imbibe for at least two days before being plated on Murashige and Skoog plates (Murashige and Skoog, 1962). Once plated, seeds were placed in 24 hours of light at  $110 \mu\text{mol}/\text{m}^2/\text{s}$  photon flux density. At 5 days post germination, seeds were transplanted into packs of soil (SunGro Sunshine Mix #1), previously fertilised with 250 ml per pack of 1 g/l Plant-Prod All-Purpose Fertilizer 20-20-20. The transplanted seedlings were placed under 9 hours/day light at  $110 \mu\text{mol}/\text{m}^2/\text{s}$  in 75-80% relative humidity at  $22^\circ\text{C}$  for the duration of the experiment. Plants were bottom watered and soil was kept moist unless otherwise

stated. Plants were fertilised every two weeks from date of transplanting to the end of the experiment. If completing a PAMP-triggered immunity (PTI) induction experiment 1  $\mu\text{M}$  flg22 was infiltrated into the abaxial side of leaves 24 hours before inoculation with *Pseudomonas syringae pv. tomato* (*Pst*).

TABLE 2.1: *Arabidopsis* plant lines used in this study.

Ecotypes and mutant plant lines	Relevant properties
Col-0	Wild type
<i>sid2-2</i>	SA biosynthesis mutant; ARR defective
<i>efr</i>	PAMP receptor mutant
<i>fls2</i>	PAMP receptor mutant
<i>bik1</i>	PTI signaling mutant
<i>bak1-3</i>	PTI signaling mutant

## 2.2 Bacterial growth and inoculations

For ARR and PTI experiments, *Pst* was grown in king's B media (20 g/L proteose peptone #3, 1% (v/v) glycerol, 1.5 g/L dibasic potassium phosphate, 15 g/L agar for solid media) with 50  $\mu\text{g}/\text{ml}$  kanamycin unless otherwise stated. Once *Pst* was in the exponential phase ( $\text{OD}_{600} = 0.1\text{-}0.6$ ), bacteria were spun down at 1000 x g for 7 minutes. After this, the supernatant was discarded, the pellet was resuspended in 10 mM  $\text{MgCl}_2$  and diluted to  $10^6$  cfu  $\text{ml}^{-1}$ . For maximal stomatal aperture, the abaxial side of leaves was pressure infiltrated with a needless syringe between one and six hours after lights turned on each day. To not overwhelm the plant defences only 3-5 leaves were inoculated per plant.

TABLE 2.2: Bacterial strains and plasmids used in this study.

Bacterial strain or plasmid	Relevant properties	Reference or source
<i>Pseudomonas syringae</i>		
<i>Pst</i> pVSP1	<i>Pst</i> with empty cloning vector; Kan <sup>r</sup> Rif <sup>r</sup>	This lab
<i>Pst</i> pDSK-GFPuv	<i>Pst</i> with GFP expression plasmid; Kan <sup>r</sup> Rif <sup>r</sup>	(Wang et al., 2007)
<i>Pst</i> <sub>165K</sub>	Contains a spontaneously 165 kb duplication (Bao et al., 2014; Markel et al., 2016); Rif <sup>r</sup> ; also known as PS1	(Markel et al., 2016)
<i>Pst</i> <sub>165K</sub> $\Delta$ algD	Alginate deficient mutant of <i>Pst</i> <sub>165K</sub>	(Markel et al., 2016)
<i>Pst</i> <sub>165K</sub> $\Delta$ algD $\Delta$ algU <i>mucAB</i>	Alginate and AlgU mutant of <i>Pst</i> <sub>165K</sub>	(Markel et al., 2016)
<i>E. coli</i>		
DH5 $\alpha$	Wild type	
Plasmids		
pDSK-GFPuv	GFP expression plasmid; Kan <sup>r</sup>	(Wang et al., 2007)
pVSP1	Empty cloning vector; Kan <sup>r</sup>	
pET29b LTP2	pET29B expression plasmid with DIR1	Dan Liu

For RNA-sequencing, at the indicated time-points infiltrated leaves were collected, weighed (400 to 1000 mg), and immediately flash frozen in liquid nitrogen. Samples were then stored at -80°C until RNA isolation.

For bacterial quantification, three days post inoculation, infected leaves were surface sterilised (50% (v/v) ethanol, 1% (v/v) bleach and 49% (v/v) sterile ddH<sub>2</sub>O) and blotted dry. Eight leaf discs per replicate were cut from inoculated tissue using 0.6 mm cork borers. Leaf discs were suspended in 1 ml of 0.1% silwet L-77 solution and shaken for one hour. Following this, the solution was diluted and 10  $\mu$ l aliquots were plated on king's B agar plates. Bacteria were then allowed to grow for 2 days. After which, a microscope was used to quantify bacterial colonies.

## **2.3 RNA isolation**

Frozen leaf tissue (100 mg) was ground in a pre-cooled mortar filled with liquid nitrogen by vigorous grinding with a pestle and never allowed to thaw. According to the manufacturer's instructions, Trizol reagent (Invitrogen) was used to isolate total RNA from frozen leaf tissue and RNA was precipitated using isopropanol. Additionally, RNA was resuspended and then purified on-column using the Qiagen RNeasy mini kit (74104). Once washed of organic contaminants, the column was dried through centrifugation and RNA was resuspended in 40  $\mu$ l RNase-free H<sub>2</sub>O. The presence of organic contaminants was measured using a Nanodrop. Samples with low 260/230 or 260/280 values (<1.8) were not sequenced. Residual DNA was degraded using 4  $\mu$ l of Sigma-Aldrich DNase I (AMPD1-1KT) per reaction. RNA integrity was qualitatively observed by running 1  $\mu$ g of total RNA on a 1% agarose gel for 1 hour at 100 volts. Total RNA gels were imaged using a ChemiDoc gel imager. Samples that showed signs of degradation were not sequenced. Signs of degradation include, a fainter 28S rRNA band compared to the 18S rRNA band and/or smearing of the lower rRNA bands.

## **2.4 Library preparation and sequencing**

The sequencing facility (GeneWiz) purified mRNA transcripts from total RNA samples using oligo-dT attached magnetic beads which bind to the poly(A) tail of mRNA transcripts. The purified mRNA transcripts were then fragmented to the desired size range and primers were then attached fragmented transcripts to allow

reverse transcription to form the first cDNA strand. The RNA template was then removed, and the second strand of cDNA was transcribed. To prevent self-ligation of the synthesized cDNA, the 3' ends of these strands were acetylated. Adapters were then ligated to DNA fragments and PCR amplification was used to amplify fragments with ligated adapters. The completed library was checked for quality and quantity to ensure successful sequencing. Samples were then diluted to 10 nM and finally were pooled.

DNA fragments were then allowed to bind to complementary adapter sequences on an Illumina HiSeq flow cell, where bridge amplification allows for generation of a cluster of forward and reverse strands. Reverse strands are subsequently cleaved and washed away. The forward strand was then sequenced. After sequencing the first read, the DNA fragment was attached to a set of nucleotides which are specific to each sample, and bridge polymerisation restores the cluster to forward and reverse reads. This time the forward read is cleaved and washed away. The reverse read was sequenced in a similar manner as the forward read.

## 2.5 Antibacterial growth curve assays

Antibacterial assays with pure SA were performed as described previously (Wilson et al., 2017). Briefly, overnight cultures of *Pst* DC3000 were grown in king's B medium. Cells were centrifuged and the pellets washed two times with *hrp*-inducing minimal media (HIM) (50 mM potassium phosphate, 10 mM D-fructose, 7.6 mM (NH<sub>4</sub>)<sub>2</sub>SO<sub>2</sub>, 6.8 mM MgCl–2, 1.7 mM NaCl, pH 5.7) or king's B (Huynh et al., 1989). Bacterial cultures were then diluted to an optical density (OD600)

of 0.1. Aliquots of 160  $\mu\text{l}$  of HIM- or king's B-diluted bacterial culture were added to each well of a 96-well plate. SA was first serially diluted in 100% ethanol to concentrations that ranged from 250 to 0.5 mM. 3.2  $\mu\text{l}$  aliquots of the serial dilutions were added to 160  $\mu\text{l}$  of bacterial solution concentration to reach the indicated final concentration. The 96-well plate was incubated with shaking at 26°C for 72 hours. Optical density at 600nm was measured every 15 mins using a Tecan Sunrise plate reader. After 72 hours, 10  $\mu\text{l}$  aliquots of the cell suspension were spotted onto a king's B agar plate and observed two days later to test for bactericidal activity.

## 2.6 Biofilm formation assays

Biofilm formation assays with pure SA were performed as described previously (Wilson et al., 2017). Briefly, overnight cultures of *Pst* DC3000 were grown in king's B medium. Overnights were centrifuged and the pellets washed with HIM and then diluted to an OD<sub>600</sub> of 0.005. During biofilm formation assays, evaporation causes non-adherent cells to stick to the sides of the well, these non-adherent cells are then stained, leading to artificially high values of biofilm formation. This effect is called the edge effect as it is most severe around the edge of the plate. To avoid the edge effect on biofilm formation, a 96-well plate was prepared by adding 200  $\mu\text{l}$  aliquots of sterile water to the edge wells (Shukla and Rao, 2017). Aliquots of 150  $\mu\text{l}$  of HIM-bacteria mixture were added to each well of a 96-well plate. A range of SA concentrations was tested by undergoing serial dilutions of SA. 3  $\mu\text{l}$  of the diluted SA mixtures were added to respective wells. The final concentrations of SA are indicated in the figures. If not otherwise indicated, bacteria were grown

without shaking at room temperature (21-23°C). Optical density at 600 nm was measured at 24, 48 and 72 hours. After which, the wells were rinsed twice with distilled water to remove non-adherent bacteria. The peptidoglycan layer of the remaining adherent cells was stained with 200  $\mu$ l aliquots of 0.1% crystal violet was added to the washed wells. After 10 minutes of staining, crystal violet was discarded, and the excess stain was removed by rinsing four times with distilled water. Plates were left upside-down for 1-3 days to dry. Once dry, 200  $\mu$ l aliquots of glacial acetic acid were added to each well to dissolve the crystal violet stain back into solution. After 15-20 minutes, the solution was mixed by pipetting and the optical density at 570 nm was measured to determine biofilm formation.

## 2.7 Statistical analysis

After bacterial quantification, significant differences between treatment groups were determined using ANOVA and assumptions were tested using the Shapiro-Wilk and Levene tests for normality and homogeneity, respectively. This was all packaged together in an R package named Garrett's *Arabidopsis* Resource Package (GARP). As well as bacterial quantification analysis, this package includes a program for comparing antimicrobial growth assays by performing a T-test at each time-point and determine statistical differences between lines. Separate from GARP, the GitHub page linked above includes all code used to perform any statistical analysis for RNA-sequencing.



# Chapter 3

## Investigating the role of alginate in protecting *Pst* from the antimicrobial effects of salicylic acid

### Preface and contributions

Sections 3.1 and 3.2 have been prepared for a portion of the paper to be submitted to the journal MPMI. Garrett Nunn performed all the experiments contained within this chapter. Experiments were designed by Garrett Nunn and Robin Cameron. The transgenic *Pseudomonas syringae* *pv.* *tomato* (*Pst*) lines used in this chapter were obtained from Dr. B Swingle (Cornell University; *Pst*<sub>165K</sub>, *Pst*<sub>165K</sub>  $\Delta$ *algD* and *Pst*<sub>165K</sub>  $\Delta$ *algU mucAB*  $\Delta$ *algD*) and Dr. KS Mysore (Noble Research Institute; *Pst* pDSK-GFPuv). Conjugation of the *Pst*<sub>165K</sub>  $\Delta$ *algD* and *Pst*<sub>165K</sub>  $\Delta$ *algU mucAB*  $\Delta$ *algD* strains with the GFP expression vector (pDSK-GFPuv) was performed by Noah Xiao.

### 3.1 *In vitro* growth of *Pst* alginate mutants

Evidence from the Cameron lab suggests that the ability of *Pst*<sub>165K</sub> (the wild type provided by the Swingle lab) to produce alginate contributes to bacterial success *in planta* as demonstrated by observing fewer biofilm-like aggregates in alginate-deficient *Pst*<sub>165K</sub>  $\Delta$ *algD*, and *Pst*<sub>165K</sub>  $\Delta$ *algU mucAB*  $\Delta$ *algD*, an alginate and the ECF AlgU mutant, compared to wild-type *Pst* pDSK-GFPuv (Fufeng, 2019). To obtain support for these *in planta* results, *in vitro* growth and biofilm assays were performed to examine the importance of alginate production for *Pst* grown in liquid culture and biofilm assays. The growth of *Pst*<sub>165K</sub>  $\Delta$ *algD* and *Pst*<sub>165K</sub>  $\Delta$ *algU mucAB*  $\Delta$ *algD* was compared to wild type in rich media (King's B) and HIM media (Huynh et al., 1989). The low pH and nutrient-poor HIM media was chosen as these environmental conditions mimic the leaf intercellular space. In *Pst*<sub>165K</sub>'s B media, the growth pattern of *Pst*<sub>165K</sub>  $\Delta$ *algD* and *Pst*<sub>165K</sub>  $\Delta$ *algU mucAB*  $\Delta$ *algD* was similar to wild-type *Pst*<sub>165K</sub> (Fig. 3.1A&B), suggesting that the absence of alginate and the stress response regulator AlgU, does not negatively impact *Pst* growth in rich media.

In leaf intercellular space-mimicking media (HIM), alginate-deficient *Pst*<sub>165K</sub>  $\Delta$ *algD* grew similarly to wild-type *Pst*<sub>165K</sub> (Fig. 3.1D), while *Pst*<sub>165K</sub>  $\Delta$ *algU mucAB*  $\Delta$ *algD* grew significantly less between 24 and 68 hours (Fig. 3.1C). This indicates that leaf intercellular space-mimicking media negatively affected the growth of *Pst*<sub>165K</sub>  $\Delta$ *algU mucAB*  $\Delta$ *algD* compared to wild-type or *Pst*<sub>165K</sub>  $\Delta$ *algD*, suggesting that the ability to produce alginate is not important for growth in HIM

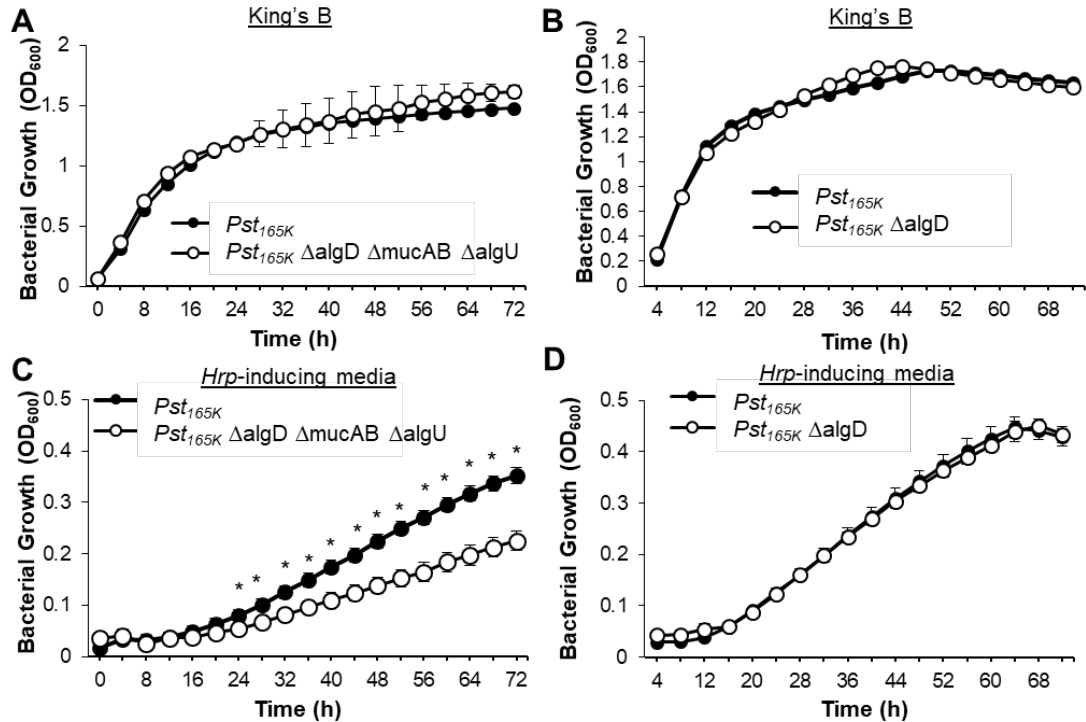


FIGURE 3.1: **Growth of *Pst*<sub>165K</sub> Δ*algU* *mucAB* Δ*algD* and *Pst*<sub>165K</sub> Δ*algD* in rich and minimal media.** The growth of wild-type *Pst*<sub>165K</sub> was compared to either *Pst*<sub>165K</sub> Δ*algD* (A&C), or *Pst*<sub>165K</sub> Δ*algU* *mucAB* Δ*algD* (B&D) in *hrp*-inducing minimal media (A&B) or *Pst*<sub>165K</sub>'s B media (C&D). Bacteria were grown overnight in King's B media, then pelleted and resuspended in the indicated media. Following this, bacteria were diluted to OD<sub>600</sub> to 0.1 and grown in a clear 96-well plate at 26°C with shaking. The optical density of each well was observed at 600 nm every 15 minutes for 72 hours. Each data point represents the average of four wells. Error bars represent the standard deviation. Asterisks indicate significant differences (T-test, p-value < 0.05). These experiments were repeated at least three times with similar results.

media which mimics the low pH and low nutrient characteristics of the intercellular space. In contrast, these results suggest the AlgU sigma factor, which induces expression of alginate and type 3 secretion system (T3SS) gene expression, is important for growth in intercellular-mimicking media. These data provide support for Fufeng (2019) *in planta* data that demonstrated that in the absence of alginate

and T3SS gene expression, *Pst*<sub>165K</sub>  $\Delta$ *algU mucAB  $\Delta$ algD* levels and biofilm-like aggregates were reduced compared to wild-type *Pst*.

### 3.2 Effect of salicylic acid on growth of *Pst* $\Delta$ *algD* and *Pst* $\Delta$ *algU mucAB $\Delta$ algD*

During PAMP-triggered immunity (PTI), preliminary evidence indicates that Salicylic acid (SA) accumulates in the intercellular space (Fufeng et al., 2020) as it does during ARR where it is thought to act as an antimicrobial and antibiofilm agent against *Pst* (Wilson et al., 2017). To examine the role of alginate in protecting bacteria from the effects of SA during plant defense, growth of wild-type *Pst*<sub>165K</sub>, *Pst*<sub>165K</sub>  $\Delta$ *algD* and *Pst*<sub>165K</sub>  $\Delta$ *algU mucAB  $\Delta$ algD* was examined in leaf intercellular space-mimicking media (HIM) supplemented with SA. Growth of wild-type and alginate-deficient *Pst*<sub>165K</sub>  $\Delta$ *algD* was inhibited at SA concentrations of  $\geq 2$  mM (Fig. 3.2A&B). However, growth of the *Pst*<sub>165K</sub>  $\Delta$ *algU mucAB  $\Delta$ algD* mutant was inhibited at lower SA concentrations of  $\geq 1$  mM, suggesting that AlgU function contributes to coping with the antimicrobial activity of SA (Fig. 3.2C).

To investigate if AlgU function is required to protect *Pst* against the bactericidal activity of SA, bacteria were cultured for 72 hours in apoplast-mimicking minimal media supplemented with SA, followed by washing pelleted cells with fresh media, thus reducing residual bactericidal activity. The culture was plated on king's B media with appropriate antibiotics to determine if viable cells remained. *Pst*<sub>165K</sub>  $\Delta$ *algU mucAB  $\Delta$ algD* colonies were not observed from wells containing 2 mM

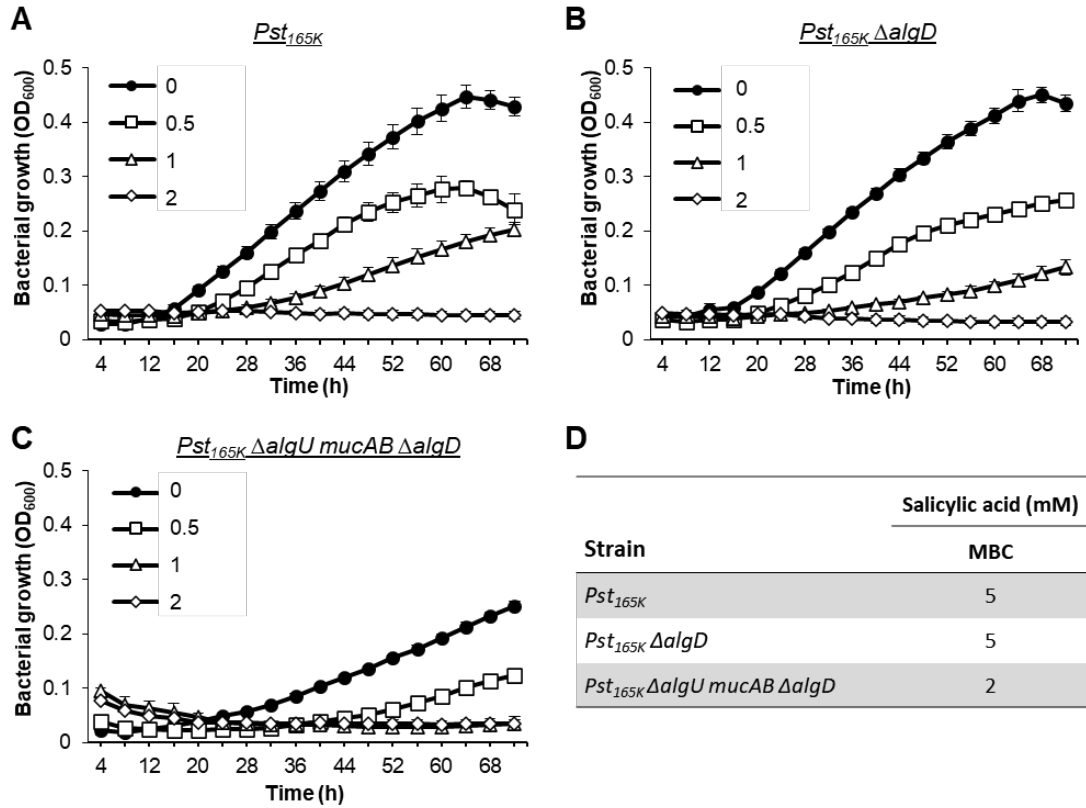


FIGURE 3.2: Antibacterial activity of SA on *Pst*<sub>165K</sub>  $\Delta$ *algU mucAB*  $\Delta$ *algD* and *Pst*<sub>165K</sub>  $\Delta$ *algD* compared to wild-type *Pst*<sub>165K</sub>. A. *Pst*<sub>165K</sub>, B. *Pst*<sub>165K</sub>  $\Delta$ *algD*, and C. *Pst*<sub>165K</sub>  $\Delta$ *algU mucAB*  $\Delta$ *algD* were grown overnight in rich media then washed and cultured with the indicated concentrations of SA in HIM at 26°C with shaking. Each data point represents the average of four wells and error bars represent standard deviation. This experiment has been performed three times with similar results. D. The MBC represents that concentration at which no bacterial colonies were observed after incubation cultures on king’s B plates.

SA, whereas wild-type *Pst*<sub>165K</sub> colonies were observed from wells containing 2 mM SA but not from wells containing 5 mM SA (Fig. 3.2D). In additional experiments, in which SA-supplemented cultures were not washed with fresh media, higher *Pst*<sub>165K</sub>  $\Delta$ *algU mucAB*  $\Delta$ *algD* SA sensitivity was observed compared to wild-type *Pst*<sub>165K</sub> (Tab. A3.1). Direct comparison of wild-type *Pst*<sub>165K</sub> and *Pst*<sub>165K</sub>  $\Delta$ *algD*

demonstrated that both bacterial strains were similarly sensitive to the bactericidal activity of SA (Fig. 3.2D). Taken together, *in vitro* growth assays indicate that *Pst*<sub>165K</sub>  $\Delta$ *algU mucAB*  $\Delta$ *algD* is more sensitive than wild-type *Pst*<sub>165K</sub> or *Pst*<sub>165K</sub>  $\Delta$ *algD* to the growth-inhibiting and bactericidal effects of SA. Given that AlgU is involved in positively regulating not only the alginate biosynthesis genes, but also the T3SS genes, these results suggest that the T3SS secreted effectors are important for protection against the antimicrobial effects of SA.

### 3.3 Effect of salicylic acid on biofilm formation by *Pst* $\Delta$ *algD* and *Pst* $\Delta$ *algU mucAB* $\Delta$ *algD*

Evidence from the Cameron lab suggests that the ability of *Pst* to produce alginate contributes to bacterial success *in planta* as demonstrated by observing fewer biofilm-like aggregates in alginate-deficient mutants, *Pst*<sub>165K</sub>  $\Delta$ *algD*, and *Pst*<sub>165K</sub>  $\Delta$ *algU mucAB*  $\Delta$ *algD*, compared to wild-type *Pst*<sub>165K</sub> (Fufeng, 2019). To provide support for these *in planta* results, the effect of SA on the ability of wild-type *Pst*<sub>165K</sub>, *Pst*<sub>165K</sub>  $\Delta$ *algD* and *Pst*<sub>165K</sub>  $\Delta$ *algU mucAB*  $\Delta$ *algD* to form biofilms *in vitro*, was examined. To do this, bacteria were cultured in intercellular-mimicking minimal media (HIM) without shaking at room temperature. Biofilm was quantified at indicated time points by staining adherent cells with crystal violet. *Pst*<sub>165K</sub>, *Pst*<sub>165K</sub>  $\Delta$ *algD*, and *Pst*<sub>165K</sub>  $\Delta$ *algU mucAB*  $\Delta$ *algD* all demonstrated a dose-dependent reduction in biofilm formation when cultured with SA

after 48 hours (Fig. 3.3). After 72 hours, biofilm formation was significantly lower at  $\geq 20 \mu\text{M}$  SA for *Pst*<sub>165K</sub> and *Pst*<sub>165K</sub>  $\Delta algD$  (Fig. 3.3A&B), whereas, *Pst*<sub>165K</sub>  $\Delta algU mucAB \Delta algD$  formed significantly lower biofilm formation at  $\geq 50 \mu\text{M}$  SA (Fig. 3.3C). However, biofilm formation by wild-type *Pst*<sub>165K</sub> was very low compared to past experiments performed with *Pst* pVSP1 (Wilson et al., 2017). For this reason, it cannot be determined whether *Pst*<sub>165K</sub>  $\Delta algU mucAB \Delta algD$  is more sensitive than wild-type *Pst* to SA or *Pst*<sub>165K</sub>  $\Delta algU mucAB \Delta algD$  forms less biofilm.

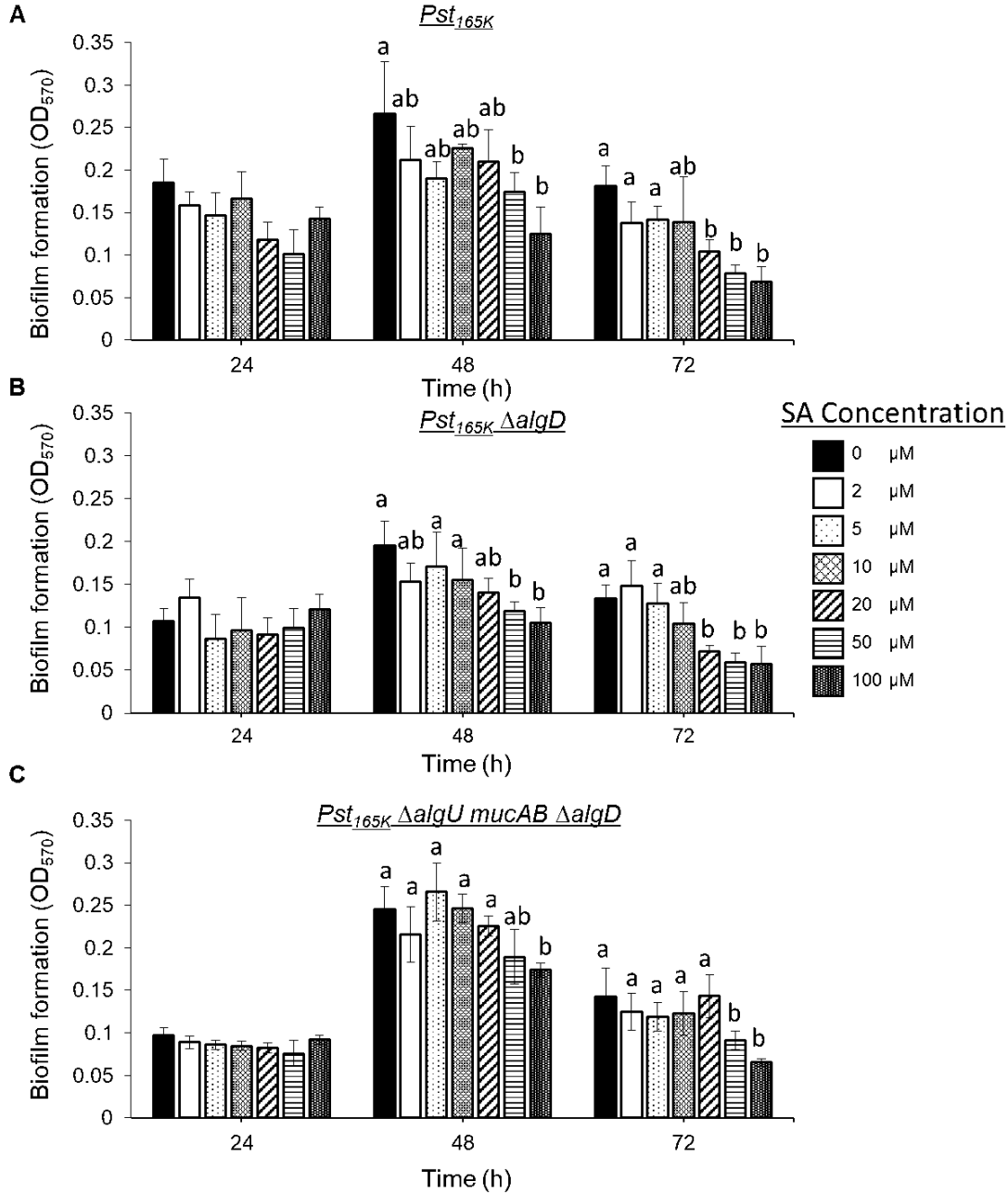


FIGURE 3.3: Antibiofilm activity of SA on *Pst*<sub>165K</sub>, *Pst*<sub>165K</sub>  $\Delta$ *algD*, and *Pst*<sub>165K</sub>  $\Delta$ *algU* *mucAB*  $\Delta$ *algD*. Bacteria were cultured in HIM without agitation in a 96-well plate. At indicated time-points, plates were rinsed to remove unattached planktonic cells and biofilms were quantified with crystal violet. Each bar represents the mean of 4 wells and error bars indicate standard deviation. Different letters indicate significant differences between groups (ANOVA, p-value <0.05).

### 3.4 The effect of bacterial strain and temperature on biofilm formation

In a previous study by Wilson et al. (2017), *Pst* pVSP1 formed higher levels of biofilm compared to *Pst*<sub>165K</sub> (Fig. 3.4; Wilson et al., 2017). Moreover, *Pst* pVSP1 biofilm formation was inhibited by lower concentrations of SA (2  $\mu$ M) (Wilson et al., 2017) compared to *Pst*<sub>165K</sub> (20  $\mu$ M) (Fig. 3.4). This led to the idea that there might be strain-dependent differences in biofilm formation. Strain-dependent differences in biofilm formation has been observed in several studies with *Pseudomonas aeruginosa* (Ude et al., 2006; Kirov et al., 2007; Gandee et al., 2015) as well as studies with *Salmonella enterica* (Lianou and Koutsoumanis, 2012) and *Listeria monocytogenes* (Poimenidou et al., 2016). Therefore, to determine if *Pst*<sub>165K</sub> does form less biofilm compared to *Pst* pVSP1, *in vitro* biofilm assays were performed with *Pst*<sub>165K</sub>, *Pst* pVSP61 (used in Wilson et al., 2017), and *Pst* pDSK-GFPuv (used in Fufeng et al., 2020, Tab. 2.2). In these experiments biofilm formation by *Pst* pVSP1 was similar to previous experiments (Fig. 3.4; Wilson et al., 2017). However, after 72 hours, the *in vitro* biofilm formation of *Pst*<sub>165K</sub> was significantly reduced compared to either *Pst* pDSK-GFPuv or *Pst* pVSP1 (Fig. 3.4). *Pst* pVSP1 consistently formed more biofilm than *Pst* pDSK-GFPuv, suggesting there are genetic differences between *Pst* strains that effect *in vitro* biofilm formation. As the biofilm formation of *Pst*<sub>165K</sub> was barely above detectable levels, a more sensitive biofilm formation assay is required to compare biofilm formation between *Pst*<sub>165K</sub>, *Pst*<sub>165K</sub>  $\Delta$ *algD*, and *Pst*<sub>165K</sub>  $\Delta$ *algU mucAB*  $\Delta$ *algD*.

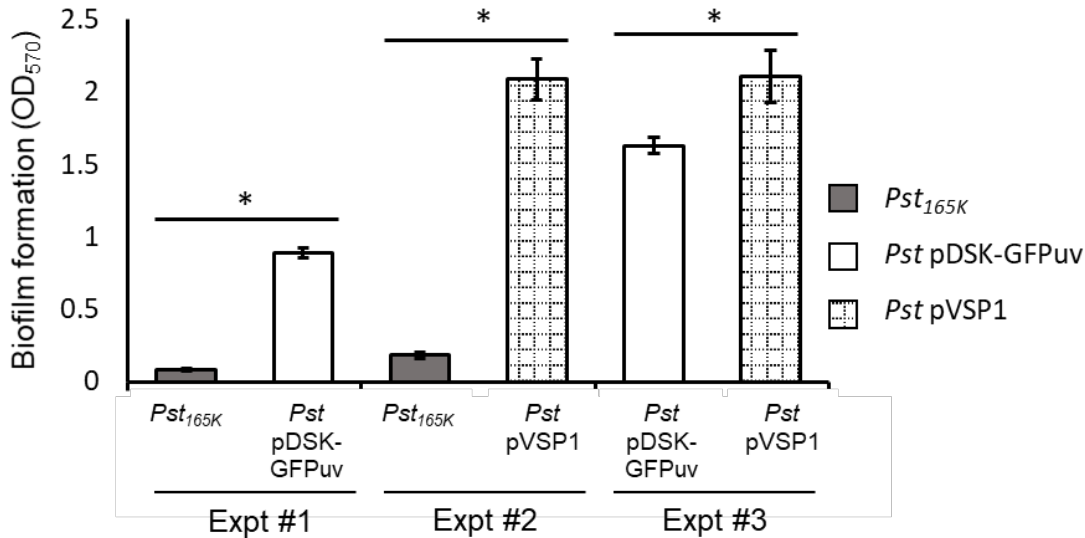
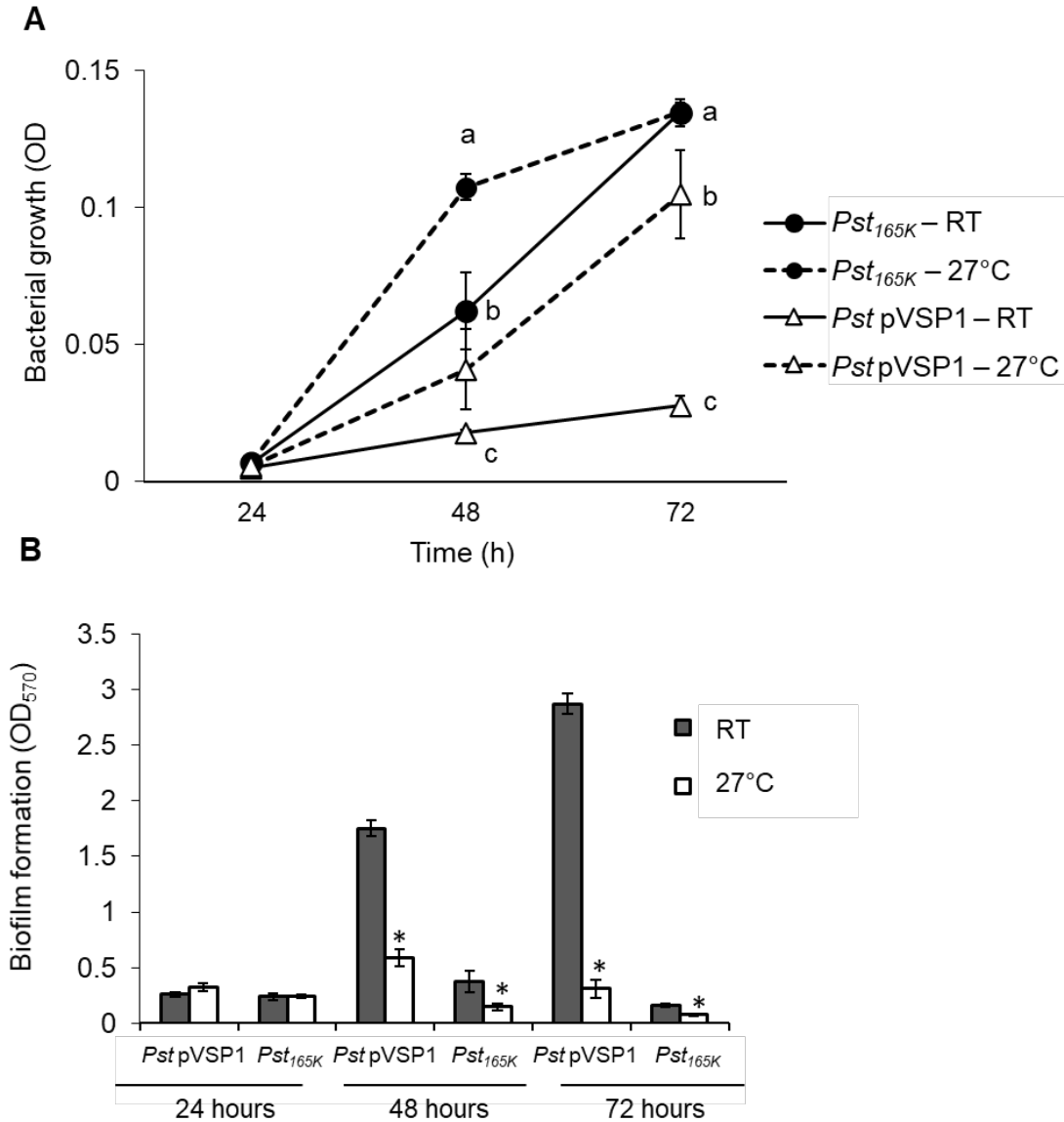


FIGURE 3.4: **Variability of biofilm formation among *Pst* strains.** Bacteria were grown in HIM at room temperature without agitation in a 96-well plate. After 72 hours, plates were rinsed to remove planktonic cells and biofilms were quantified with crystal violet. Each bar represents the mean of 4 wells and error bars indicate standard deviation. Asterisks indicate significant differences (T-test, p-value < 0.05). Each of these comparisons was performed twice with similar results.

In terms of genetic differences between these *Pst* strains, Bao et al. (2014) characterised a 165 kb duplication present in *Pst*<sub>165K</sub> (also known as PS1) that is not in the progenitor *Pst* strain originally isolated by Cuppels (1986), from which both *Pst* pDSK-GFPuv and *Pst* pVSP1 are independent descendants. Strains with this duplication had a higher growth rate in liquid culture compared to strains without, in both king's B and mannitol-glutamate minimal media, however there was no effect on *in planta* growth (Bao et al., 2014). To assess if the reduced ability to form biofilms by *Pst*<sub>165K</sub> compared to *Pst* pVSP1 was due to growth rate differences, *Pst*<sub>165K</sub> and *Pst* pVSP1, were grown in intercellular-mimicking minimal media (HIM) without agitation. At indicated time-points, planktonic cell numbers

were quantified by measuring the OD600, then the well contents were removed and rinsed followed by staining with crystal violet to assess biofilm formation. When bacteria were grown without shaking there was significantly higher numbers of planktonic cells in *Pst*<sub>165K</sub> compared to *Pst* pVSP1 at 48 and 72 hours (Fig. 3.5A). In contrast, *Pst* pVSP1 displayed higher levels of biofilm compared to the wells of *Pst*<sub>165K</sub> (Fig. 3.5B). These data support that there is a strain-dependent difference in biofilm formation. However, when conditions did not support biofilm growth (cultures were shaken continuously), the difference in planktonic cell numbers disappeared (data not shown). Therefore, when conditions support biofilm formation, this data suggest there is a negative relationship between planktonic cell numbers and biofilm formation.



**FIGURE 3.5: Temperature-dependent growth and biofilm formation in *Pst* pVSP1 and *Pst*<sub>165K</sub>.** Bacteria were grown in intercellular-mimicking media (HIM) without agitation in a 96-well plate at the indicated temperature. At indicated time-points, planktonic cell growth was quantified (A), then plates were rinsed to remove planktonic cells followed by staining with crystal violet to quantify biofilm levels (B). Each data point or bar represents the mean of 4 wells and error bars indicate standard deviation. Different letters indicate significant differences between groups (ANOVA, p-value <0.05). Asterisks indicate significant differences relative to the room temperature control (T-test, p-value <0.05). This experiment was performed once.

It has been shown that the closely related plant pathogen *Pseudomonas syringae* *pv.* *syringae* (*Pss*) down-regulates extracellular polysaccharides (EPS)-related genes when grown in king's B at 30°C compared to 20°C (Hockett et al., 2013). Therefore to assess if the reduced ability to form biofilms by *Pst*<sub>165K</sub> could be due to temperature-based effects on biofilm formation, bacteria were grown at room temperature or at 27°C. Both *Pst*<sub>165K</sub> and *Pst* pVSP1, displayed significantly higher planktonic growth at 27°C compared to room temperature at 48 and 72 hours (Fig. 3.5A). Additionally, growth at 27°C resulted in less biofilm formation for both strains (Fig. 3.5B). Based on this preliminary data it appears that higher temperatures can enhance growth after 48 hours in static cultures. A correlation matrix of data from Figure 3.6 indicates that planktonic growth at 72 hours was lower for *Pst* pDSK-GFPuv than for *Pst*<sub>165K</sub>, with *Pst* pVSP1 in the middle (Fig. 3.6). As previously mentioned, *Pst* pDSK-GFPuv forms more biofilm than *Pst*<sub>165K</sub> but less than *Pst* pVSP1 (Fig. 3.6). Modeling a multiple linear regression model to the data revealed a strong negative correlation between growth and biofilm formation (Fig. 3.6). These data suggest that the strain-dependent difference in biofilm formation could cause or be caused by a difference in planktonic growth in these static cultures.

The biofilm formation model presented in Figure 1.1 can be mapped to the data presented in this study (Fig. 3.7). *Pst* pVSP1 formed biofilms from 24 to 72 hours after which biofilm levels decreased, suggesting that the mature biofilm reached the dispersal stage of biofilm development (Fig. 1.1, 3.7). Similarly, in Figure 3.4B at room temperature, *Pst* pVSP1 formed biofilms up to 72 hours. However, when the temperature was raised to 27°C, biofilm was formed up to 48 hours, with biofilm

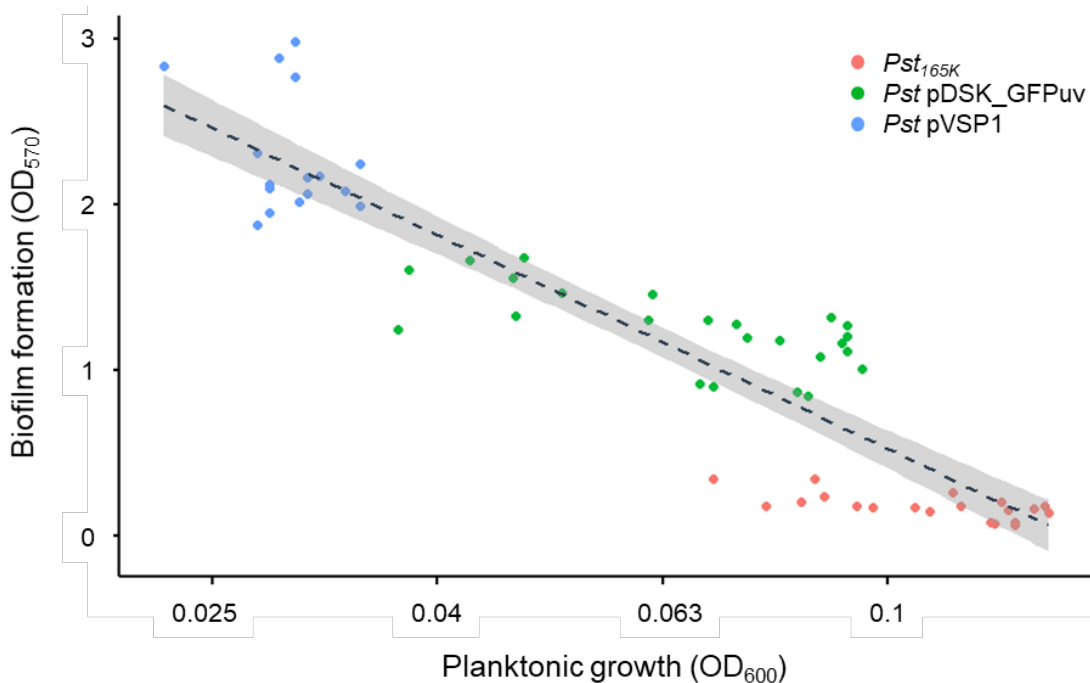


FIGURE 3.6: **Growth to biofilm formation correlation by strain.** Various strains of *Pst* were grown in intercellular-mimicking media (HIM) without agitation at room temperature for 72 hours in a 96-well plate. Each data point represents one biological replicate grown for 72 hours in HIM. The dashed line represents a multiple linear regression model (Growth  $\sim$  Biofilm formation) with an  $R^2$  value of 0.8655 and the shaded area represents a 95% confidence interval. This regression model suggests a strong negative correlation between planktonic growth and biofilm formation. The parameter for strain effects was not included during model selection as it did not contribute to significantly to growth.

levels decreasing after that, suggesting that at higher temperatures planktonic cell dispersal began earlier than at room temperature. Similarly, *Pst*<sub>165K</sub> grown at room temperature formed biofilms until 48 hours after which less biofilm was observed. These data suggest that when *Pst* strains form maximal biofilm early in the experiment, they reach the dispersal stage earlier as well.

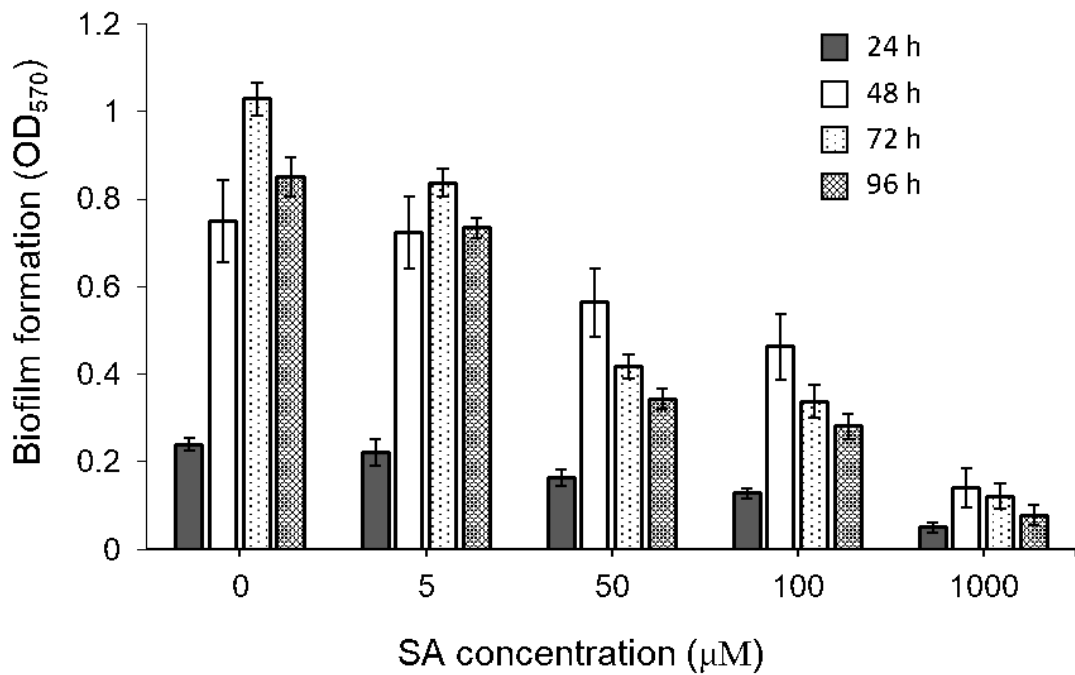


FIGURE 3.7: **Biofilm formation over time at various concentrations of SA.** *Pst* pVSP1 were cultured in HIM without agitation in a 96-well plate. At indicated time-points, plates were rinsed to remove unattached planktonic cells and biofilms were quantified with crystal violet. Each bar represents the mean of 4 wells and error bars indicate standard deviation. Different letters indicate significant differences between groups (ANOVA, p-value <0.05).



# Chapter 4

## Elucidating the ARR signaling pathway

### Preface & contributions

Experiments in this chapter were designed by Garrett Nunn and Robin Cameron. PTI-ARR experiments were conducted by Garrett Nunn. Angela Fufeng and Garrett Nunn collected tissue and quantified *in planta* bacterial levels for the RNA-Seq experiment. Garrett Nunn isolated the RNA, performed initial quality checks, sequencing was performed by GeneWiz. Garrett Nunn performed the RNA-Seq data analysis with help from Dr. Brian Golding. Figures in this section were created and designed by Garrett Nunn. All code used in this section can be found at [github.com/nunngm/RNA-sequencing](https://github.com/nunngm/RNA-sequencing).

## 4.1 Do PTI signaling components contribute to ARR?

Age-related resistance (ARR) is a strong defense response that occurs in mature plants (Kus et al., 2002). Currently, little is known about how mature plants become ARR-competent or the signaling pathway that results in a successful ARR response. It is possible that ARR may be a form of PAMP-triggered immunity (PTI) or employ components of the PTI signaling pathway. If ARR is a form of PTI, PTI signaling mutants would be defective for ARR. Preliminary studies suggested that the PTI mutants *bik1*, *efr-1* and *bak1-3* were partially ARR-incompetent compared to wild-type Col-0 (Dan-Dobre, 2018; Nunn, 2018). To confirm these observations, the ARR competence of various PTI mutants was examined by inoculating young and mature plants with *Pst*. Col-0 served as a positive control for ARR, and the SA-accumulation mutant *sid2-2* was included as a negative control for ARR (Kus et al., 2002). *In planta* bacterial levels of mature Col-0 were observed to be 9-fold lower than young plants. While the pattern recognition receptor (PRR) mutants, *efr-1* and *fls2* were partially ARR-defective as demonstrated by 2.9- and 4.7-fold lower *in planta* bacterial levels in mature compared to young plants (Fig. 4.1). The PTI signaling mutant, *bik1* was partially ARR-defective as demonstrated by 8-fold lower *in planta* bacterial levels in mature compared to young plants (Fig. 4.1), suggesting that *bik1* is partially ARR-competent. There was no significant difference between young and mature plants in the PTI signaling mutant *bak1-3*, suggesting that *bak1-3* was ARR-defective and BAK1 could be important for ARR (Fig. 4.1). The bacterial levels in young *bak1-3* plants were significantly lower than Col-0 and

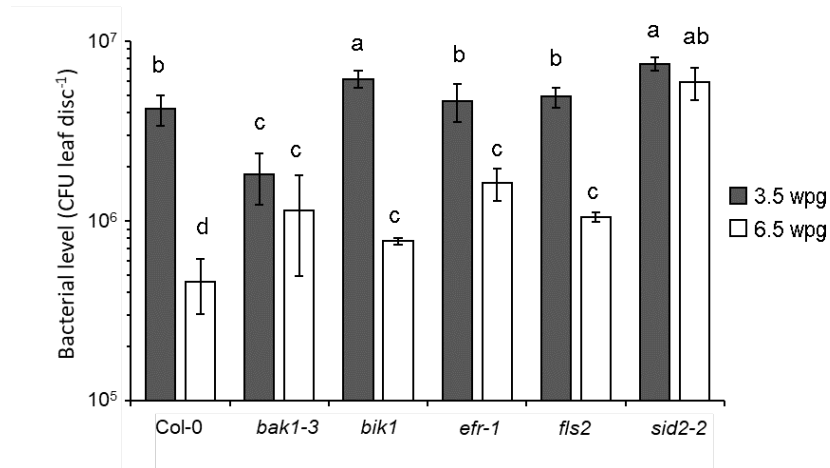


FIGURE 4.1: **ARR assay of various PTI mutants.** Plants were inoculated with  $10^6$  cfu ml<sup>-1</sup> *Pst* at either 3.5 or 6.5 weeks-post germination (wpg) and bacterial levels were quantified 3 days later. Different letters indicate significant differences (ANOVA, p-value < 0.05). This experiment was performed once.

bacterial levels in mature plants was significantly higher than Col-0 (Fig. 4.1). The reduced *Pst* levels in *bak1-3* is similar to previous research which demonstrated young *bak1-3* plants support significantly less bacteria than Col-0 (Fufeng, 2019). In summary, data from 2 experiments suggests that BIK1, EFR, and FLS2 contribute to ARR, while functional BAK1 is required for a successful ARR response.

## 4.2 RNA-sequencing to identify differentially expressed genes during ARR

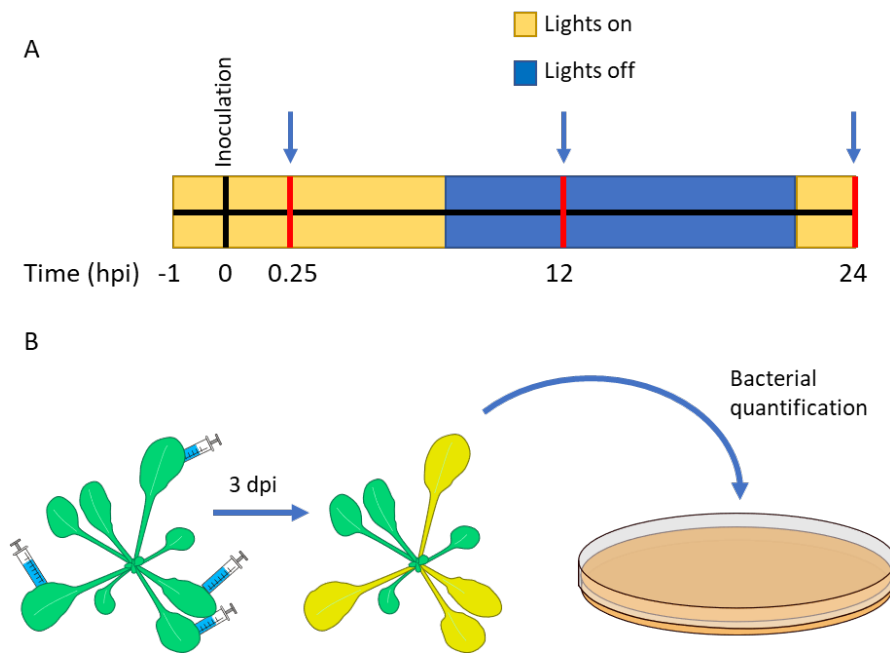


FIGURE 4.2: **RNA-sequencing experimental timeline.** Wild-type Col-0 were grown under short days (9 hour days) until plants were 3.5 or 6.5 weeks-post germination (wpg). Plants were inoculated with either 10 mM  $MgCl_2$  (mock) or  $10^6$  cfu  $ml^{-1}$  *Pst.* (A) At 0.25, 12, 24 and 36 hpi, leaf tissue was collected and flash frozen in liquid nitrogen. (B) At 72 hpi, *in planta* bacterial levels were quantified.

The popularity of RNA-sequencing has risen as the cost to perform RNA-Seq has fallen. RNA-Seq has been used to examine and found to be useful in understanding other resistance responses such as PTI and Effector-triggered immunity (ETI) (Howard et al., 2013; Mine et al., 2018). RNA-Seq was employed to identify differentially expressed genes in mature ARR-competent compared to young ARR-incompetent plants to discover genes that contribute to a successful ARR

response. Wild-type Arabidopsis (Col-0) were grown to either 3.5 or 6.5 wpg followed by inoculation with 10 mM MgCl<sub>2</sub> (mock) or *Pst*. At the indicated time-points (Fig. 4.2A) mock- or *Pst*-inoculated tissue was collected, and flash frozen on liquid nitrogen. To confirm that plants were ARR-competent, *in planta* bacterial levels were quantified in a subset of these plants (Fig. 4.2B). RNA was isolated from all samples for RNA-sequencing.

This experiment was performed twice and a strong ARR response was observed in both. In the first experiment, mature plants displayed a very strong ARR response (246-fold lower bacterial levels in mature compared to young plants). In the second experiment, mature plants exhibited a strong ARR response (64-fold lower bacterial levels in mature compared to young (Fig. 4.3). Therefore, experiment 1 was chosen for RNA-sequencing.

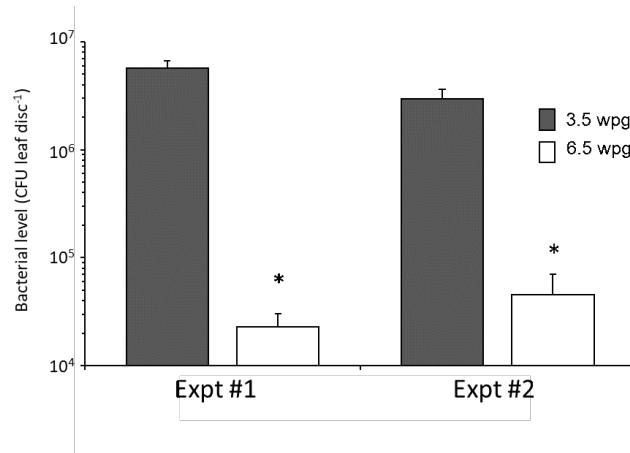


FIGURE 4.3: **Age-Related Resistance response for RNA-sequencing experiment.** Plants were inoculated with  $10^6$  cfu  $\text{ml}^{-1}$  *Pseudomonas syringae* *pv.* *tomato* at either 3.5 or 6.5 weeks-post germination (wpg) and bacterial levels were quantified 3 days later. Tissue for RNA-sequencing was collected 0.25, 12, 24 and 36 hours post-infection. Asterisks indicate significant differences (T-Test,  $p$ -value  $< 0.01$ ).

#### 4.2.1 Quality checking before sequencing

Before sequencing, several sample quality methods were used to ensure only high-quality samples were sent for sequencing. After RNA isolation, a nanodrop micro-volume spectrophotometer was used to determine the presence of protein contamination (A260/A280) or organic contaminants (A260/A230). Total RNA samples were examined for signs of RNA degradation by electrophoresis in 1% agarose. Following this, samples were shipped on dry ice to GeneWiz for RNA-sequencing. After shipping, 1  $\mu\text{l}$  of each RNA sample was run on an Agilent ScreenTape System to confirm that RNA integrity was not affected during transport (Fig. 4.4). Total RNA of *Arabidopsis* leaf tissue when run on a gel typically has two upper

bands for the larger cytosolic rRNAs (25S and 18S) and three smaller bands corresponding to the smaller organellar rRNAs (Keren et al., 2011). As the software built to determine RNA integrity number equivalent (RINe) values, was optimised for animal and bacterial samples, which only have the two upper cytosolic rRNA bands, an accurate determination of RINe is not possible. Due to this, the RINe calculated for plant leaf tissue is consistently lower than the RNA integrity number (RIN) generated from data collected by an Agilent Bioanalyzer 2100. For this reason, based on the recommendation of GeneWiz, any samples with a RINe value of  $\leq 4.0$  were excluded from RNA-sequencing (Tab. A4.1). Additionally, any sample which displayed signs of smearing of rRNA bands was removed (Fig. A4.2). For example, lane 6 (Fig. 4.4) is significantly higher quality than lane 5, since the 28S rRNA band in lane 5 is noticeably weaker than lane 6. Since mRNA would be enriched using the poly(A) enrichment method (mRNA would be removed from mixture solution and therefore purified) and there was little organic contamination in samples, the presence or absence of organic contaminants (Tab. A4.1) was not considered during sample selection.

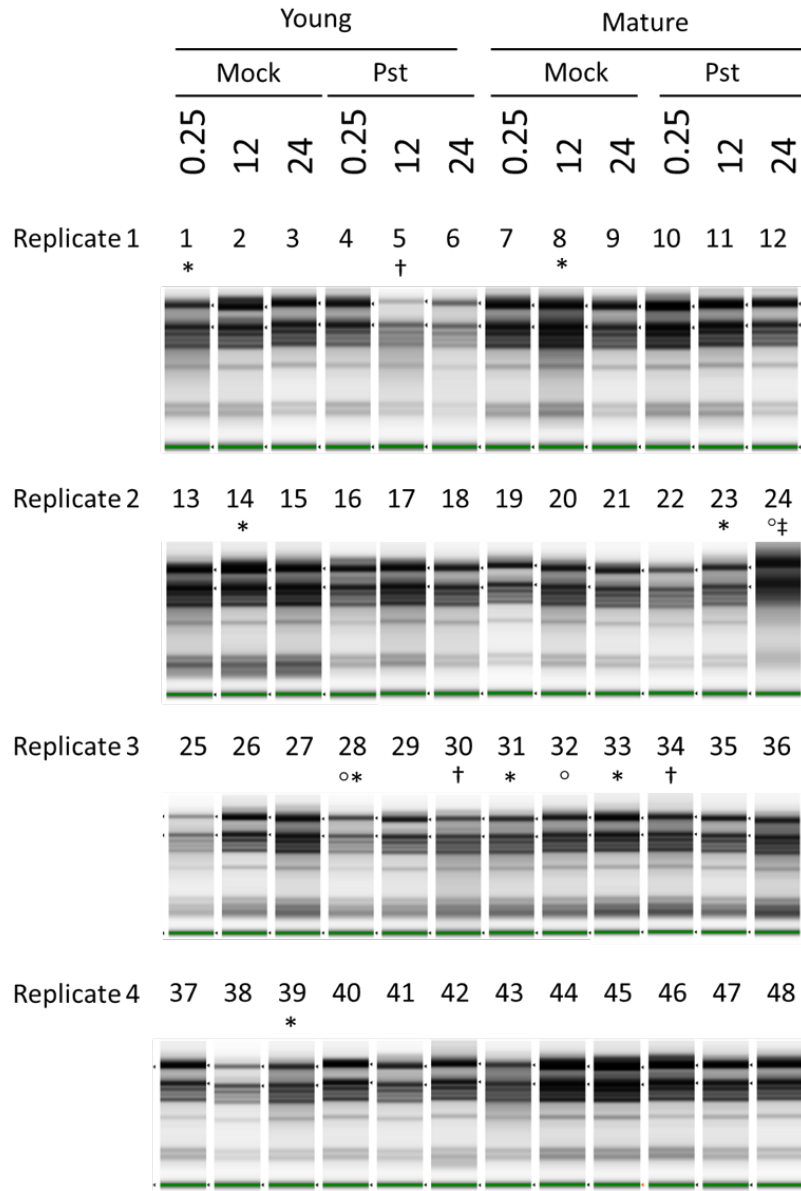


FIGURE 4.4: **RNA sample quality for RNA-sequencing.** Total RNA from leaf tissue of young or mature *Arabidopsis* plants inoculated with either  $MgCl_2$  or *Pst* was isolated using Trizol and purified on-column using a RNeasy minikit. RNA was run on 1% agarose at 100V for 1 hour. Asterisks (\*) indicate samples that met RNA-sequencing cut-offs but were not sequenced due to either lower RIN values or signs of degradation. Daggers (†) indicate samples with RIN values <4. Double daggers (‡) indicate samples with severe signs of degradation. Degree symbols (°) indicate samples with 260/230 values less than 1.75. Refer to Table A4.1 for more information.

Once the samples were sequenced, quality of the reads across each sample was assessed using fastqc, a quality control tool for high-throughput data. For the raw reads, the average phred quality score ranged from 35.7 to 35.9. A phred score is a measure of the quality of nucleobases generated by automated sequencing ranging from 1 (low quality) to 40 (high quality). A phred score of 30 indicates a 1 in 1000 probability of an incorrect base call and is generally considered to be a high-quality base. The percent of bases with phred scores  $\geq 30$  ranged from 92.7% to 93.6%. These quality scores demonstrate high quality reads even before trimming of adaptor sequences. Trimmomatic (Bolger et al., 2014) was used to trim off adapter sequences and low-quality base-pairs at 3' ends. After trimming, adapter sequences were only present in the last 5 base pairs at the 3' ends in 5% of reads, suggesting that reads were adequately trimmed for alignment.

For paired-end sequencing of 150 bp, a forward read and a reverse read are generated. The forward read is the first 150 bp of the DNA fragment starting from the 5' end, while the reverse read is the last 150 bp of the DNA fragment beginning from the 3' end. As these sequences are from the same DNA fragment together they are called a read pair. These read pairs are used together to determine the location of the mRNA transcript in the *Arabidopsis thaliana* (*Arabidopsis*) genome. Individually, low quality bases and adapters were removed from the reads. Trimmed read pairs were aligned to TAIR 10, the most recent full assembly of the *Arabidopsis* genome. For alignment, STAR was the aligner of choice as it is among the fastest and most accurate aligners currently available (Rapplee et al., 2019). After alignment, quality of aligned read pairs was analyzed using RSeQC, an RNA-seq quality control package (Wang et al., 2012). RSeQC generated a

mean inner distance plot for each sample (representative sample Fig. 4.5A). The mean mRNA insert size (the number of bp between the end of one read and the beginning of another) was negative, suggesting the reads were overlapped. Overlapping reads are often caused by short mRNA transcripts. To assess if these short transcripts were due to mRNA degradation or fragmentation of the RNA during library preparation, coverage uniformity was assessed over the length of transcripts (Fig. 4.5B). In 7/36 samples, the 5' end had a slightly lower gene body coverage, suggesting minor RNA degradation in these samples. These samples were all from mature plants and were evenly distributed amongst batches where RNA isolation was completed at different times, therefore the batches were all of similar quality. However, the other 29 samples had uniformly high coverage across the gene body indicating there was little to no degradation of RNA in these samples (Fig. 4.5B). Taken together, this suggests that the short transcripts were probably generated due to other factors and not due to mRNA degradation. One possible cause could be fragmentation during library preparation. Communication with GeneWiz confirmed that the samples were fragmented prior to sequencing.

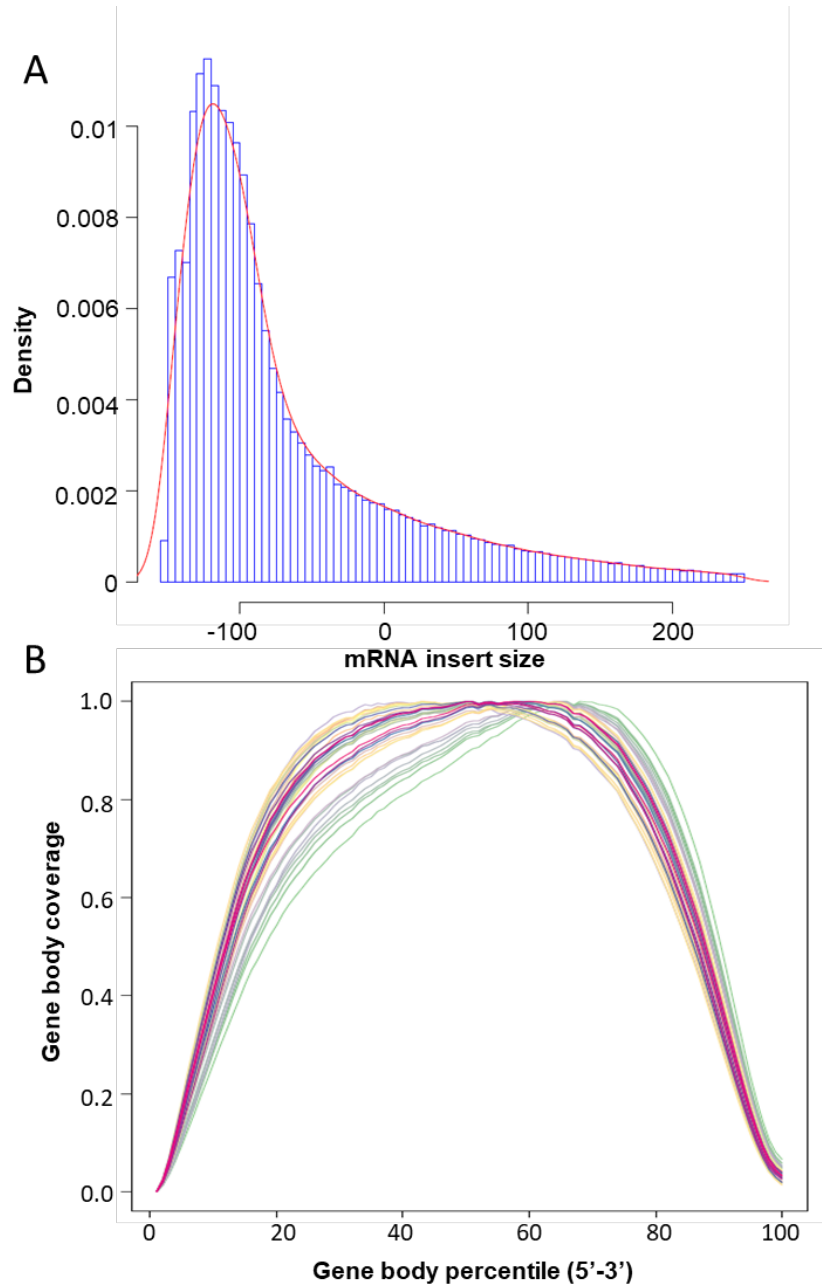
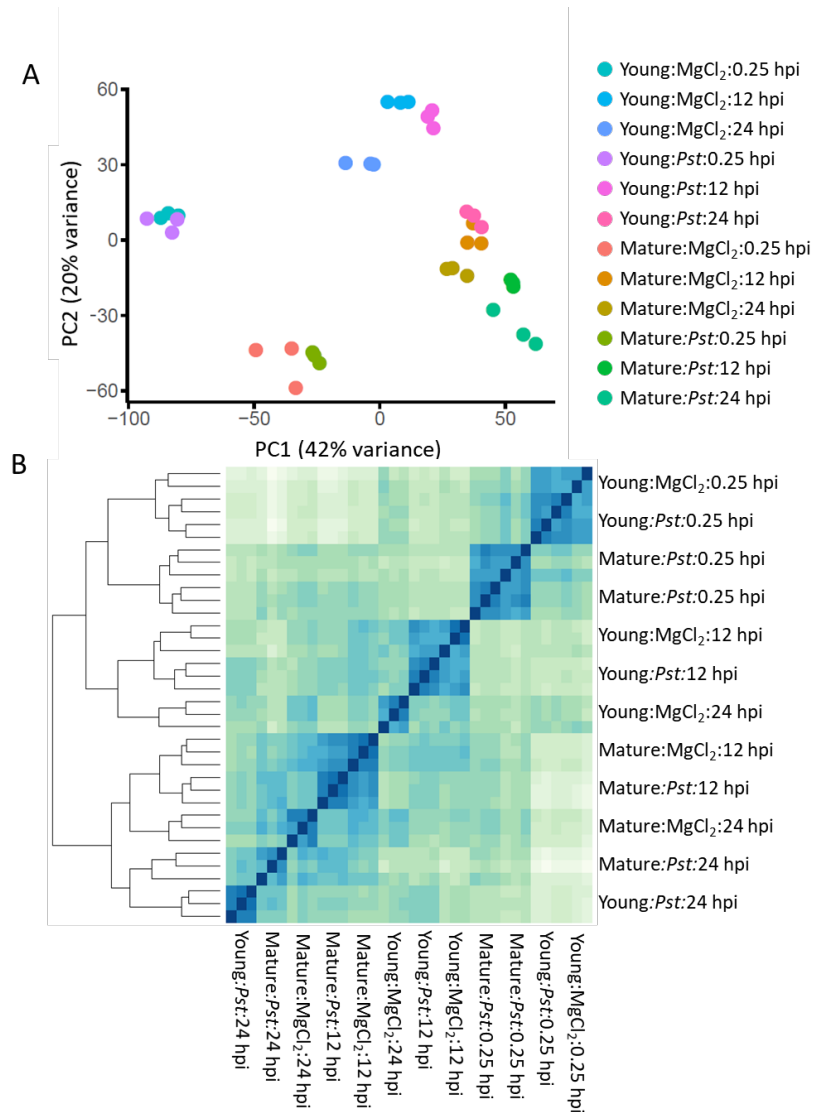


FIGURE 4.5: **RNA-seq quality checks.** (A) mRNA insert size density plot of a representative sample (Mature : MgCl<sub>2</sub> : 0.25 hpi : sample 2 : read 1). (B) Gene body coverage plot of all samples sequenced.

#### 4.2.2 Sample dispersion of young and mature plants responding to *Pst*

After assessing the quality of the reads, the number of reads pairs aligned to a given gene was counted using HTseq-count, a program that assesses the features of each read pair and determines the number of read pairs aligned to each gene (Anders et al., 2015). Read counts were normalised using the DESeq2 method for differential expression analysis using individual sample size factors to normalize count data (Love et al., 2014). A table of counts was generated and principal component analysis (PCA) was conducted on the top 10,000 genes by variance across samples to visualise the effect of experimental variables and batch effects. Samples within treatment groups clustered together and there were no major outliers among the samples (Fig. 4.6). The only samples from different treatments that grouped together were young mock- and *Pst*-inoculated plants at 0.25 hpi, suggesting these plants responded similarly (Fig. 4.6A). Next, a distance comparison between each sample was calculated by comparing the normalized read counts of every gene. This was used to create a distance matrix which then underwent hierarchical clustering to determine which samples had the highest similarity (Fig. 4.6B). This supported the results of the PCA, finding that young plant samples inoculated with mock- or *Pst* at 0.25 hpi grouped together. The hierarchical cluster analysis also revealed that for young or mature plants, samples at 0.25 hpi and 12 hpi grouped together, while samples at 24 hpi did not. This suggests that the highest level of differential gene expression occurred at 24 hpi, with less differences in gene expression at 0.25 and 12 hpi.



**FIGURE 4.6: RNA-sequencing sample dispersion plots.** Tissue from plants inoculated with *Pseudomonas syringae* *pv.* *tomato* at 3.5- and 6.5-weeks-post germination was collected at 0.25, 12 and 24 hpi. RNA-sequencing reads were aligned to the *Arabidopsis* genome (TAIR10) and counted using STAR and HTSeq respectively. After reads were normalized with DESeq2, principal component analysis (A) and hierarchical clustering (B) was performed on samples. Each row/column of the distance matrix (B) represents one sample. All treatment groups clustered together therefore for clarity the label was only shown once for every three samples.

### 4.2.3 Modeling and differential gene expression analysis during Age-Related Resistance

The purpose of this RNA-Seq experiment was to identify ARR-specific genes by comparing the transcriptomes of young ARR-incompetent and ARR-competent mature plants using DESeq2 (Love et al., 2014). The initial analysis observed, the 15 most up- and down-regulated genes in response to *Pst* in mature plants (Fig. A4.2,A4.3), which was compared to genes in which the young response to *Pst* appeared to differ. Two issues arose in this analysis, (i) gene expression changed significantly across timepoints and (ii) direct comparison of *Pst*-inoculated young and mature plants does not take into consideration the plant response to the inoculation procedure. To address the first issue, samples were analyzed based on hours post-inoculation (hpi). This was the simplest way to avoid addressing how expression changed over the course of the experiment, but it is a shortcoming that will be addressed in the future. However, this is also a shortcoming in this analysis as the speed at which genes are expressed in response to *Pst*, cannot be analyzed. To identify which genes are differentially expressed in response to *Pst*, a model was used for DESeq2 analysis to first analyze how genes expression changed in response to *Pst* compared to mock inoculation and then compare this response between age groups.

To validate the RNA-Seq data, the expression of a number of genes known to be involved in ARR was examined. ICS1 was shown to be induced in response to *Pst* in young and mature plants as demonstrated by RNA gel blot and RT-PCR analysis (Rusterucci et al., 2005; Wilson et al., 2017). Similar results were

observed in the ARR RNA-seq dataset, where ICS1 transcript accumulation at 24 hpi was enhanced in young (3.4-fold) and mature (5.5-fold) plants compared to the corresponding mock-inoculated plants (Fig. 4.7A). Interestingly, SOC1 expression did not appear to respond to *Pst* in young plants but was induced in mature plants (1.7-fold) at 24 hpi (Fig. 4.7C). However, JAZ10, a protein involved in attenuating the response to jasmonic acid (JA) (Moreno et al., 2013), was strongly induced in response to *Pst* young (77-fold) compared to mature plants (4-fold) (Fig. 4.7B). Interestingly, JAZ10 expression is induced in response to *Pst* in a coronatine-dependent manner in young plants (Demianski et al., 2012), suggesting that *Pst*-produced coronatine is not affecting mature *Arabidopsis* plants. WRKY53, a regulator involved in Salicylic acid (SA) response pathways, was induced in response to *Pst* at 12 (1.7-fold) and 24 (2.3-fold) hpi in mature, but not young plants (Fig. 4.7D). As previous research demonstrated that WRKY53 expression is SA-inducible (Sarkar et al., 2018) and SA accumulates in mature but not young plants at 24 hpi (Cameron and Zaton, 2004; Carviel et al., 2014; Wilson et al., 2017), SA may act as signal to up-regulate WRKY53 mature plants during ARR.

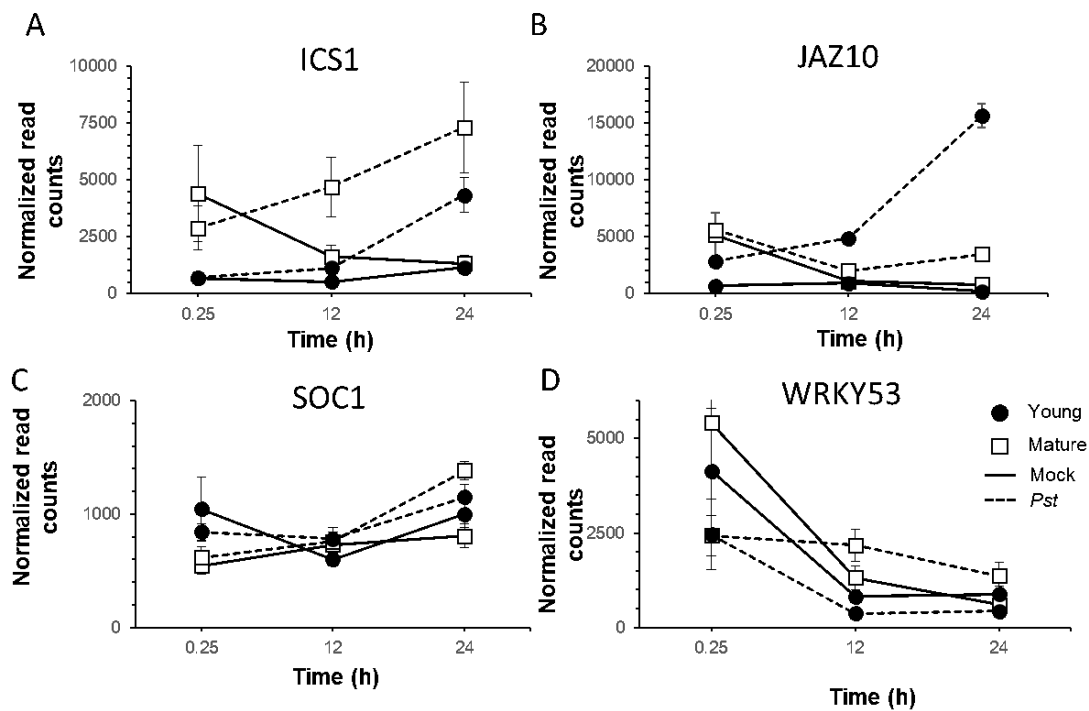


FIGURE 4.7: **Differential gene expression during infection of young and mature plants.** Plants were inoculated with  $10^6$  cfu  $\text{ml}^{-1}$  *Pseudomonas syringae pv. tomato* at either 3.5- or 6.5-weeks post-germination (wpg). Tissue for RNA-sequencing was collected at 0.25, 12, and 24 hours post-infection. Reads were aligned to the Arabidopsis genome (TAIR10) using STAR and counted using HT-Seq. Read counts were normalized using DESeq2. A&C represent genes in which young and mature plants responded similarly to *Pst*. B&D represent genes where young and mature plants responded differently to *Pst*. Each data point represents the average of three biological replicates and error bars represent standard deviation.

#### 4.2.4 Functional analysis of genes expressed or suppressed during Age-Related Resistance

To gain insight into the nature of age-related differentially expressed genes, comparative GO analysis was performed. Genes more highly induced in response to *Pst* in mature plants than young plants at 0.25 hpi were associated with the gene ontology (GO) terms, signal transduction, response to auxin, response to gibberellin, cell surface receptor signaling pathways, defense response, and phenylpropanoid metabolic processes. Genes more highly induced in response to *Pst* in young plants than mature plants at 0.25 hpi were associated with the GO terms, response to wounding, response to jasmonic acid, defense response, response to other organisms, regulation of defense response, response to oxidative stress, carbohydrate derivative transport and cellular carbohydrate metabolic process. At other timepoints, genes associated with the GO terms, regulation of defense were more highly expressed in response to *Pst* in mature plants than young plants at 12 hpi, while at 24 hpi, genes associated with the GO term defense response to bacteria, were more highly expressed in response to *Pst* in mature plants compared to young plants. The relative expression of genes related to the GO terms regulation of defense response at 12 hpi and defense response to bacteria at 24 hpi was calculated. Hierarchical clustering was then performed based on the relative expression pattern of these genes (Fig. 4.8). Genes in Clade I (Fig. 4.8A) represent those associated with the GO term, regulation of defense. This clade contained JAZ3/6/8/10, in which the change in expression in response to *Pst* was age dependent. These proteins were previously shown to be expressed in response to *Pst*

in a coronatine-dependent manner in young plants (Demianski et al., 2012).

Clade II (Fig. 4.8B) contains genes associated with the GO term defense response to bacterium which clustered based on an increase in expression in response to *Pst* in mature ARR-competent, but not young ARR-incompetent plants. Genes in this clade include the glutathione S-transferase proteins GSTF6 and GSTF7 (Fig. 4.8). GSTF6 was previously be found to be important for camalexin biosynthesis and therefore may be involved in DHCA biosynthesis (Su et al., 2011) and could contribute to ARR, as Dihydrocamalexin acid (DHCA) was demonstrated to be involved in ARR (Kempthorne, 2018).

Clade III (Fig. 4.8B) contains genes which clustered based on a decrease in expression in response to *Pst* in young ARR-incompetent plants but an increase in expression in response to *Pst* in mature ARR-competent plants. This clade includes another glutathione S-transferase, GSTF2, which is a putative SA-binding protein involved in defense (Manohar et al., 2015). Previous research demonstrated that GSTF2 was induced after 24 hours post inoculation with avirulent *Pst* or treatment with SA via soil drench (Lieberherr et al., 2003).

Clade III also contains several other genes associated with the GO term defense response such as an ATP-binding cassette transporter pleiotropic drug resistance8 (PDR8) and the transcription factor MYB51. MYB51 is involved in regulation of indole glucosinolate biosynthesis by up-regulating CYP79B2 and CYP79B3 (Gigolashvili et al., 2007). As the *cyp79b2 cyp79b3* double mutant is partially ARR-defective (Kempthorne, 2018), this suggests that MYB51 could contribute to ARR

through activation of CYP79B2 and CYP79B3. The ATP-binding cassette transporter PDR8 is involved in transport of defence compounds out of the plant cell (reviewed in Chapter 1.8.3). The induction of PDR8 in mature but not young plants suggests that transport of defence compounds into the intercellular space contributes to ARR. Interestingly, this clade also includes the lectin receptor kinase LecRK-IV.3, which was induced at 12 hpi in response to *Pst* in mature but not young plants. LecRK-IV.3 was induced in response to SA and overexpression conferred enhanced resistance to the fungal pathogen *B. cinera*, suggesting that LecRK-IV.3 could also contribute to defense against *Pst* (Huang et al., 2013).

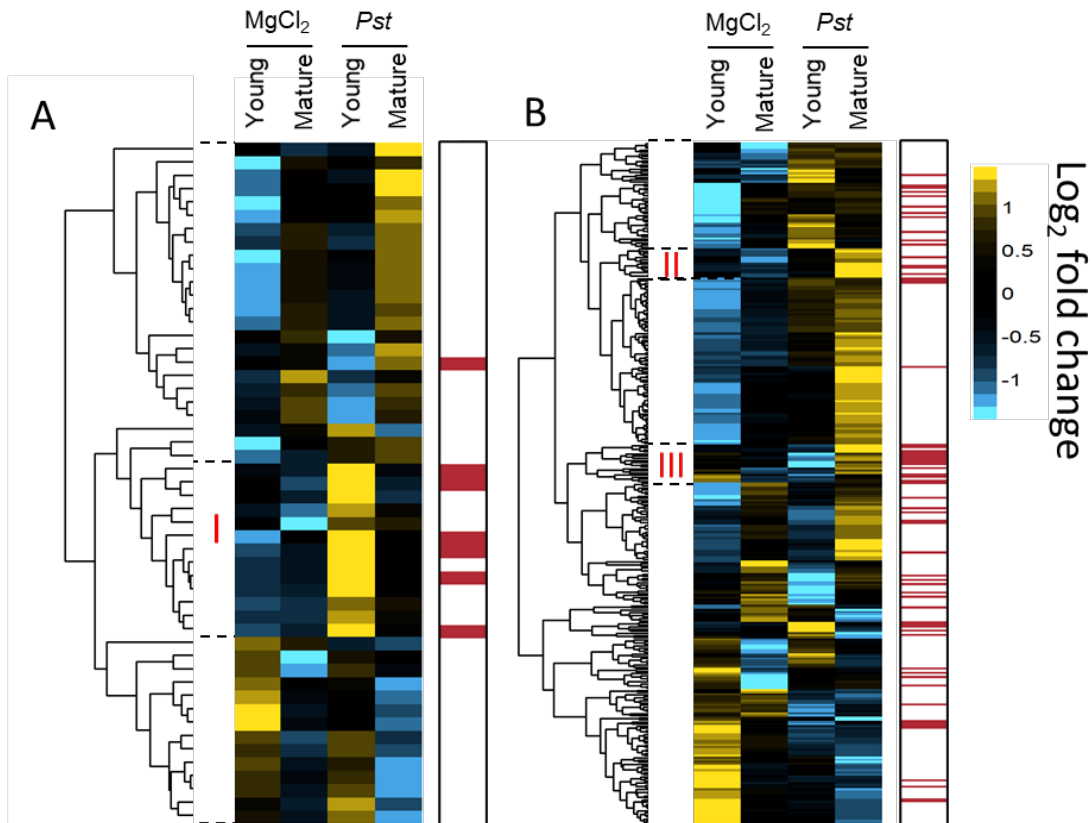


FIGURE 4.8: **Functional analysis of defense-related genes in response to *Pst* in young and mature plants.** Hierarchical clustering (blue/yellow heatmap) of relative expression of GO term genes, regulation of defense at 12 hpi with MgCl<sub>2</sub> or *Pst* (A) and GO term genes, defense response to bacterium at 24 hpi with MgCl<sub>2</sub> or *Pst* (B). Genes in which plant age significantly contributed to the change in expression in response to *Pst* are represented by red lines to the right of each heatmap (FDR < 0.05). Each row represents a different gene. Clades of interest are indicated by dashed lines. The phylogeny tree beside each heatmap demonstrates the similarity in expression patterns among these genes.

# Chapter 5

## Discussion

### 5.1 The role of AlgU during *Pst* growth in the leaf intercellular space-mimicking environment

The effect of Salicylic acid (SA) on the growth and biofilm formation of *Pseudomonas syringae* pv. *tomato* (*Pst*) was investigated using the *Pst* alginate production mutant *Pst*<sub>165K</sub>  $\Delta$ *algD* and the alginate-deficient ECF sigma factor mutant *Pst*<sub>165K</sub>  $\Delta$ *algU mucAB*  $\Delta$ *algD* in leaf intercellular space-mimicking media (HIM). Over 72 hours in liquid culture, the *Pst*<sub>165K</sub>  $\Delta$ *algU mucAB*  $\Delta$ *algD* mutant grew less well than wild type and *Pst*<sub>165K</sub>  $\Delta$ *algD*. Whereas in rich media (king's B) *Pst*<sub>165K</sub>  $\Delta$ *algU mucAB*  $\Delta$ *algD* grew similarly to wild type and *Pst*<sub>165K</sub>  $\Delta$ *algD*. The observed growth difference between *Pst*<sub>165K</sub>  $\Delta$ *algU mucAB*  $\Delta$ *algD* and wild-type *Pst*<sub>165K</sub> in HIM, but not king's B suggests that a nutrient deficiency in HIM impacts growth in *Pst*<sub>165K</sub>  $\Delta$ *algU mucAB*  $\Delta$ *algD*. Previously Kim et al. (2009) demonstrated the nutrient deficiency of the leaf intercellular space-mimicking minimal media (HIM)

by growing *Pst* to stationary phase in leaf intercellular space-mimicking minimal media (HIM) then sub-culturing in fresh media. Each subsequent subculture of *Pst* in fresh HIM media resulted in a reduced growth rate suggesting, a nutrient deficiency in HIM (Kim et al., 2009). To identify the deficient nutrient, *Pst* was grown in a continuous flow culture in HIM to stationary phase, after which the culture was supplemented with various nutrients. Growth would spike when the stationary phase culture was supplemented with iron, but not other nutrients (Kim et al., 2009), suggesting that HIM may contain less iron than king’s B media. The slow reduction in growth rate over subsequent subcultures could be due to release of *Pst*-stored iron to supplement growth. *Pst* is thought to sequester iron while growing in iron-rich media such as king’s B media, as genes involved in iron storage are induced in iron rich media (Buell et al., 2003; Butcher et al., 2011). Iron sequestration is important for the growth of *Pseudomonas aeruginosa*, as growth in higher iron concentrations enhanced the growth rate of *P. aeruginosa* when transferred to iron-deficient growth media (Eschelman et al., 2017). During the experiments presented in this thesis, *Pst* was cultured in a high-iron growth media (king’s B), perhaps allowing it to sequester iron before it was transferred to HIM media for growth assays. This suggests that wild-type *Pst*<sub>165K</sub> could more effectively sequester iron compared to *Pst*<sub>165K</sub>  $\Delta algU$  *mucAB*  $\Delta algD$ , thereby leading to the enhanced growth rate observed for wild-type *Pst*<sub>165K</sub>.

The reduced growth rate in HIM of *Pst*<sub>165K</sub>  $\Delta algU$  *mucAB*  $\Delta algD$  mutants was probably not due to mutations in the MucA and MucB genes as both of these gene products repress AlgU activity and AlgU is deleted in this strain (Xie et al., 1996; Mathee et al., 1997). The single mutant *Pst*<sub>165K</sub>  $\Delta algD$  grows at the same rate as

wild-type *Pst*<sub>165K</sub> in HIM suggesting that AlgD does not contribute to the growth deficiency of *Pst*<sub>165K</sub>  $\Delta$ *algU mucAB  $\Delta$ algD*. Therefore, the growth rate reduction of *Pst*<sub>165K</sub>  $\Delta$ *algU mucAB  $\Delta$ algD* could be due to the deletion of AlgU. This makes sense given that AlgU regulates many cellular processes including induction of genes involved in mobilisation of iron and suppression of genes involved in motility (Markel et al., 2016) both of which have been implicated in affecting growth rate.

The preceding paragraphs suggest that insufficient iron in HIM may have reduced the growth of *Pst*<sub>165K</sub>  $\Delta$ *algU mucAB  $\Delta$ algD* and deletion of AlgU could be the reason *Pst*<sub>165K</sub>  $\Delta$ *algU mucAB  $\Delta$ algD* grew poorly in HIM. It is possible that AlgU positively regulates iron storage/release in *Pst*<sub>165K</sub>, however little is known about iron storage/release systems in *Pst*. Fortunately, *P. aeruginosa* iron storage/release systems have been well characterized. BACTERIOFERRITIN B (BfrB) is thought to perform several functions including catalyzing the oxidation of water-soluble accessible iron (Fe<sup>2+</sup>) to inaccessible oxidized iron (Fe<sup>3+</sup>) to sequester iron, followed by forming an interlaced structure around the oxidized iron to store it and accepting electrons to reduce oxidized iron back into usable Fe<sup>2+</sup> when iron is needed by the cell (Andrews et al., 2003; Liu and Theil, 2005; Wang et al., 2015). BFR-ASSOCIATED FERREDOXIN (Bfd) is thought to play a role in iron release, as studies *in vitro* demonstrate that Bfd interacts with BfrB leading to the release of BfrB-stored iron (Wang et al., 2015). Additionally *in vitro* studies indicate that both BfrB and Bfd are required by *P. aeruginosa* for enhanced growth in low iron media after bacteria are transferred from a high-iron culture to low-iron culture (Eschelman et al., 2017). This data demonstrates that in *P. aeruginosa*, Bfd and BfrB are required for growth in iron-limited media.

It is possible that the *P. syringae* orthologs of BfrB and Bfd function like those in *P. aeruginosa* to promote growth in iron limiting conditions. Like in *P. aeruginosa*, the *Pst* orthologs PsBFRB (PSPTO\_4160) and PsBFD (PSPTO\_4159) are adjacent to one another (Buell et al., 2003). A MUSCLE alignment performed for this thesis found that the nucleotide sequences of *P. aeruginosa* PAO1 and *Pst* are 78% identical for BfrB and 71% identical for Bfd (Stover et al., 2000; Buell et al., 2003; Edgar, 2004), providing support that these *Pst* genes are *P.aeruginosa* orthologs. Additional evidence supporting the idea that PsBFRB and PsBFD are required for growth in iron limiting media was obtained by expression analysis. Similar to *P. aeruginosa* (Palma et al., 2003), expression of PsBFRB and PsBFD was elevated (143-fold and 408-fold respectively) in iron-limiting compared to iron-rich media (Bronstein et al., 2008). Similar expression profiles and nucleotide sequences of *P. aeruginosa* and *Pst* BfrB and Bfd suggests these proteins function in iron storage, sequestration and release in *Pst*. A connection between AlgU and PsBFRB and PsBFD was demonstrated when AlgU overexpressing *Pst*<sub>165K</sub> was grown in rich king’s B media and up-regulation of PsBFD and down-regulation of PsBFRB, was observed (Markel et al., 2016). Furthermore, 23 iron- and siderophore-related genes were up-regulated, while only 6 were down-regulated by AlgU overexpression (Markel et al., 2016). Taken together, these data support a model in which in iron-limited media AlgU activates expression of PsBFD and mobilisation of stored iron that is necessary for growth of *Pst* in iron-limiting media. This could be tested by supplementing HIM media with iron to determine if iron alleviates the growth difference between wild-type *Pst*<sub>165K</sub> and *Pst*<sub>165K</sub>  $\Delta algU$  *mucAB*  $\Delta algD$ .

It is important not to equate growth in leaf intercellular space-mimicking media with growth in the leaf intercellular space because they are similar, but not identical (Huynh et al., 1989). Recently, a transcriptome study revealed that global gene expression of *Pst* during *in vitro* growth in king’s B or HIM was significantly different from gene expression during *in planta* growth providing evidence that HIM and *in planta* growth conditions are very different (Nobori et al., 2018).

## 5.2 The role of alginate in protecting *Pst* against the growth inhibitory effects of SA

To examine the role of alginate in protecting bacteria from the effects of SA during plant defense, growth of wild-type, *Pst*<sub>165K</sub>  $\Delta$ *algD* and *Pst*<sub>165K</sub>  $\Delta$ *algU mucAB*  $\Delta$ *algD* was examined in leaf intercellular space-mimicking media (HIM). *Pst*<sub>165K</sub>  $\Delta$ *algU mucAB*  $\Delta$ *algD* was twice as sensitive to the growth inhibitory effects of SA than wild-type *Pst*<sub>165K</sub> and *Pst*<sub>165K</sub>  $\Delta$ *algD*. *Pst*<sub>165K</sub>  $\Delta$ *algU mucAB*  $\Delta$ *algD* was more sensitive to the bactericidal effects of SA than wild-type *Pst*<sub>165K</sub> and *Pst*<sub>165K</sub>  $\Delta$ *algD*. This suggests that the regulatory activity of AlgU, but not the ability to produce alginate, is required to protect *Pst* against the antimicrobial effects of SA.

One possible explanation for the enhanced sensitivity to SA of *Pst*<sub>165K</sub>  $\Delta$ *algU mucAB*  $\Delta$ *algD* could be due to the absence of AlgU and therefore an inability to express multi-drug efflux pumps. AlgU expression has been implicated in expression of multi-drug efflux pumps as AlgU overexpression in *Pst*<sub>165K</sub>  $\Delta$ *algU mucAB* induced expression of MexE (Markel et al., 2016). In other bacteria, multi-drug

efflux (MEX) pumps contribute to antibiotic resistance by expelling antibiotics from the cytoplasm to the outside of the cell and it is possible that MEX pumps perform a similar function in *Pst* (Aeschlimann, 2003). Some MEX pumps are involved in the response to plant defensive phenolic acids. For example, *Erwinia chrysanthemi* expressed AcrA, an ortholog of *P. aeruginosa* MexA, in response to treatment with salicylic acid, benzoic acid and trans-cinnamic acid (Ravirala et al., 2007). In *P. aeruginosa*, the MexAB-OprM pump is the MEX pump with the broadest antibiotic substrate specificity (Aeschlimann, 2003). In *Pst*, deletion of the MexAB ortholog led to enhanced sensitivity when cultured in the presence of a number antimicrobials such as ampicillin, fusaric acid and chloramphenicol (Stoitsova et al., 2008). Deletion of MexAB in *Pseudomonas syringae pv. syringae* (*Pss*) resulted in reduced bacterial success on the surface of bean leaves compared to wild type (Stoitsova et al., 2008). Additionally, analysis of the *in planta* transcriptome of *Pst* demonstrated that the MEX pump MexEF-OprN was expressed during PAMP-triggered immunity (PTI) and Effector-triggered immunity (ETI) (Nobori et al., 2018). Previous research revealed that during both PTI and ETI, SA accumulates in the intercellular space (Carviel et al., 2014; Fufeng et al., 2020). These studies combined suggest that bacteria in the leaf intercellular space could express MEX pumps to expel antimicrobials like SA from the bacterial cytoplasm. In the future, it would be useful to investigate if MexA and MexE are expressed in *Pst* in response to media containing SA, as this could link MEX pump expression to SA and provide evidence that *Pst* protects itself from the antimicrobial effects of SA by expelling it from the cell.

In *Pss*, AlgU regulatory activity contributes to protecting *Pss* from several environmental stressors, including oxidative stress (Keith and Bender, 1999). *Pst* AlgU regulatory activity may also perform this function by reducing the oxidative effects of high concentrations of intercellular SA. Intercellular washing fluids collected from *Arabidopsis* responding to *Pst* with an ARR response contain 50 to 100  $\mu\text{M}$  SA (Wilson et al., 2017). Similar concentrations of SA result in oxidative stress in *Escherichia coli* (Cattò et al., 2017).

### 5.3 Exploring conditions that effect *Pst* biofilm formation

One of the original objectives of this thesis was to obtain support for *in planta* biofilm-like aggregate formation data which suggested that AlgD and AlgU contribute to *Pst* biofilm formation during infection, by examining *in vitro* biofilm formation by *Pst*<sub>165K</sub>  $\Delta algD$  pDSK-GFPuv and *Pst* pDSK-GFPuv. However these *Pst* strains were found to produce little biofilm in these experiments, therefore *Pst*<sub>165K</sub> biofilm formation was compared to the strain used in previous experiments *Pst* pVSP61, and the strain used to examine *in planta* biofilm-like aggregate formation, *Pst* pDSK-GFPuv. *Pst*<sub>165K</sub> was observed to produce less biofilm compared to *Pst* pVSP1 and *Pst* pDSK-GFPuv.

Biofilm formation by *Pst*<sub>165K</sub>  $\Delta algD$  and *Pst*<sub>165K</sub>  $\Delta algU$  *mucAB*  $\Delta algD$  and *Pst*<sub>165K</sub> were similarly low and due to the insufficient sensitivity of the biofilm formation assay, it was not possible to compare biofilm formation in *Pst*<sub>165K</sub>, *Pst*<sub>165K</sub>

$\Delta algD$  and  $Pst_{165K} \Delta algU mucAB \Delta algD$ .

Variability in biofilm formation among different isolates of the same species has been well documented in *E. coli* (González et al., 2017), *Bacillus cereus* (Kwon et al., 2017) and in some *Pseudomonads* including *P. aeruginosa* and *Pst* (Ude et al., 2006). All three *Pst* strains in this thesis are descendents from the same *Pst* DC3000 strain originally isolated by Diane Cuppels (Cuppels, 1986) and yet there is strain-to-strain variability. One reason for this variability could be due to differences in growth rates. During biofilm assays in which bacteria are cultured in HIM without agitation, planktonic  $Pst_{165K}$  cells had a faster growth rate compared to  $Pst_{165K} \Delta algD$  and  $Pst_{165K} \Delta algU mucAB \Delta algD$ , but formed less biofilm, suggesting there is a trade-off between planktonic growth and biofilm formation. The faster growth rate of  $Pst_{165K}$  (also known as PS1) could be due to a 165 Kb duplication, which is associated with a faster planktonic growth rate in minimal media, compared to *Pst* without this duplication (Bao et al., 2014). However, this 165 Kb duplication had no effect on bacterial growth in tomato (Bao et al., 2014). Bao et al. (2014) suggest that the duplication occurred spontaneously and has been maintained because of the faster growth rate. None of the genes present in the 165 Kb duplication are known suppressors of biofilm formation. Therefore, reduced biofilm formation in  $Pst_{165K}$  could be due to the faster growth rate of planktonic cells.

Another possibility for what causes the difference in biofilm formation is the presence or absence of plasmids in each strain as high-copy number plasmids have been associated with enhanced biofilm formation ( 2.2-fold) in *Escherichia coli*

(Mathlouthi et al., 2018). *Pst*<sub>165K</sub> does not carry a plasmid, while *Pst* pVSP1 carries pVSP1 which originates from pVS1 a low-copy-number *P. aeruginosa* plasmid (Itoh et al., 1984; Kunkel et al., 1993) and *Pst* pDSK-GFPuv carries pDSK-GFPuv a high-copy number plasmid from *P. syringae* (Keen et al., 1988; Wang et al., 2007; Bao et al., 2014; Markel et al., 2016). If high plasmid copy number was associated with enhanced biofilm formation like it is in *E. coli* (Mathlouthi et al., 2018), the strain with the highest copy number plasmid would form the most biofilm. However, this was not the case, as *Pst* pVSP1, containing a low copy number plasmid, formed more biofilm than the high copy number strain *Pst* pDSK-GFPuv. Additionally, biofilm formation of *Pst*<sub>165K</sub>  $\Delta$ algD (no plasmid) and *Pst*<sub>165K</sub>  $\Delta$ algD pDSK-GFPuv (with plasmids) was very similar, suggesting that plasmid copy-number probably does not affect biofilm formation and therefore does not explain the differences in biofilm formation observed between *Pst*<sub>165K</sub>, *Pst*<sub>165K</sub>  $\Delta$ algD and *Pst*<sub>165K</sub>  $\Delta$ algU *mucAB*  $\Delta$ algD.

While carrying out biofilm assays, temperature effects on biofilm formation were observed. Data presented in this thesis suggests that independent of strain, higher planktonic growth and lower biofilm formation was associated with higher temperatures. In *Pst* pVSP1 cultured without shaking at room temperature (22 to 24°C), total adhered biomass peaked at 72 hours and then declined by 96 hours (this thesis and Wilson et al., 2017), while at 27°C, adhered biomass peaked at a lower level than at room temperature after just 48 hours and declined by 72 hours, suggesting that higher temperatures not only promote less biofilm formation, but also speeds up the biofilm formation cycle (planktonic cells to biofilm formation to dispersal of planktonic cells).

At room temperature (22 to 24°C), *Pst*<sub>165K</sub> biofilm formation peaked at 48 hours, which is similar to *Pst* pVSP1 grown at 27°C. Additionally, the amount of biofilm formed at 48 hours by *Pst* pVSP1 and *Pst*<sub>165K</sub> cultured at 27°C, was similar. The similarities of *Pst*<sub>165K</sub> at room temperature and *Pst* pVSP1 at 27°C suggests a similar cause for the lower level of biofilm formation. Moreover, during biofilm assays, planktonic growth of *Pst* pVSP1 at 27°C was similar to planktonic growth of *Pst*<sub>165K</sub> at room temperature (22 to 24°C). This suggests a link between biofilm formation and the growth rate of planktonic cells.

These data support a connection between growth rate of planktonic cells and biofilm formation. As mentioned above *Pst* pVSP1 formed abundant biofilms after 72h with fewer planktonic cells, while *Pst*<sub>165K</sub> formed little biofilm with abundant planktonic cells. A correlation matrix (Chapter 3) supported this, demonstrating planktonic growth negatively correlated with the amount of biofilm formed.

The biofilm matrix is largely composed of extracellular polysaccharides and it is predicted that culturing bacteria in media with excess carbon and limited nutrients, will stimulate bacteria to produce extracellular polysaccharides (EPS) (Sutherland, 2001). In support of this model, *Pst* cultured in nutrient- and carbon-rich conditions formed little biofilm, while *Pst* cultured in low-pH, nutrient-poor conditions but with excess fructose formed abundant biofilm (Wilson et al., 2017). Petrova and Sauer (2012) suggest that nutrient limitation stimulates biofilm formation. However, if phosphate levels were below a threshold value, this was observed to inhibit biofilm formation in *Pseudomonas aureofaciens* (Monds et al., 2001). This suggests that if nutrient levels drop too low, it will negatively impact the

ability to form biofilms (Petrova and Sauer, 2012). This may account for the observation that *Pst*<sub>165K</sub> formed biofilm up to 48 hours after which biofilm formation was highly reduced by 72 hours, perhaps due to using up the nutrients in the culture. Carbohydrate starvation has been shown to induce dispersal of biofilms in continuous flow cultures of *P. aeruginosa* (Huynh et al., 2012). Kim et al. (2009) showed that *Pst* grown in HIM, used 70% of the fructose in the culture by stationary phase at 48 hours. For the experiments presented in this thesis, faster growing *Pst* may have used up all the carbon in HIM more quickly than slower growing *Pst* and therefore reached starvation earlier which may have negatively impacted biofilm formation.

### 5.3.1 SA as an antibiofilm agent

During these studies, *Pst* pVSP1 formed biofilms over 72 hours after which total adhered biomass was reduced at 96 hours, suggesting that *Pst* biofilms began to disperse after 72 hours. However, when *Pst* was cultured in HIM with  $\geq 20 \mu\text{M}$  SA, the total adhered biomass reached a peak at 48 hours, while *Pst* cultured without SA reached a higher peak at 72 hours. These results suggest that *Pst* entered the dispersal phase early as a result of SA treatment (this thesis; Wilson et al., 2017) and SA acts as an antibiofilm agent by promoting early dispersal of aggregates.

Evidence supporting the idea that SA acts to disperse biofilms comes from experiments in which *E. coli* was cultured in media supplemented with 50 to 100  $\mu\text{M}$  SA and planktonic cell dispersal from biofilms, was observed (Cattò et al., 2017). Culturing in the presence of SA also resulted in lower polysaccharide and

protein levels within the biofilms of *E. coli* (Cattò et al., 2017), supporting previous research in the lab which demonstrated that 50 to 100  $\mu\text{M}$  SA inhibited *in planta* *Pst* growth and 2 to 10  $\mu\text{M}$  SA inhibited *in vitro* *Pst* biofilm formation (Wilson et al., 2017).

If SA acts to disperse *Pst* biofilms, this would add to the mechanisms by which SA acts in the leaf intercellular space to prevent infection by *Pst* and potentially other bacterial pathogens. SA may enhance the effect of other plant-produced antimicrobials by enhancing biofilm dispersal, as dispersed biofilms are thought to be more susceptible to the effects of antibiotics (Gupta et al., 2013; Muñoz-Egea et al., 2013; Kim and Lee, 2016; Sharma et al., 2019). Additionally, *P. aeruginosa* cultured in the presence of SA was found to enhance the effect of the antibiotic, ciprofloxacin (Prithiviraj et al., 2005).

### 5.3.2 Exploring EPS composition of *Pst* biofilms

Studies to explore the composition of Pseudomonas biofilms have employed *in vitro* methods such as continuous flow cells or static biofilm assays, therefore our understanding of biofilm composition and formation during infection of plants is severely limited. Recently, concanavalin A (ConA)-TRITC and calcofluor white (CFW) staining of *Pst*-inoculated *Arabidopsis* leaves demonstrated that *Pst* biofilm-like aggregated cells were surrounded by polysaccharides providing evidence that these *Pst* aggregates are indeed *in planta* biofilms (Fufeng et al., 2020). A possible future direction is to use these *in planta* staining methods to more comprehensively elucidate the composition of *Pst* biofilms during infection. This could be done by

staining various EPS deficient *Pst* strains ( $\Delta wssBC$ ,  $\Delta lscBC$ , and  $\Delta algD$ ) with ConA and CFW to determine which components are present in *Pst* biofilms.

CFW binds to  $\beta(1,3)$  and  $\beta(1,4)$  polysaccharides that are found in cellulose and chitin (Harrington and Hageage, 2003). It is possible that *Pst* biofilms in *Arabidopsis* contain cellulose (Fufeng et al., 2020), because CFW specifically binds to cellulose and CFW stained the air-liquid biofilms of wild-type *Pst*, but not biofilms of cellulose-deficient mutants (Farias et al., 2019). If CFW specifically binds cellulose in *Pst* biofilms during infection of *Arabidopsis*, then the cellulose production mutant *Pst*  $\Delta wssBC$  should not stain with CFW. Additionally, it is possible that *Pst*  $\Delta wssBC$  is not able to form biofilms. *In planta* experiments with *Pst* and *Pst*  $\Delta wssBC$  will shed light on whether cellulose is an important component of *Pst* biofilms.

ConA-TRITC stained *Pst* biofilm-like aggregates in inoculated *Arabidopsis* leaves, suggesting that *Pst* biofilms contain the EPS alginate (Fufeng et al., 2020). However, a number of experiments suggest that ConA-TRITC does not always detect alginate in *Pseudomonas* biofilms. Purified alginate from *P. aeruginosa* was bound by ConA, specifically to the mannuronic acid component (Fig. 1.2; Strathmann et al., 2002; Laue et al., 2006). However, experiments with wild-type and levan-deficient *Pseudomonas syringae* *pv.* *glycinea* (*Psg*) mutants demonstrated that ConA bound to the levan (Laue et al., 2006). Additionally, treatment of wild-type biofilms with the levan-degrading enzyme, levanase disrupted binding of ConA (Laue et al., 2006). Furthermore, there was no binding of ConA to biofilms of levan-deficient and alginate-producing *Psg* (Laue et al., 2006). These *in vitro* data suggest that ConA binds *Psg* levan, but not *Psg* alginate (Laue et al., 2006). Given

that *Pst* and *Psg* are different pathovars of the same species it is tempting to speculate that ConA binds to *Pst* levan and does not bind to *Pst* alginate. This could be tested by ConA staining of *in planta* biofilms of alginate- and levan-deficient mutants of *Pst*.

## 5.4 ARR

### 5.4.1 Contribution of PTI components to ARR

To determine if PTI is an important part of ARR, the ARR competence of the PTI mutants *bak1-3*, *bik1*, *efr-1*, and *fls2*, was examined. PTI mutants, *bik1*, *efr-1*, and *fls2* were partially ARR-defective while *bak1-3* was completely defective for ARR. These results suggest that the PRRs EFR and FLS2 contribute to some extent to a successful ARR response, while the coreceptor BAK1 is required for ARR. This supports the idea that ARR may be associated with the priming of defence prior to infection, as it is thought that primed defences are associated with elevated expression of PRR proteins and the co-receptor BAK1 (Conrath et al., 2015). However, this experiment was completed once and therefore must be repeated to confirm these results. Previous experiments with just mature plants demonstrated that *bak1-3*, *efr-1* and *fls2* displayed an ARR defect compared to wild-type Col-0.

### 5.4.2 RNA-sequencing

RNA-Seq was employed to identify differentially expressed genes in mature ARR-competent compared to young ARR-incompetent plants to discover genes that contribute to a successful ARR response. RNA-sequencing revealed that in response to *Pst*, young plants expressed genes associated with the GO term response to jasmonic acid, while in mature plants these same genes were not induced in response to *Pst*. This suggests that young, but not mature plants were affected by *Pst*-produced coronatine, an analog of JA-Ile that stimulates the jasmonic acid (JA) defense pathway. Possible reasons for why mature plants were not affected by coronatine include (i) the JA response pathway was not stimulated by coronatine in mature plants, (ii) coronatine production by *Pst* was inhibited by mature plants, (iii) coronatine did not reach the cytoplasm of mature plants. The idea that coronatine does not stimulate the JA pathway in mature plants is supported by the finding that *coi1-17*, a mutant of COI1 which acts as a receptor for coronatine or JA-Ile, had a modestly enhanced ARR response (Al-Daoud and Cameron, 2011).

The RNA-sequencing analysis also found that the SA-binding glutathione S-transferase GSTF2 (Manohar et al., 2015) was down-regulated in response to *Pst* in young plants but up-regulated in response to *Pst* in mature plants. GSTF2 could contribute to ARR by aiding in transport of bioactive compounds out of the cell (Dixon et al., 2012). As GSTF2 is an SA binding protein, it is possible that GSTF2 aids in transporting SA out of the cell (Manohar et al., 2015).

## 5.5 Conclusions

The work presented here significantly contributes to our understanding of ARR and further characterises the antimicrobial effects of SA against *Pst*. While alginate is important for biofilm formation in some bacterial species, the ability to produce alginate does not contribute to protecting *Pst* from the antimicrobial effects of SA *in vitro*. However, the alginate regulator AlgU appears to be important for growth in leaf intercellular space-mimicking minimal media (HIM), possibly due to its regulation of the T3SS and iron storage and uptake genes. AlgU also appears to contribute to resistance against the growth inhibiting and bactericidal effects of SA. This work also provides evidence that several components of the PTI signaling pathway contribute to ARR. Additionally, transcriptomes from susceptible young and mature ARR-competent plants responding to *Pst* were obtained. These transcriptomes make up a rich dataset that can be examined for years to come and will enhance our understanding of ARR. For example, comparative transcriptome analysis of young and mature plants revealed that JA pathway genes are expressed in young plants during a susceptible interaction with *Pst*, but are not expressed in mature plants responding with an ARR response. This may indicate that ARR could involve desensitization or suppression of the JA-Ile analog coronatine. The findings in this thesis enhance our understanding of how plants respond to bacterial infection over the course of their development, and this knowledge may be useful in designing crops with enhanced disease resistance.

# Chapter A

## Appendix

### A3 Chapter 3 Appendix

TABLE A3.1: Minimum inhibitory and bactericidal activities of SA.

Strain	MIC <sub>100</sub> (mM)	MBC (mM)
<i>Pst</i> <sub>165K</sub>	1 (1/3)	2 (3/8)
	2 (2/3)	5 (5/8)
<i>Pst</i> <sub>165K</sub> $\Delta$ algD	1 (2/4)	2 (2/6)
	2 (2/4)	5 (4/6)
<i>Pst</i> <sub>165K</sub> $\Delta$ algD $\Delta$ mucAB $\Delta$ algU	0.5 (1/5)	1 (1/6)
	1 (4/5)	2 (3/6)
		5 (2/6)

MIC<sub>100</sub> = Minimum concentration required to completely inhibit growth,  
MBC = Minimum bactericidal activity. Parentheses indicate ratio of experiments  
that resulted with the correlated MIC.

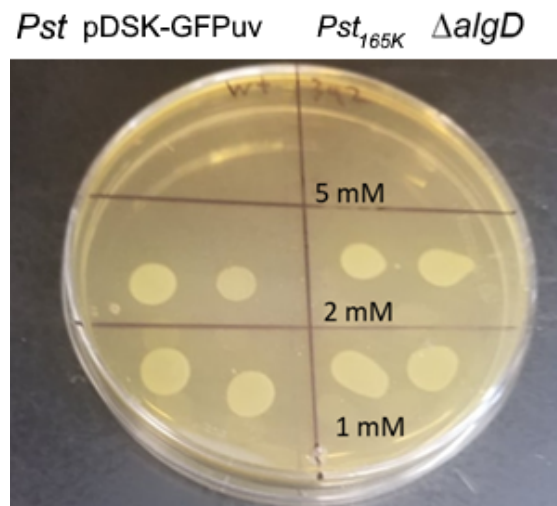


FIGURE A3.1: Bactericidal activity of SA on wild type *Pst* pDSK-GFPuv and *Pst*<sub>165K</sub>  $\Delta$ algD. After 72 hours of growth in HIM with indicated concentration of SA, 10  $\mu$ l spots of bacteria were plated on king's B agar plates. After 2 days, the plates were imaged.

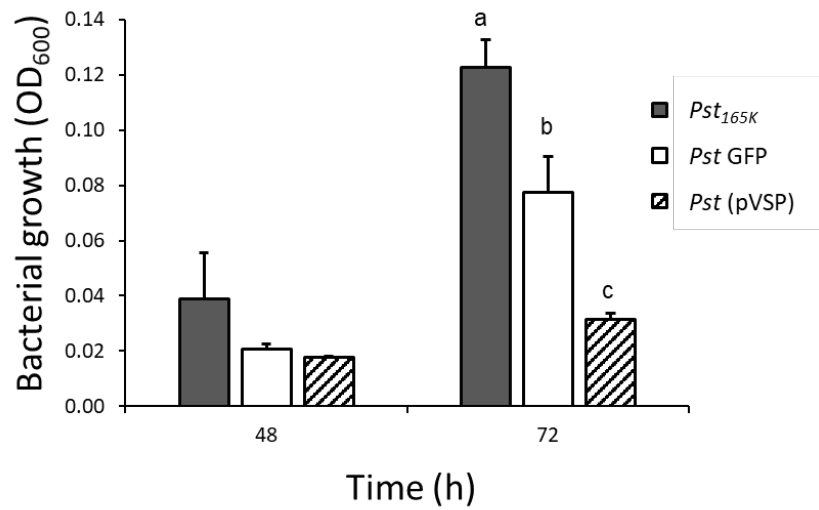


FIGURE A3.2: **Summary of growth of various *Pst* isolates without agitation.** This data represents a summary of several experiments, meaning that these cell lines have not all been directly compared at one time. Each bar represents the average of the mean for 4 independently conducted experiments. For each of these experiments, bacteria were grown on a 96-well microplate for up to 72 hours without agitation at room temperature. After either 48 or 72 hours, the optical density of 4 wells per cell type was measured before non-adherent cells were discarded to measure biofilm formation.

## A4 Chapter 4 Appendix

TABLE A4.1: RNA sample quality for RNA-sequencing of ARR.

Sample ID	ng/ μl	260/ 280	260/ 230	RINe <sup>a</sup>	Sample ID	ng/ μl	260/ 280	260/ 230	RINe <sup>a</sup>
1*	332.0	2.00	2.28	4.4	25	178.8	2.01	2.03	4.6
2	382.2	2.09	2.15	5.1	26	328.2	2.00	2.16	5.4
3	317.5	2.02	2.18	4.6	27	571.1	2.06	2.05	4.2
4	334.5	1.99	2.23	5.5	28*	197.4	1.99	1.62	4.8
5*	184.2	2.06	1.94	3.9	29	312.4	2.00	2.13	5.0
6	166.5	2.06	2.07	4.7	30*	360.5	1.98	1.83	3.7
7	252.2	2.03	2.46	4.6	31*	403.0	2.05	1.75	4.0
8*	628.6	2.09	2.14	4.0	32	424.3	2.06	1.31	4.2
9	328.5	1.96	2.14	4.6	33*	509.4	2.05	1.78	4.5
10	531.5	2.11	2.40	4.7	34*	510.2	2.07	2.22	3.9
11	643.7	2.10	2.14	4.8	35	437.8	2.06	2.01	4.6
12	288.2	1.99	2.34	4.9	36	508.3	2.08	2.07	4.3
13	595.1	2.09	2.23	4.6	37	275.9	2.01	2.19	5.5
14*	666.7	2.06	2.20	5.1	38	156.5	2.07	2.26	5.3
15	576.6	2.05	2.07	4.2	39*	302.4	2.02	2.26	4.1
16	330.7	2.01	2.24	5.2	40	290.3	2.07	2.22	5.2
17	506.0	2.08	2.04	4.4	41	255.8	2.05	2.26	5.0
18	335.1	1.98	2.02	4.6	42	399.5	2.09	2.09	4.8
19	251.6	2.05	2.31	5.3	43	317.6	2.03	2.32	4.0
20	346.6	2.00	2.08	4.1	44	616.4	2.10	2.35	4.5
21	344.0	1.99	2.18	5.4	45	605.8	2.10	2.33	4.6
22	218.3	2.05	2.12	5.4	46	488.0	2.14	2.32	5.1
23*	287.4	2.04	2.18	4.5	47	413.3	2.17	2.24	4.8
24	323.0	1.99	1.38	4.4	48	403.2	2.14	2.25	4.9

\* = samples that were not sequenced, <sup>a</sup> RINe = RNA integrity number equivalent

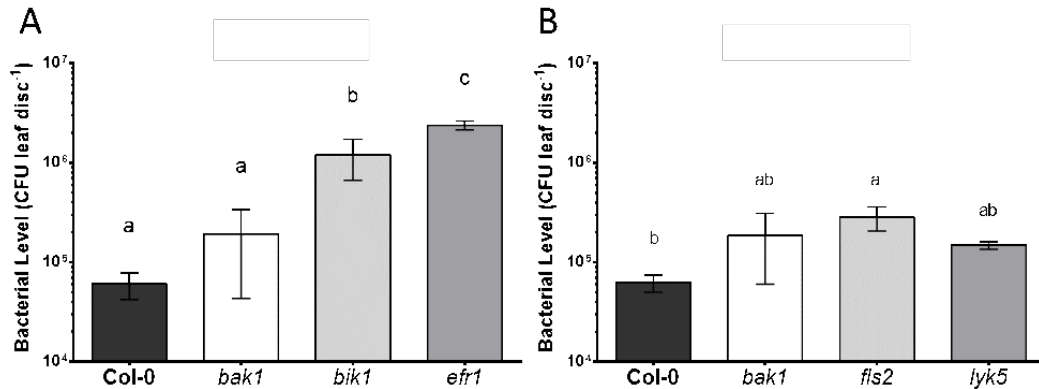


FIGURE A4.1: **Preliminary data on bacterial growth in mature plants of PTI mutants.** Wild-type Col-0, *bak1-3*, *bik1*, *efr-1*, and *fls2* were inoculated with 10<sup>6</sup> cfu ml<sup>-1</sup> *Pst* at 7 weeks post-germination (wpg) and bacterial levels were quantified 3 days later. Different letters indicate significant differences (ANOVA, p-value < 0.05). (A) Adapted from Nunn (2018). (B) A reanalysis based on raw data in Dan-Dobre (2018).

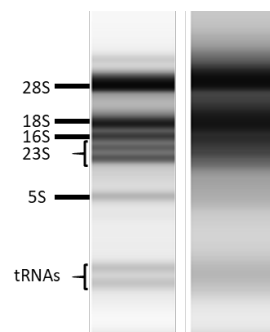


FIGURE A4.2: **Comparison of rRNA banding in intact and degraded total RNA samples from leafy tissue.** Total RNA isolated from leafy tissue of mature *Arabidopsis* plants 24 hours after infection with *Pst* was run on an Agilent TapeStation. Intact RNA (left) is distinctive from degraded RNA (right) by prominent clear and distinct banding of rRNA.

TABLE A4.2: The top up-regulated genes in *Pst* compared to mock-inoculated mature plants at 24 hpi.

Accession Number	Gene Name	Mature (log <sub>2</sub> fold change)	Padj (FDR) <sup>a</sup>	Young (log <sub>2</sub> fold change)	Padj (FDR) <sup>a</sup>
AT5G19890	AT5G19890	5.812	0.001204	5.334	0.002064
AT4G37390	BRU6	5.772	5.55E-06	3.327	0.008559
AT1G11925	AT1G11925	5.624	0.0007	4.913	1.73E-06
AT3G13610	F6'H1	5.548	4.68E-14	4.243	3.42E-09
AT5G63600	FLS5	5.546	0.00874	4.955	0.009188
AT2G44000	AT2G44000	5.446	0.000322	-0.864	0.35956
AT1G76480	AT1G76480	5.415	0.000903	3.763	0.000827
AT1G68450	PDE337	5.412	0.000796	1.730	0.061894
AT2G44070	AT2G44070	5.379	0.001169	2.525	0.047923
AT1G69920	GSTU12	5.239	1.16E-08	2.648	0.00023
AT2G41260	M17	5.149	0.011986	-0.099	0.958035
AT1G65970	TPX2	5.142	0.000447	1.119	0.241151
AT3G01420	DOX1	4.889	1.07E-05	1.908	0.098631
AT2G29470	GSTU3	4.784	3.04E-10	1.725	0.025982
AT1G22110	AT1G22110	4.780	0.004346	-0.644	0.575329

<sup>a</sup> The adjusted P-value using the FDR method (Benjamini and Hochberg, 1995).

TABLE A4.3: The top down-regulated genes in *Pst* compared to mock-inoculated mature plants at 24 hpi.

Accession Number	Gene Name	Mature (log <sub>2</sub> fold change)	Padj (FDR) <sup>a</sup>	Young (log <sub>2</sub> fold change)	Padj (FDR) <sup>a</sup>
AT2G41240	BHLH100	-6.593	8.30E-05	-3.458	0.121181
AT4G39250	RL1	-6.159	0.000515	-0.279	0.914992
AT3G21330	AT3G21330	-5.845	1.54E-06	-4.339	9.20E-05
AT3G56970	bHLH38	-5.528	0.001603	-3.307	0.168583
AT1G04180	YUC9	-5.233	5.70E-06	0.724	0.770786
AT5G02760	APD7	-5.056	1.94E-06	-4.410	1.85E-12
AT3G56980	bHLH39	-5.007	0.003176	-1.436	0.553537
AT3G58120	BZIP61	-4.919	9.53E-05	-2.638	1.57E-08
AT3G27970	AT3G27970	-4.871	0.000145	-2.993	0.000207
AT1G55200	AT1G55200	-4.708	0.001397	1.723	0.001042
AT4G06195	NA	-4.502	0.00473	-3.535	0.01053
AT4G32280	IAA29	-4.483	9.43E-10	-4.197	2.46E-05
AT3G27500	AT3G27500	-4.424	0.007521	-2.621	0.139098
AT2G14247	AT2G14247	-4.422	0.003424	-0.599	0.748574
AT1G32780	AT1G32780	-4.362	0.002344	-1.943	8.28E-05

<sup>a</sup> The adjusted P-value using the FDR method (Benjamini and Hochberg, 1995).



# Bibliography

- Aeschlimann, J. R. (2003). The role of multidrug efflux pumps in the antibiotic resistance of *Pseudomonas aeruginosa* and other gram-negative bacteria. *Pharmacotherapy* 23(7), 916–924. ISSN: 02770008.
- Al-Daoud, F. and Cameron, R. K. (2011). ANAC055 and ANAC092 contribute non-redundantly in an EIN2-dependent manner to Age-Related Resistance in *Arabidopsis*. *Physiological and Molecular Plant Pathology* 76(3-4), 212–222. ISSN: 08855765.
- Amasino, R. (2010). Seasonal and developmental timing of flowering. *The Plant Journal* 61(6), 1001–1013. ISSN: 09607412.
- Anders, S., Pyl, P. T., and Huber, W. (2015). HTSeq—a Python framework to work with high-throughput sequencing data. *Bioinformatics* 31(2), 166–169. ISSN: 14602059.
- Andrews, S. C., Robinson, A. K., and Rodríguez-Quñones, F. (2003). Bacterial iron homeostasis. *FEMS Microbiology Reviews* 27(2-3), 215–237. ISSN: 01686445.

## BIBLIOGRAPHY

---

- Appel, H. M., Fescemyer, H., Ehltling, J., Weston, D., Rehrig, E., Joshi, T., Xu, D., Bohlmann, J., and Schultz, J. (2014). Transcriptional responses of *Arabidopsis thaliana* to chewing and sucking insect herbivores. *Frontiers in Plant Science* 5(November), 1–20. ISSN: 1664462X.
- Axtell, M. J. and Staskawicz, B. J. (2003). Initiation of RPS2-specified disease resistance in *Arabidopsis* is coupled to the AvrRPT2-directed elimination of RIN4. *Cell* 112, 369–377. ISSN: 17511097.
- Bao, Z., Stodghill, P. V., Myers, C. R., Lam, H., Wei, H. L., Chakravarthy, S., Kvitko, B. H., Collmer, A., Cartinhour, S. W., Schweitzer, P., and Swingle, B. (2014). Genomic plasticity enables phenotypic variation of *Pseudomonas syringae* pv. tomato DC3000. *PLoS ONE* 9(2). ISSN: 19326203.
- Benjamini, Y. and Hochberg, Y. (1995). Controlling the False Discovery Rate : A Practical and Powerful Approach to Multiple Testing Author ( s ): Yoav Benjamini and Yosef Hochberg Source : Journal of the Royal Statistical Society . Series B ( Methodological ), Vol . 57 , No . 1 ( 1995 ), Publi. *Journal of the Royal Statistical Society* 57(1), 289–300.
- Bevan, M. and Walsh, S. (2005). The *Arabidopsis* genome: A foundation for plant research. *Genome Research* 15, 1632–1642. ISSN: 10889051.
- Bolger, A. M., Lohse, M., and Usadel, B. (2014). Trimmomatic: a flexible trimmer for Illumina sequence data. *Bioinformatics* 30(15), 2114–2120.
- Boller, T. and Felix, G. (2009). A renaissance of elicitors: perception of microbe-associated molecular patterns and danger signals by pattern-recognition receptors. *Annual Review of Plant Biology* 60(1), 379–406. ISSN: 1543-5008.
- Bronstein, P. A., Filiatrault, M. J., Myers, C. R., Rutzke, M., Schneider, D. J., and Cartinhour, S. W. (2008). Global transcriptional responses of *Pseudomonas*

## BIBLIOGRAPHY

---

- syringae DC3000 to changes in iron bioavailability in vitro. *BMC Microbiology* 8, 1–15. ISSN: 14712180.
- Brooks, D. M., Hernández-Guzmán, G., Kloek, A. P., Alarcón-Chaidez, F., Sreedharan, A., Rangaswamy, V., Peñaloza-Vázquez, A., Bender, C. L., and Kunkel, B. N. (2004). Identification and characterization of a well-defined series of coronatine biosynthetic mutants of *Pseudomonas syringae* pv. tomato DC3000. *Molecular Plant-Microbe Interactions* 17(2), 162–174. ISSN: 08940282.
- Bruegger, B. B. and Keen, N. T. (1979). Specific elicitors of glyceollin accumulation in the *Pseudomonas glycinea*-soybean host-parasite system. *Physiological Plant Pathology* 15(1), 43–51. ISSN: 00484059.
- Buell, C. R., Joardar, V., Lindeberg, M., Selengut, J., Paulsen, I. T., Gwinn, M. L., Dodson, R. J., Deboy, R. T., Durkin, A. S., Kolonay, J. F., Madupu, R., Daugherty, S., Brinkac, L., Beanan, M. J., Haft, D. H., Nelson, W. C., Davidsen, T., Zafar, N., Zhou, L., Liu, J., Yuan, Q., Khouri, H., Fedorova, N., Tran, B., Russell, D., Berry, K., Utterback, T., Van Aken, S. E., Feldblyum, T. V., D'Ascenzo, M., Deng, W.-L., Ramos, A. R., Alfano, J. R., Cartinhour, S., Chatterjee, A. K., Delaney, T. P., Lazarowitz, S. G., Martin, G. B., Schneider, D. J., Tang, X., Bender, C. L., White, O., Fraser, C. M., and Collmer, A. (2003). The complete genome sequence of the Arabidopsis and tomato pathogen *Pseudomonas syringae* pv. tomato DC3000. *Proceedings of the National Academy of Sciences of the United States of America* 100(18), 10181–10186. ISSN: 00278424.
- Butcher, B. G., Bronstein, P. A., Myers, C. R., Stodghill, P. V., Bolton, J. J., Markel, E. J., Filiatrault, M. J., Swingle, B., Gaballa, A., Helmann, J. D., Schneider, D. J., and Cartinhour, S. W. (2011). Characterization of the Fur

## BIBLIOGRAPHY

---

- regulon in *Pseudomonas syringae* pv. tomato DC3000. *Journal of Bacteriology* 193(18), 4598–4611. ISSN: 00219193.
- Cai, R., Lewis, J., Yan, S., Liu, H., Clarke, C. R., Campanile, F., Almeida, N. F., Studholme, D. J., Lindeberg, M., Schneider, D., Zaccardelli, M., Setubal, J. C., Morales-Lizcano, N. P., Bernal, A., Coaker, G., Baker, C., Bender, C. L., Lemman, S., and Vinatzer, B. A. (2011). The plant pathogen *Pseudomonas syringae* pv. tomato is genetically monomorphic and under strong selection to evade tomato immunity. *PLoS Pathogens* 7(8). ISSN: 15537366.
- Cameron, R. K. and Zaton, K. (2004). Intercellular salicylic acid accumulation is important for age-related resistance in *Arabidopsis* to *Pseudomonas syringae*. *Physiological and Molecular Plant Pathology* 65(4), 197–209. ISSN: 08855765.
- Campbell, E. J., Schenk, P. M., Kazan, K., Penninckx, I. A.M. A., Anderson, J. P., Maclean, D. J., Cammue, B. P. A., Ebert, P. R., and Manners, J. M. (2003). Pathogen-responsive expression of a putative ATP-binding cassette transporter gene conferring resistance to the diterpenoid sclareol is regulated by multiple defense signaling pathways in *Arabidopsis*. *Plant Physiology* 133(3), 1272–1284. ISSN: 00320889.
- Campe, R., Langenbach, C., Leissing, F., Popescu, G. V., Popescu, S. C., Goellner, K., Beckers, G. J. M., and Conrath, U. (2016). ABC transporter PEN3/PDR8/ABCG36 interacts with calmodulin that, like PEN3, is required for *Arabidopsis* nonhost resistance. *New Phytologist* 209, 294–306. ISSN: 14698137.
- Cao, Y., Liang, Y., Tanaka, K., Nguyen, C. T., Jedrzejczak, R. P., Joachimiak, A., and Stacey, G. (2014). The kinase LYK5 is a major chitin receptor in *Arabidopsis* and forms a chitin-induced complex with related kinase CERK1. *eLife* 3, e03766. ISSN: 2050084X.

## BIBLIOGRAPHY

---

- Carella, P., Wilson, D. C., and Cameron, R. K. (2015). Some things get better with age: differences in salicylic acid accumulation and defense signaling in young and mature *Arabidopsis*. *Frontiers in plant science* 5, 775. ISSN: 1664-462X.
- Carella, P., Wilson, D. C., Kempthorne, C. J., and Cameron, R. K. (2016). Vascular Sap Proteomics: Providing Insight into Long-Distance Signaling during Stress. *Frontiers in Plant Science* 7(May), 1–8. ISSN: 1664-462X.
- Carviel, J. L., Al-Daoud, F., Neumann, M., Mohammad, A., Provart, N. J., Moeder, W., Yoshioka, K., and Cameron, R. K. (2009). Forward and reverse genetics to identify genes involved in the age-related resistance response in *Arabidopsis thaliana*. *Molecular Plant Pathology* 10(5), 621–634. ISSN: 14646722.
- Carviel, J. L., Wilson, D. C., Isaacs, M., Carella, P., Catana, V., Golding, B., Weretilnyk, E. A., and Cameron, R. K. (2014). Investigation of intercellular salicylic acid accumulation during compatible and incompatible *Arabidopsis*-*Pseudomonas syringae* interactions using a fast neutron-generated mutant allele of EDS5 identified by genetic mapping and whole-genome sequencing. *PLoS ONE* 9(3), e88608. ISSN: 19326203.
- Cattò, C., Grazioso, G., Dell’Orto, S., Gelain, A., Villa, S., Marzano, V., Vitali, A., Villa, F., Cappitelli, F., and Forlani, F. (2017). The response of *Escherichia coli* biofilm to salicylic acid. *Biofouling* 33(3), 235–251. ISSN: 10292454.
- Cezairliyan, B. O. and Sauer, R. T. (2009). Control of *P. aeruginosa* AlgW protease cleavage of MucA by peptide signals and MucB. *Molecular Microbiology* 72(2), 368–379. ISSN: 15378276.
- Chinchilla, D., Bauer, Z., Regenass, M., Boller, T., and Felix, G. (2006). The *Arabidopsis* receptor kinase FLS2 binds flg22 and determines the specificity of flagellin perception. *Plant Cell* 18(2), 465–476. ISSN: 10404651.

## BIBLIOGRAPHY

---

- Chinchilla, D., Zipfel, C., Robatzek, S., Kemmerling, B., Nürnberger, T., Jones, J. D. G., Felix, G., and Boller, T. (2007). A flagellin-induced complex of the receptor FLS2 and BAK1 initiates plant defence. *Nature* 448, 497–500. ISSN: 0028-0836.
- Choi, J., Kim, K.-T., Jeon, J., and Lee, Y.-H. (2013). Fungal plant cell wall-degrading enzyme database: a platform for comparative and evolutionary genomics in fungi and Oomycetes. *BMC Genomics* 14(Suppl 5), S7. ISSN: 14712164.
- Conrath, U., Beckers, G. J., Langenbach, C. J., and Jaskiewicz, M. R. (2015). Priming for Enhanced Defense. *Annual Review of Phytopathology* 53(1), 97–119. ISSN: 0066-4286.
- Cui, H., Tsuda, K., and Parker, J. E. (2015). Effector-triggered immunity: from pathogen perception to robust defense. *Annual Review of Plant Biology* 66, 487–511. ISSN: 1543-5008.
- Cuppels, D. A. (1986). Generation and characterization of Tn5 insertion mutations in *Pseudomonas syringae* pv. tomato. *Applied and Environmental Microbiology* 51(2), 323–327. ISSN: 00992240.
- Dan-Dobre, M. (2018). Investigating the role of PAMP-triggered immunity in age-related resistance in *Arabidopsis* and chemically induced resistance in cucumber. Bachelor's thesis. McMaster University.
- Davies, D. G. and Marques, C. N. H. (2009). A fatty acid messenger is responsible for inducing dispersion in microbial biofilms. *Journal of Bacteriology* 191(5), 1393–1403. ISSN: 00219193.
- Dean, J. V. and Mills, J. D. (2004). Uptake of salicylic acid 2-O- $\beta$ -D-glucose into soybean tonoplast vesicles by an ATP-binding cassette transporter-type mechanism. *Physiologia Plantarum* 120(4), 603–612. ISSN: 00319317.

## BIBLIOGRAPHY

---

- Dean, J. V., Shah, R. P., and Mohammed, L. A. (2003). Formation and vacuolar localization of salicylic acid glucose conjugates in soybean suspension cultures. *Physiologia Plantarum* 118, 328–336. ISSN: 00320935.
- Demianski, A. J., Chung, K. M., and Kunkel, B. N. (2012). Analysis of Arabidopsis JAZ gene expression during *Pseudomonas syringae* pathogenesis. *Molecular Plant Pathology* 13(1), 46–57. ISSN: 14646722.
- Dempsey, D. A., Vlot, A. C., Wildermuth, M. C., and Klessig, D. F. (2011). Salicylic Acid Biosynthesis and Metabolism. *The Arabidopsis Book* 9, e0156. ISSN: 1543-8120.
- Deng, W., Ying, H., Helliwell, C. A., Taylor, J. M., Peacock, W. J., and Dennis, E. S. (2011). FLOWERING LOCUS C (FLC) regulates development pathways throughout the life cycle of Arabidopsis. *Proceedings of the National Academy of Sciences of the United States of America* 108(16), 6680–6685. ISSN: 00278424.
- Desveaux, D., Subramaniam, R., Després, C., Mess, J.-N., Lévesque, C., Fobert, P. R., Dangl, J. L., and Brisson, N. (2004). A "Whirly" transcription factor is required for salicylic acid-dependent disease resistance in Arabidopsis. *Developmental Cell* 6(2), 229–240. ISSN: 15345807.
- Develey-Rivière, M.-P. and Galiana, E. (2007). Resistance to pathogens and host developmental stage: A multifaceted relationship within the plant kingdom. *New Phytologist* 175(3), 405–416. ISSN: 0028646X.
- Díaz-Salazar, C., Calero, P., Espinosa-Portero, R., Jiménez-Fernández, A., Wirebrand, L., Velasco-Domínguez, M. G., López-Sánchez, A., Shingler, V., and Govantes, F. (2017). The stringent response promotes biofilm dispersal in *Pseudomonas putida*. *Scientific Reports* 7(18055). ISSN: 20452322.

## BIBLIOGRAPHY

---

- Ding, Y., Sun, T., Ao, K., Peng, Y., Zhang, Y., Li, X., and Zhang, Y. (2018). Opposite roles of salicylic acid receptors NPR1 and NPR3/4 in transcriptional regulation of plant immunity. *Cell* 173(6), 1454–1467. ISSN: 10974172.
- Dixon, D. P., Sellars, J. D., and Edwards, R. (2012). The Arabidopsis phi class glutathione transferase AtGSTF2: binding and regulation by biologically active heterocyclic ligands. *Biochemical Journal* 438(1).
- Doggett, R. G. (1969). Incidence of mucoid *Pseudomonas aeruginosa* from clinical sources. *Applied Microbiology* 18(5), 936–937. ISSN: 00036919.
- Edgar, R. C. (2004). MUSCLE: A multiple sequence alignment method with reduced time and space complexity. *BMC Bioinformatics* 5, 1–19. ISSN: 14712105.
- Eschelman, K., Yao, H., Punchi Hewage, A. N. D., Deay, J. J., Chandler, J. R., and Rivera, M. (2017). Inhibiting the BfrB:Bfd interaction in *Pseudomonas aeruginosa* causes irreversible iron accumulation in bacterioferritin and iron deficiency in the bacterial cytosol. *Metallomics* 9(6), 646–659.
- Evans, L. R. and Linker, A. (1973). Production and characterization of the slime polysaccharide of *Pseudomonas aeruginosa*. *Journal of Bacteriology* 116(2), 915–924. ISSN: 00219193.
- Fakhr, M. K., Peñaloza-Vázquez, A., Chakrabarty, A. M., and Bender, C. L. (1999). Regulation of alginate biosynthesis in *Pseudomonas syringae* pv. *syringae*. *Journal of Bacteriology* 181(11), 3478–3485. ISSN: 00219193.
- Farias, G. A., Olmedilla, A., and Gallegos, M. T. (2019). Visualization and characterization of *Pseudomonas syringae* pv. *tomato* DC3000 pellicles. *Microbial Biotechnology* 12(4), 688–702. ISSN: 17517915.

## BIBLIOGRAPHY

---

- Ferreira, A. O., Myers, C. R., Gordon, J. S., Martin, G. B., Vencato, M., Collmer, A., Wehling, M. D., Alfano, J. R., Moreno-Hagelsieb, G., Lamboy, W. F., Declerck, G., Schneider, D. J., and Cartinhour, S. W. (2006). Whole-genome expression profiling defines the HrpL regulon of *Pseudomonas syringae* pv. tomato DC3000, allows de novo reconstruction of the Hrp cis element, and identifies novel coregulated genes. *Molecular Plant-Microbe Interactions* 19(11), 1167–1179. ISSN: 08940282.
- Flemming, H.-C. (1993). Biofilms and environmental protection. *Water Science and Technology* 27(7-8), 1–10. ISSN: 02731223.
- Flemming, H.-c., Neu, T. R., and Wozniak, D. J. (2007). The EPS matrix: The “house of biofilm cells”. *Journal of Bacteriology* 189(22), 7945–7947.
- Fragniere, C., Serrano, M., Abou-Mansour, E., Métraux, J.-P., and L’Haridon, F. (2011). Salicylic acid and its location in response to biotic and abiotic stress. *FEBS Letters* 585(12), 1847–1852. ISSN: 00145793.
- Fu, Z. Q., Yan, S., Saleh, A., Wang, W., Ruble, J., Oka, N., Mohan, R., Spoel, S. H., Tada, Y., Zheng, N., and Dong, X. (2012). NPR3 and NPR4 are receptors for the immune signal salicylic acid in plants. *Nature* 486(7402), 228–232.
- Fufeng, A. B. (2019). Investigation of SAR-associated small molecules as inducers of resistance in cucumber and biofilm formation by *Pseudomonas syringae* pv. tomato in *Arabidopsis*. Master’s thesis.
- Fufeng, A. B., Xiao, N. W., Nunn, G. M., Halim, A., and Cameron, R. K. (2020). Suppression of bacterial biofilm formation contributes to PAMP-triggered immunity in the *Arabidopsis*-*Pseudomonas syringae* pv. tomato interaction. unpublished.

## BIBLIOGRAPHY

---

- Gandee, L., Hsieh, J.-T., Sperandio, V., Moreira, C. G., Lai, C.-H., and Zimmern, P. E. (2015). The efficacy of immediate versus delayed antibiotic administration on bacterial growth and biofilm production of selected strains of uropathogenic *Escherichia coli* and *Pseudomonas aeruginosa*. *International Brazilian Journal of Urology* 41(1), 67–77. ISSN: 16776119.
- Garcion, C., Lohmann, A., Lamodièrre, E., Catinot, J., Buchala, A., Doermann, P., and Métraux, J.-P. (2008). Characterization and biological function of the ISOCHORISMATE SYNTHASE2 gene of *Arabidopsis*. *Plant Physiology* 147(3), 1279–1287. ISSN: 00320889.
- Geng, X., Jin, L., Shimada, M., Kim, M. G., and Mackey, D. (2014). The phyto-toxin coronatine is a multifunctional component of the virulence armament of *Pseudomonas syringae*. *Planta* 240(6), 1149–1165. ISSN: 14322048.
- Gigolashvili, T., Berger, B., Mock, H.-P., Müller, C., Weisshaar, B., and Flügge, U.-I. (2007). The transcription factor HIG1/MYB51 regulates indolic glucosinolate biosynthesis in *Arabidopsis thaliana*. *Plant Journal* 50(5), 886–901. ISSN: 1365313X.
- Gilbert, G. S. and Parker, I. M. (2010). Rapid evolution in a plant-pathogen interaction and the consequences for introduced host species. *Evolutionary Applications* 3(2), 144–156. ISSN: 17524563.
- Gilbert, P., Das, J., and Foley, I (1997). Biofilm susceptibility to antimicrobials. *Advances in Dental Research* 11(1), 160–167. ISSN: 08959374.
- Glombitza, S., Dubuis, P.-H., Thulke, O., Welzl, G., Bovet, L., Götz, M., Affenzeller, M., Geist, B., Hehn, A., Asnaghi, C., Ernst, D., Seidlitz, H. K., Gundlach, H., Mayer, K. F., Martinoia, E., Werck-Reichhart, D., Mauch, F., and Schäffner, A. R. (2004). Crosstalk and differential response to abiotic and biotic

## BIBLIOGRAPHY

---

- stressors reflected at the transcriptional level of effector genes from secondary metabolism. *Plant Molecular Biology* 54(6), 817–835. ISSN: 01674412.
- Goldstein, I. J. and Poretz, R. D. (1986). Isolation, physicochemical characterization, and carbohydrate-binding specificity of lectins. In: *The lectins: properties, functions, and applications in biology and medicine*. Ed. by I. E. Liener, N. Sharon, and I. J. Goldstein. Academic Press, Inc. ISBN: 0-12-449945-7.
- Gomila, M., Peña, A., Mulet, M., Lalucat, J., and García-Valdés, E. (2015). Phylogenomics and systematics in *Pseudomonas*. *Frontiers in Microbiology* 6, 214. ISSN: 1664302X.
- González, M. J., Robino, L., Iribarnegaray, V., Zunino, P., and Scavone, P. (2017). Effect of different antibiotics on biofilm produced by uropathogenic *Escherichia coli* isolated from children with urinary tract infection. *Pathogens and Disease* 75(4), 1–9. ISSN: 2049632X.
- Grasdalen, H. (1983). High-field, <sup>1</sup>H-n.m.r. spectroscopy of alginate: sequential structure and linkage conformations. *Carbohydrate Research* 118(C), 255–260. ISSN: 00086215.
- Gregis, V., Andrés, F., Sessa, A., Guerra, R. F., Simonini, S., Mateos, J. L., Torti, S., Zambelli, F., Prazzoli, G. M., Bjerkan, K. N., Grini, P. E., Pavese, G., Colombo, L., Coupland, G., and Kater, M. M. (2013). Identification of pathways directly regulated by SHORT VEGETATIVE PHASE during vegetative and reproductive development in *Arabidopsis*. *Genome Biology* 14(6), R56. ISSN: 1474760X.
- Gupta, K., Marques, C. N. H., Petrova, O. E., and Sauer, K. (2013). Antimicrobial tolerance of *pseudomonas aeruginosa* biofilms is activated during an early

## BIBLIOGRAPHY

---

- developmental stage and requires the two-component hybrid sagS. *Journal of Bacteriology* 195(21), 4975–4987. ISSN: 00219193.
- Harrington, B. J. and Hageage, G. J. (2003). Calcofluor white: a review of its uses and applications in clinical mycology and parasitology. *Laboratory Medicine* 34(5), 361–367. ISSN: 0007-5027.
- Hay, I. D., Ur Rehman, Z., Moradali, M. F., Wang, Y., and Rehm, B. H. A. (2013). Microbial alginate production, modification and its applications. *Microbial Biotechnology* 6, 637–650.
- He, Y., Xu, J., Wang, X., He, X., Wang, Y., Zhou, J., Zhang, S., and Meng, X. (2019). The Arabidopsis pleiotropic drug resistance transporters PEN3 and PDR12 mediate camalexin secretion for resistance to *Botrytis cinerea*. *The Plant cell* 31(9), 2206–2222. ISSN: 1532298X.
- Heese, A, Hann, D. R., Gimenez-Ibanez, S, Jones, A. M. E., He, K, Li, J, Schroeder, J. I., Peck, S. C., and Rathjen, J. P. (2007). The receptor-like kinase SERK3/BAK1 is a central regulator of innate immunity in plants. *Proceedings of the National Academy of Sciences* 104(29), 12217–12222. ISSN: 0027-8424.
- Henry, E., Yadeta, K. A., and Coaker, G. (2013). Recognition of bacterial plant pathogens: local, systemic and transgenerational immunity. *New Phytologist* 199, 908–915. ISSN: 15378276.
- Hockett, K. L., Burch, A. Y., and Lindow, S. E. (2013). Thermo-regulation of genes mediating motility and plant interactions in *Pseudomonas syringae*. *PLoS ONE* 8(3). ISSN: 19326203.

## BIBLIOGRAPHY

---

- Howard, B. E., Hu, Q., Babaoglu, A. C., Chandra, M., Borghi, M., Tan, X., He, L., Winter-Sederoff, H., Gassmann, W., Veronese, P., and Heber, S. (2013). High-throughput RNA sequencing of *Pseudomonas*-infected *Arabidopsis* reveals hidden transcriptome complexity and novel splice variants. *PLoS ONE* 8(10).
- Huang, P., Ju, H.-W., Min, J.-H., Zhang, X., Kim, S.-H., Yang, K.-Y., and Kim, C. S. (2013). Overexpression of L-type lectin-like protein kinase 1 confers pathogen resistance and regulates salinity response in *Arabidopsis thaliana*. *Plant Science* 203-204, 98–106. ISSN: 01689452.
- Hurley, B., Subramaniam, R., Guttman, D. S., and Desveaux, D. (2014). Proteomics of effector-triggered immunity (ETI) in plants. *Virulence* 5(7), 752–760. ISSN: 21505608.
- Huynh, T. V., Dahlbeck, D., and Staskawicz, B. J. (1989). Bacterial blight of soybean: regulation of a pathogen gene determining host cultivar specificity. *Science* 245, 1374–1377.
- Huynh, T. T., McDougald, D., Klebensberger, J., Al Qarni, B., Barraud, N., Rice, S. A., Kjelleberg, S., and Schleheck, D. (2012). Glucose starvation-induced dispersal of *Pseudomonas aeruginosa* biofilms is cAMP and energy dependent. *PLoS ONE* 7(8). ISSN: 19326203.
- Hwang, J.-U., Song, W.-Y., Hong, D., Ko, D., Yamaoka, Y., Jang, S., Yim, S., Lee, E., Khare, D., Kim, K., Palmgren, M., Yoon, H. S., Martinoia, E., and Lee, Y. (2016). Plant ABC transporters enable many unique aspects of a terrestrial plant’s lifestyle. *Molecular Plant* 9(3), 338–355. ISSN: 17529867.
- Itoh, Y., Watson, J. M., Haas, D., and Leisinger, T. (1984). Genetic and molecular characterization of the *Pseudomonas* plasmid pVS1. *Plasmid* 11(3), 206–220. ISSN: 10959890.

## BIBLIOGRAPHY

---

- Jensen, L. J., Skovgaard, M., Sicheritz-Ponten, T., Hensen, N. T., Johansson, H., Jorgensen, M. K., Kiil, K., Hallin, P. F., and Ussery, D. (2004). Comparative genomics of four *Pseudomonas* species. In: *Pseudomonas*. Ed. by J.-L. Ramos. Springer, Boston, MA.
- Jin, Q., Hu, W., Brown, I., McGhee, G., Hart, P., Jones, A. L., and He, S. Y. (2001). Visualization of secreted Hrp and Avr proteins along the Hrp pilus during type III secretion in *Erwinia amylovora* and *Pseudomonas syringae*. *Molecular Microbiology* 40(5), 1129–1139. ISSN: 0950382X.
- Jovanovic, M., Lawton, E., Schumacher, J., and Buck, M. (2014). Interplay among *Pseudomonas syringae* HrpR, HrpS and HrpV proteins for regulation of the type III secretion system. *FEMS Microbiology Letters* 356(2), 201–211. ISSN: 15746968.
- Kaplan, J. B. (2010). Biofilm dispersal: mechanisms, clinical implications , and potential therapeutic uses. *Journal of Dental Research* 89(3), 205–218.
- Kazachkova, Y., Eshel, G., Pantha, P., Cheeseman, J. M., Dassanayake, M., and Barak, S. (2018). Halophytism: What have we learnt from *Arabidopsis thaliana* relative model systems? *Plant Physiology* 178(3), 972–988. ISSN: 15322548.
- Keen, N. T., Tamaki, S, Kobayashi, D, and Troilinger, D (1988). Improved brood-host-range plasmids for DNA cloning in Gram-negative bacteria. *Gene* 70, 191–197.
- Keith, L. M. W. and Bender, C. L. (1999). AlgT ( 22 ) Controls Alginate Production and Tolerance to Environmental Stress in. *Journal of Bacteriology* 181(23), 7176–7184.
- Kemphorne, C. J. (2018). Intercellular dihydrocamalexin acid contributes to ARR. Master’s thesis. McMaster University.

## BIBLIOGRAPHY

---

- Keren, I., Abudraham, S., Shaya, F., and Ostersetzer-Biran, O. (2011). An optimized method for the analysis of plant mitochondria RNAs by Northern blotting. *Journal of Endocytobiosis and Cell Research* 21(March), 34–42.
- Khare, D., Choi, H., Huh, S. U., Bassin, B., Kim, J., Martinoia, E., Sohn, K. H., Paek, K.-H., Lee, Y., and Chrispeels, M. J. (2017). Arabidopsis ABCG34 contributes to defense against necrotrophic pathogens by mediating the secretion of camalexin. *Proceedings of the National Academy of Sciences of the United States of America* 114(28), E5712–E5720. ISSN: 10916490.
- Kim, B. J., Park, J. H., Park, T. H., Bronstein, P. A., Schneider, D. J., Cartinhour, S. W., and Shuler, M. L. (2009). Effect of iron concentration on the growth rate of *Pseudomonas syringae* and the expression of virulence factors in hrp-inducing minimal medium. *Applied and Environmental Microbiology* 75(9), 2720–2726. ISSN: 00992240.
- Kim, M. G., Da Cunha, L., McFall, A. J., Belkhadir, Y., DebRoy, S., Dangl, J. L., and Mackey, D. (2005). Two *Pseudomonas syringae* type III effectors inhibit RIN4-regulated basal defense in Arabidopsis. *Cell* 121(5), 749–759. ISSN: 00928674.
- Kim, S.-K. and Lee, J.-H. (2016). Biofilm dispersion in *Pseudomonas aeruginosa*. *Journal of Microbiology* 54(2), 71–85. ISSN: 19763794.
- Kinkema, M., Fan, W., and Dong, X. (2000). Nuclear localization of NPR1 is required for activation of PR gene expression. *The Plant Cell* 12(12), 2339–2350. ISSN: 10404651.

## BIBLIOGRAPHY

---

- Kirov, S. M., Webb, J. S., O'May, C. Y., Reid, D. W., Woo, J. K. K., Rice, S. A., and Kjelleberg, S. (2007). Biofilm differentiation and dispersal in mucoid *Pseudomonas aeruginosa* isolates from patients with cystic fibrosis. *Microbiology* 153(10), 3264–3274. ISSN: 13500872.
- Kubicek, C. P., Starr, T. L., and Glass, N. L. (2014). Plant cell wall-degrading enzymes and their secretion in plant-pathogenic fungi. *Annual Review of Phytopathology* 52(1), 427–451. ISSN: 0066-4286.
- Kunkel, B. N., Bent, A. F., Dahlbeck, D., Innes, R. W., and Staskawicz, B. J. (1993). RPS2, an arabidopsis disease resistance locus specifying recognition of *Pseudomonas syringae* strains expressing the avirulence gene *avrRpt2*. *Plant Cell* 5(8), 865–875. ISSN: 10404651.
- Kunze, G., Zipfel, C., Robatzek, S., Niehaus, K., Boller, T., and Felix, G. (2004). The N terminus of bacterial elongation factor Tu elicits innate immunity in *Arabidopsis* plants. *The Plant Cell* 16(12), 3496–3507. ISSN: 1040-4651.
- Kus, J. V., Zaton, K., Sarkar, R., and Cameron, R. K. (2002). Age-related resistance in *Arabidopsis* is a developmentally regulated defense response to *Pseudomonas syringae*. *The Plant cell* 14(2), 479–490. ISSN: 1040-4651.
- Kwon, M., Hussain, M. S., and Oh, D. H. (2017). Biofilm formation of *Bacillus cereus* under food-processing-related conditions. *Food Science and Biotechnology* 26(4), 1103–1111. ISSN: 12267708.
- Lal, N. K., Nagalakshmi, U., Hurlburt, N. K., Flores, R., Bak, A., Sone, P., Ma, X., Song, G., Walley, J., Shan, L., He, P., Casteel, C., Fisher, A. J., and Dinesh-Kumar, S. P. (2018). The receptor-like cytoplasmic kinase BIK1 localizes to the nucleus and regulates defense hormone expression during plant innate immunity. *Cell Host Microbe* 23(4), 485–497.

## BIBLIOGRAPHY

---

- Laluk, K. and Mengiste, T. (2010). Necrotroph attacks on plants: Wanton destruction or covert extortion? *The Arabidopsis Book* 8, e0136. ISSN: 1543-8120.
- Lam, H. N., Chakravarthy, S., Wei, H.-L., BuiNguyen, H., Stodghill, P. V., Collmer, A., Swingle, B. M., and Cartinhour, S. W. (2014). Global analysis of the HrpL regulon in the plant pathogen *Pseudomonas syringae* pv. tomato DC3000 reveals new regulon members with diverse functions. *PLoS ONE* 9(8). ISSN: 19326203.
- Laue, H., Schenk, A., Li, H., Lambertsen, L., Neu, T. R., Molin, S., and Ullrich, M. S. (2006). Contribution of alginate and levan production to biofilm formation by *Pseudomonas syringae*. *Microbiology* 152(10), 2909–2918. ISSN: 13500872.
- Lefèvre, F. and Boutry, M. (2018). Towards identification of the substrates of ATP-binding cassette transporters. *Plant Physiology* 178(1), 18–39. ISSN: 15322548.
- Li, C.-M., Brown, I., Mansfield, J., Stevens, C., Boureau, T., Romantschuk, M., and Taira, S. (2002). The Hrp pilus of *Pseudomonas syringae* elongates from its tip and acts as a conduit for translocation of the effector protein HrpZ. *EMBO Journal* 21(8), 1909–1915. ISSN: 02614189.
- Li, D., Liu, C., Shen, L., Wu, Y., Chen, H., Robertson, M., Helliwell, C. A., Ito, T., Meyerowitz, E., and Yu, H. (2008). A repressor complex governs the integration of flowering signals in *Arabidopsis*. *Developmental Cell* 15(1), 110–120. ISSN: 15345807.
- Li, H. and Ullrich, M. S. (2001). Characterization and mutational analysis of three allelic *lsc* genes encoding levansucrase in *Pseudomonas syringae*. *Journal of Bacteriology* 183(11), 3282–3292. ISSN: 00219193.

## BIBLIOGRAPHY

---

- Lianou, A. and Koutsoumanis, K. P. (2012). Strain variability of the biofilm-forming ability of *Salmonella enterica* under various environmental conditions. *International Journal of Food Microbiology* 160(2), 171–178. ISSN: 01681605.
- Lieberherr, D., Wagner, U., Dubuis, P. H., Métraux, J. P., and Mauch, F. (2003). The rapid induction of glutathione S-transferases AtGSTF2 and AtGSTF6 by avirulent *Pseudomonas syringae* is the result of combined salicylic acid and ethylene signaling. *Plant and Cell Physiology* 44(7), 750–757. ISSN: 00320781.
- Lin, W., Li, B., Lu, D., Chen, S., Zhu, N., He, P., and Shan, L. (2014). Tyrosine phosphorylation of protein kinase complex BAK1/BIK1 mediates *Arabidopsis* innate immunity. *Proceedings of the National Academy of Sciences* 111(9), 3632–3637. ISSN: 0027-8424.
- Liu, J., Liu, B., Chen, S., Gong, B.-Q., Chen, L., Zhou, Q., Xiong, F., Wang, M., Feng, D., Li, J.-F., Wang, H.-B., and Wang, J. (2018). A tyrosine phosphorylation cycle regulates fungal activation of a plant receptor Ser/Thr kinase. *Cell Host and Microbe* 23(2), 241–253. ISSN: 19346069.
- Liu, X. and Theil, E. C. (2005). Ferritins: Dynamic management of biological iron and oxygen chemistry. *Accounts of Chemical Research* 38(3), 167–175. ISSN: 00014842.
- Loper, J. E., Hassan, K. A., Mavrodi, D. V., Davis, E. W., Lim, C. K., Shaffer, B. T., Elbourne, L. D. H., Stockwell, V. O., Hartney, S. L., Breakwell, K., Henkels, M. D., Tetu, S. G., Rangel, L. I., Kidarsa, T. A., Wilson, N. L., Mortel, J. E. van de, Song, C., Blumhagen, R., Radune, D., Hostetler, J. B., Brinkac, L. M., Durkin, A. S., Kluepfel, D. A., Wechter, W. P., Anderson, A. J., Kim, Y. C., Pierson, L. S., Pierson, E. A., Lindow, S. E., Kobayashi, D. Y., Raaijmakers, J. M., Weller, D. M., Thomashow, L. S., Allen, A. E., and

## BIBLIOGRAPHY

---

- Paulsen, I. T. (2012). Comparative genomics of plant-associated pseudomonas spp.: Insights into diversity and inheritance of traits involved in multitrophic interactions. *PLoS Genetics* 8(7). ISSN: 15537390.
- Love, M., Anders, S., and Huber, W. (2014). *Differential analysis of count data – the DESeq2 package*. ISBN: 0000000000.
- Lu, X., Dittgen, J., Pislewska-Bednarek, M., Molina, A., Schneider, B., Svatos, A., Doubsky, J., Schneeberger, K., Weigel, D., Bednarek, P., and Schulze-Lefert, P. (2015). Mutant allele-specific uncoupling of penetration3 functions reveals engagement of the ATP-binding cassette transporter in distinct tryptophan metabolic pathways. *Plant Physiology* 168(3), 814–827. ISSN: 15322548.
- Ma, S.-W., Morris, V. L., and Cuppels, D. A. (1991). *Characterization of a DNA Region Required for Production of the Phytotoxin Coronatine by Pseudomonas syringae pv. tomato*.
- Mackey, D., Holt, B. F., Wiig, A., and Dangl, J. L. (2002). RIN4 interacts with Pseudomonas syringae type III effector molecules and is required for RPM1-mediated resistance in Arabidopsis. *Cell* 108(6), 743–754. ISSN: 00928674.
- Mann, E. E. and Wozniak, D. J. (2012). Pseudomonas biofilm matrix composition and niche biology. *FEMS Microbiology Review* 36(4), 893–916.
- Manohar, M., Tian, M., Moreau, M., Park, S.-W., Choi, H. W., Fei, Z., Friso, G., Asif, M., Manosalva, P., Von Dahl, C. C., Shi, K., Ma, S., Dinesh-Kumar, S. P., O’doherly, I., Schroeder, F. C., Van Wijk, K. J., and Klessig, D. F. (2015). Identification of multiple salicylic acid-binding proteins using two high throughput screens. *Frontiers in Plant Science* 5(777), 1–14. ISSN: 1664462X.

## BIBLIOGRAPHY

---

- Markel, E., Stodghill, P., Bao, Z., Myers, C. R., and Swingle, B. (2016). AlgU controls expression of virulence genes in *Pseudomonas syringae* pv. tomato DC3000. *Journal of Bacteriology* 198(17), 2330–2344.
- Martin, D. W., Schurr, M. J., Yu, H, and Deretic, V (1994). Analysis of promoters controlled by the putative sigma factor AlgU regulating conversion to mucoidy in *Pseudomonas aeruginosa*: relationship to  $\sigma(E)$  and stress response. *Journal of Bacteriology* 176(21), 6688–6696. ISSN: 00219193.
- Maruri-López, I., Aviles-Baltazar, N. Y., Buchala, A., and Serrano, M. (2019). Intra and extracellular journey of the phytohormone salicylic acid. *Frontiers in Plant Science* 10(April), 1–11. ISSN: 1664462X.
- Mateos, J. L., Madrigal, P., Tsuda, K., Rawat, V., Richter, R., Romera-Branchat, M., Fornara, F., Schneeberger, K., Krajewski, P., and Coupland, G. (2015). Combinatorial activities of SHORT VEGETATIVE PHASE and FLOWERING LOCUS C define distinct modes of flowering regulation in *Arabidopsis*. *Genome Biology* 16(31), 1–23. ISSN: 1474760X.
- Matern, A., Böttcher, C., Eschen-Lippold, L., Westermann, B., Smolka, U., Döll, S., Trempel, F., Aryal, B., Scheel, D., Geisler, M., and Rosahl, S. (2019). A substrate of the ABC transporter PEN3 stimulates bacterial flagellin (flg22)-induced callose deposition in *Arabidopsis thaliana*. *Journal of Biological Chemistry* 294(17), 6857–6870. ISSN: 1083351X.
- Mathee, K., McPherson, C. J., and Ohman, D. E. (1997). Posttranslational control of the algT (algU)-encoded  $\sigma_{22}$  for expression of the alginate regulon in *Pseudomonas aeruginosa* and localization of its antagonist proteins MucA and MucB (AlgN). *Journal of Bacteriology* 179(11), 3711–3720. ISSN: 00219193.

## BIBLIOGRAPHY

---

- Mathlouthi, A, Pennacchietti, E, and De Biase, D (2018). Effect of temperature, pH and plasmids on in vitro biofilm formation in *Escherichia coli*. *Acta Naturae* 10(4), 129–132. ISSN: 20758251.
- Mine, A., Seyfferth, C., Kracher, B., Berens, M. L., Becker, D., and Tsuda, K. (2018). The defense phytohormone signaling network enables rapid, high-amplitude transcriptional reprogramming during effector-triggered immunity[OPEN]. *Plant Cell* 30(6), 1199–1219. ISSN: 1532298X.
- Mitra, P. P. and Loqué, D. (2014). Histochemical staining of *Arabidopsis thaliana* secondary cell wall elements. *Journal of Visualized Experiments* (87), 1–11. ISSN: 1940087X.
- Mittal, S. and Davis, K. R. (1995). *Role of the phytotoxin coronatine in the infection of Arabidopsis thaliana by Pseudomonas syringae pv. tomato.*
- Mohr, C. D., Hibler, N. S., and Deretic, V (1991). AlgR, a response regulator controlling mucoidy in *Pseudomonas aeruginosa*, binds to the FUS sites of the algD promoter located unusually far upstream from the mRNA start site. *Journal of Bacteriology* 173(16), 5136–5143. ISSN: 00219193.
- Monds, R. D., Silby, M. W., and Khris Mahanty, H (2001). Expression of the Pho regulon negatively regulates biofilm formation by *Pseudomonas aureofaciens* PA147-2. *Molecular Microbiology* 42(2), 415–426. ISSN: 0950382X.
- Moreno, J. E., Shyu, C., Campos, M. L., Patel, L. C., Chung, H. S., Yao, J., He, S. Y., and Howe, G. A. (2013). Negative feedback control of jasmonate signaling by an alternative splice variant of JAZ10. *Plant Physiology* 162(2), 1006–1017. ISSN: 00320889.

## BIBLIOGRAPHY

---

- Mulet, M., Lalucat, J., and García-Valdés, E. (2010). DNA sequence-based analysis of the *Pseudomonas* species. *Environmental Microbiology* 12(6), 1513–1530. ISSN: 14622912.
- Müller, T. M., Böttcher, C., Morbitzer, R., Götz, C. C., Lehmann, J., Lahaye, T., and Glawischnig, E. (2015). TRANSCRIPTION ACTIVATOR-LIKE EFFECTOR NUCLEASE-mediated generation and metabolic analysis of camalexin-deficient *cyp71a12 cyp71a13* double knockout lines. *Plant Physiology* 168(3), 849–858. ISSN: 15322548.
- Muñoz-Egea, M.-C., García-Pedrazuela, M., Mahillo, I., García, M. J., and Esteban, J. (2013). Autofluorescence as a tool for structural analysis of biofilms formed by nonpigmented rapidly growing mycobacteria. *Applied and Environmental Microbiology* 79(3), 1065–1067. ISSN: 00992240.
- Murashige, T. and Skoog, F. (1962). A revised medium for rapid growth and bioassays with tobacco tissue cultures. *Physiologia Plantarum* 15.
- Nawrath, C., Heck, S., Parinthewong, N., and Métraux, J.-P. (2002). EDS5, an essential component of salicylic acid-dependent signaling for disease resistance in *Arabidopsis*, is a member of the MATE transporter family. *Plant Cell* 14(1), 275–286. ISSN: 10404651.
- Nekrasov, V., Li, J., Batoux, M., Roux, M., Chu, Z.-H., Lacombe, S., Rougon, A., Bittel, P., Kiss-Papp, M., Chinchilla, D., Esse, H. P. van, Jorda, L., Schwessinger, B., Nicaise, V., Thomma, B. P.H. J., Molina, A., Jones, J. D. G., and Zipfel, C. (2009). Control of the pattern-recognition receptor EFR by an ER protein complex in plant immunity. *The EMBO Journal* 28, 3428–3438. ISSN: 0261-4189.

## BIBLIOGRAPHY

---

- Nobori, T., Velásquez, A. C., Wu, J., Kvitko, B. H., Kremer, J. M., Wang, Y., He, S. Y., and Tsuda, K. (2018). Transcriptome landscape of a bacterial pathogen under plant immunity. *Proceedings of the National Academy of Sciences of the United States of America* 115(13), E3055–E3064. ISSN: 10916490.
- Nunn, G. M. (2018). Commercial compounds induce resistance and investigating an association between age-related resistance and PAMP-triggered immunity. Bachelor’s thesis. McMaster University.
- Oerke, E. C. (2006). Crop losses to pests. *Journal of Agricultural Science* 144(1), 31–43. ISSN: 00218596.
- Osman, S. F., Fett, W. F., and Fishman, M. L. (1986). Exopolysaccharides of the phytopathogen *Pseudomonas syringae* pv. *glycinea*. *Journal of Bacteriology* 166(1), 66–71. ISSN: 00219193.
- O’Toole, G. A. (2010). Microtiter dish biofilm formation assay. *Journal of Visualized Experiments* (47), 10–11. ISSN: 1940087X.
- Palma, M., Worgall, S., and Quadri, L. E. N. (2003). Transcriptome analysis of the *Pseudomonas aeruginosa* response to iron. *Archives of Microbiology* 180(5), 374–379. ISSN: 03028933.
- Panchal, S., Roy, D., Chitrakar, R., Price, L., Breitbach, Z. S., Armstrong, D. W., and Melotto, M. (2016). Coronatine facilitates *Pseudomonas syringae* infection of arabidopsis leaves at night. *Frontiers in Plant Science* 7. ISSN: 1664462X.
- Pearson, J. P., Van Delden, C., and Iglewski, B. H. (1999). Active efflux and diffusion are involved in transport of *Pseudomonas aeruginosa* cell-to-cell signals. *Journal of Bacteriology* 181(4), 1203–1210. ISSN: 00219193.

## BIBLIOGRAPHY

---

- Petrova, O. E. and Sauer, K. (2012). Sticky situations: Key components that control bacterial surface attachment. *Journal of Bacteriology* 194(10), 2413–2425. ISSN: 00219193.
- Poimenidou, S. V., Chrysadaku, M., Tzakoniati, A., Bikouli, V. C., Nychas, G.-J., and Skandamis, P. N. (2016). Variability of *Listeria monocytogenes* strains in biofilm formation on stainless steel and polystyrene materials and resistance to peracetic acid and quaternary ammonium compounds. *International Journal of Food Microbiology* 237, 164–171. ISSN: 18793460.
- Prada-Ramírez, H. A., Pérez-Mendoza, D., Felipe, A., Martínez-Granero, F., Rivilla, R., Sanjuán, J., and Gallegos, M.-T. (2016). AmrZ regulates cellulose production in *Pseudomonas syringae* pv. tomato DC3000. *Molecular Microbiology* 99(5), 960–977. ISSN: 13652958.
- Prithiviraj, B, Bais, H. P., Weir, T, Suresh, B, Najarro, E. H., Dayakar, B. V., Schweizer, H. P., and Vivanco, J. M. (2005). Down regulation of virulence factors of *Pseudomonas aeruginosa* by salicylic acid attenuates its virulence on *Arabidopsis thaliana* and *Caenorhabditis elegans*. *Infection and Immunity* 73(9), 5319–5328.
- Qiu, D., Eisinger, V. M., Rowen, D. W., and Yu, H. D. (2007). Regulated proteolysis controls mucoid conversion in *Pseudomonas aeruginosa*. *Proceedings of the National Academy of Sciences of the United States of America* 104(19), 8107–8112. ISSN: 00278424.
- Raplee, I. D., Evsikov, A. V., and De Evsikova, C. M. (2019). Aligning the aligners: Comparison of rna sequencing data alignment and gene expression quantification tools for clinical breast cancer research. *Journal of Personalized Medicine* 9(2). ISSN: 20754426.

## BIBLIOGRAPHY

---

- Ravirala, R. S., Barabote, R. D., Wheeler, D. M., Reverchon, S., Tatum, O., Malouf, J., Liu, H., Pritchard, L., Hedley, P. E., Birch, P. R. J., Toth, I. K., Payton, P., and San Francisco, M. J. D. (2007). Efflux pump gene expression in *Erwinia chrysanthemi* is induced by exposure to phenolic acids. *Molecular Plant-Microbe Interactions* 20(3), 313–320. ISSN: 08940282.
- Roux, M., Schwessinger, B., Albrecht, C., Chinchilla, D., Jones, A., Holtton, N., Malinovsky, F. G., Tör, M., Vries, S. de, and Zipfel, C. (2011). The Arabidopsis leucine-rich repeat receptor-like kinases BAK1/SERK3 and BKK1/SERK4 are required for innate immunity to hemibiotrophic and biotrophic pathogens. *The Plant Cell* 23(6), 2440–2455. ISSN: 1040-4651.
- Rusterucci, C., Zhao, Z., Haines, K., Mellersh, D., Neumann, M., and Cameron, R. K. (2005). Age-related resistance to *Pseudomonas syringae* pv. tomato is associated with the transition to flowering in Arabidopsis and is effective against *Peronospora parasitica*. *Physiological and Molecular Plant Pathology* 66(6), 222–231. ISSN: 08855765.
- Sarkar, S., Das, A., Khandagale, P., Maiti, I. B., Chattopadhyay, S., and Dey, N. (2018). Interaction of Arabidopsis TGA3 and WRKY53 transcription factors on Cestrum yellow leaf curling virus (CmYLCV) promoter mediates salicylic acid-dependent gene expression in planta. *Planta* 247(1), 181–199. ISSN: 14322048.
- Sauer, K., Camper, A. K., Ehrlich, G. D., Costerton, J. W., and Davies, D. G. (2002). *Pseudomonas aeruginosa* displays multiple phenotypes during development as a biofilm. *Journal of Bacteriology* 184(4), 1140–1154.
- Savary, S., Willocquet, L., Pethybridge, S. J., Esker, P., McRoberts, N., and Nelson, A. (2019). The global burden of pathogens and pests on major food crops. *Nature Ecology and Evolution* 3(3), 430–439. ISSN: 2397334X.

## BIBLIOGRAPHY

---

- Serrano, M., Wang, B., Aryal, B., Garcion, C., Abou-Mansour, E., Heck, S., Geisler, M., Mauch, F., Nawrath, C., and Métraux, J.-P. (2013). Export of salicylic acid from the chloroplast requires the multidrug and toxin extrusion-like transporter EDS5. *Plant Physiology* 162(4), 1815–1821. ISSN: 00320889.
- Sharma, D., Misba, L., and Khan, A. U. (2019). Antibiotics versus biofilm: An emerging battleground in microbial communities. *Antimicrobial Resistance and Infection Control* 8(76). ISSN: 20472994.
- Shukla, S. K. and Rao, T. S. (2017). An improved crystal violet assay for biofilm quantification in 96-wel microtitre plate. *bioRxiv*, 1–10.
- Simpson, G. G. and Dean, C. (2002). Arabidopsis, the rosetta stone of flowering time? *Science* 296(April), 285–289.
- Spanu, P. D. and Panstruga, R. (2017). Editorial: Biotrophic plant-microbe interactions. *Frontiers in Plant Science* 8(February), 1–4. ISSN: 1664462X.
- Stauber, J. L., Loginicheva, E., and Schechter, L. M. (2012). Carbon source and cell density-dependent regulation of type III secretion system gene expression in *Pseudomonas syringae* pathovar tomato DC3000. *Research in Microbiology* 163(8), 531–539. ISSN: 09232508.
- Stein, M., Dittgen, J., Sanchez-Rodriguez, C., Hou, B.-H., Molina, A., Schulze-Lefert, P., Lipka, V., and Somerville, S. (2006). Arabidopsis PEN3/PDR8, an ATP binding cassette transporter, contributes to nonhost resistance to inappropriate pathogens that enter by direct penetration. *The Plant Cell* 18, 731–746.
- Stoitsova, S. O., Braun, Y., Ullrich, M. S., and Weingart, H. (2008). Characterization of the RND-type multidrug efflux pump MexAB-OprM of the plant

## BIBLIOGRAPHY

---

- pathogen *Pseudomonas syringae*. *Applied and Environmental Microbiology* 74(11), 3387–3393. ISSN: 00992240.
- Stover, C. K., Pham, X. Q., Erwin, A. L., Mizoguchi, S. D., Warrenner, P., Hickey, M. J., Brinkman, F. S. L., Hufnagle, W. O., Kowalk, D. J., Lagrou, M, Garber, R. L., Goltry, L, Tolentino, E, Westbrook-Wadman, S, Yuan, Y, Brody, L. L., Coulter, S. N., Folger, K. R., Kas, A, Larbig, K, Lim, R, Smith, K, Spencer, D, Wong, G. K. S., Wu, Z, Paulsen, I. T., Relzer, J, Saler, M. H., Hancock, R. E. W., Lory, S, and Olson, M. V. (2000). Complete genome sequence of *Pseudomonas aeruginosa* PAO1, an opportunistic pathogen. *Nature* 406(6799), 959–964. ISSN: 00280836.
- Strader, L. C. and Bartel, B. (2009). The Arabidopsis PLEIOTROPIC DRUG RESISTANCE8/ABCG36 ATP binding cassette transporter modulates sensitivity to the auxin precursor indole-3-butyric acid. *The Plant Cell* 21(7), 1992–2007. ISSN: 10404651.
- Strathmann, M., Wingender, J., and Flemming, H.-C. (2002). Application of fluorescently labelled lectins for the visualization and biochemical characterization of polysaccharides in biofilms of *Pseudomonas aeruginosa*. *Journal of Microbiological Methods* 50(3), 237–248. ISSN: 01677012.
- Su, T., Xu, J., Li, Y., Lei, L., Zhao, L., Yang, H., Feng, J., Liu, G., and Rena, D. (2011). Glutathione-indole-3-acetonitrile is required for camalexin biosynthesis in *Arabidopsis thaliana*. *Plant Cell* 23(1), 364–380. ISSN: 10404651.
- Sutherland, I. W. (2001). Biofilm exopolysaccharides: A strong and sticky framework. *Microbiology* 147(1), 3–9. ISSN: 13500872.

## BIBLIOGRAPHY

---

- Tatnell, P. J., Russell, N. J., and Gacesa, P. (1994). GDP-mannose dehydrogenase is the key regulatory enzyme in alginate biosynthesis in *Pseudomonas aeruginosa*: evidence from metabolite studies. *Microbiology* 140(7), 1745–1754. ISSN: 13500872.
- Torrens-Spence, M. P., Bobokalonova, A., Carballo, V., Glinkerman, C. M., Pluskal, T., Shen, A., and Weng, J.-K. (2019). PBS3 and EPS1 complete salicylic acid biosynthesis from isochorismate in *Arabidopsis*. *Molecular Plant* 12(12), 1577–1586. ISSN: 17529867.
- Truman, W., Zabala, M. T. de, and Grant, M. (2006). Type III effectors orchestrate a complex interplay between transcriptional networks to modify basal defence responses during pathogenesis and resistance. *The Plant Journal* 46(1), 14–33. ISSN: 09607412.
- Tsuda, K. and Katagiri, F. (2010). Comparing signaling mechanisms engaged in pattern-triggered and effector-triggered immunity. *Current Opinion in Plant Biology* 13(4), 459–465. ISSN: 13695266.
- Tsuda, K. and Somssich, I. E. (2015). Transcriptional networks in plant immunity. *New Phytologist* 206(3), 932–947. ISSN: 14698137.
- Tsuda, K., Mine, A., Bethke, G., Igarashi, D., Botanga, C. J., Tsuda, Y., Glazebrook, J., Sato, M., and Katagiri, F. (2013). Dual Regulation of Gene Expression Mediated by Extended MAPK Activation and Salicylic Acid Contributes to Robust Innate Immunity in *Arabidopsis thaliana*. *PLoS Genetics* 9(12). ISSN: 15537390.
- Ude, S., Arnold, D. L., Moon, C. D., Timms-Wilson, T., and Spiers, A. J. (2006). Biofilm formation and cellulose expression among diverse environmental *Pseudomonas* isolates. *Environmental Microbiology* 8(11), 1997–2011. ISSN: 14622912.

## BIBLIOGRAPHY

---

- Uquillas, C., Letelier, I., Blanco, F., Jordana, X., and Holuigue, L. (2004). NPR1-independent activation of immediate early salicylic acid-responsive genes in *Arabidopsis*. *Molecular Plant-Microbe Interactions* 17(1), 34–42. ISSN: 08940282.
- Vaca, E., Behrens, C., Theccanat, T., Choe, J.-Y., and Dean, J. V. (2017). Mechanistic differences in the uptake of salicylic acid glucose conjugates by vacuolar membrane-enriched vesicles isolated from *Arabidopsis thaliana*. *Physiologia Plantarum* 161(3), 322–338. ISSN: 13993054.
- Velasco, V. M. E., Mansbridge, J., Bremner, S., Carruthers, K., Summers, P. S., Sung, W. W. L., Champigny, M. J., and Weretilnyk, E. A. (2016). Acclimation of the crucifer *Eutrema salsugineum* to phosphate limitation is associated with constitutively high expression of phosphate-starvation genes. *Plant Cell and Environment* 39(8), 1818–1834. ISSN: 13653040.
- Vlot, A. C., Dempsey, D. A., and Klessig, D. F. (2009). Salicylic Acid, a Multifaceted Hormone to Combat Disease. *Annual Review of Phytopathology* 47(1), 177–206. ISSN: 0066-4286.
- Waite, R. D., Papakonstantinou, A., Littler, E., and Curtis, M. A. (2005). Transcriptome analysis of *Pseudomonas aeruginosa* growth: comparison of gene expression in planktonic cultures and developing and mature biofilms. *Journal of Bacteriology* 187(18), 6571–6576.
- Wang, K., Kang, L., Anand, A., Lazarovits, G., and Mysore, K. S. (2007). Monitoring in planta bacterial infection at both cellular and whole-plant levels using the green fluorescent protein variant GFPuv. *New Phytologist* 174(1), 212–223. ISSN: 0028646X.
- Wang, L., Wang, S., and Li, W. (2012). RSeQC: quality control of RNA-seq experiments. *Bioinformatics* 28(16), 2184–2185. ISSN: 13674803.

## BIBLIOGRAPHY

---

- Wang, Y., Yao, H., Cheng, Y., Lovell, S., Battaile, K. P., Midaugh, C. R., and Rivera, M. (2015). Characterization of the Bacterioferritin/Bacterioferritin Associated Ferredoxin Protein-Protein Interaction in Solution and Determination of Binding Energy Hot Spots. *Biochemistry* 54(40), 6162–6175. ISSN: 15204995.
- Whalen, M. C., Innes, R. W., Bent, A. F., and Staskawicz, B. J. (1991). Identification of *Pseudomonas syringae* pathogens of *Arabidopsis* and a bacterial locus determining avirulence on both *Arabidopsis* and soybean. *The Plant Cell* 3(1), 49–59. ISSN: 10404651.
- Wildermuth, M. C., Dewdney, J., Wu, G., and Ausubel, F. M. (2001). Isochorismate synthase is required to synthesize salicylic acid for plant defense. *Nature* 414, 562–565. ISSN: 00280836.
- Wilson, D. C., Carella, P., Isaacs, M., and Cameron, R. K. (2013). The floral transition is not the developmental switch that confers competence for the *Arabidopsis* age-related resistance response to *Pseudomonas syringae* pv. tomato. *Plant Molecular Biology* 83(3), 235–246. ISSN: 01674412.
- Wilson, D. C., Kempthorne, C. J., Carella, P., Liscombe, D. K., and Cameron, R. K. (2017). Age-related resistance in *Arabidopsis thaliana* involves the MADS-domain transcription factor SHORT VEGETATIVE PHASE and direct action of salicylic acid on *Pseudomonas syringae*. *Molecular Plant-Microbe Interactions* 30(11), 919–929. ISSN: 0894-0282.
- Wu, Y., Zhang, D., Chu, J. Y., Boyle, P., Wang, Y., Brindle, I. D., De Luca, V., and Després, C. (2012). The *Arabidopsis* NPR1 protein is a receptor for the plant defense hormone salicylic acid. *Cell Reports* 1(6), 639–647. ISSN: 22111247.

## BIBLIOGRAPHY

---

- Xiang, T., Zong, N., Zou, Y., Wu, Y., Zhang, J., Xing, W., Li, Y., Tang, X., Zhu, L., Chai, J., and Zhou, J.-M. (2008). Pseudomonas syringae effector AvrPto blocks innate immunity by targeting receptor kinases. *Current Biology* 18(1), 74–80. ISSN: 09609822.
- Xie, Z.-D., Hershberger, C. D., Shankar, S., Ye, R. W., and Chakrabarty, A. M. (1996). Sigma factor-anti-sigma factor interaction in alginate synthesis: inhibition of AlgT by MucA. *Journal of Bacteriology* 178(16), 4990–4996. ISSN: 00219193.
- Xin, X.-F. and He, S. Y. (2013). Pseudomonas syringae pv. tomato DC3000: a model pathogen for probing disease susceptibility and hormone signaling in plants. *Annual Review of Phytopathology* 51, 473–498. ISSN: 0066-4286.
- Xin, X.-F., Kvitko, B., and He, S. Y. (2018). Pseudomonas syringae: what it takes to be a pathogen. *Nature Reviews Microbiology* 16(5), 316–328.
- Yamasaki, K., Motomura, Y., Yagi, Y., Nomura, H., Kikuchi, S., Nakai, M., and Shiina, T. (2013). Chloroplast envelope localization of EDS5, an essential factor for salicylic acid biosynthesis in Arabidopsis thaliana. *Plant Signaling and Behavior* 8(4). ISSN: 15592316.
- Yan, S. and Dong, X. (2014). Perception of the plant immune signal salicylic acid. *Current Opinion in Plant Biology* 20, 64–68. ISSN: 08966273.
- Yu, J., Penaloza-Vazquez, A., Chakrabarty, A. M., and Bender, C. L. (1999). Involvement of the exopolysaccharide alginate in the virulence and epiphytic fitness of Pseudomonas syringae pv. syringae. *Molecular Microbiology* 33(4), 712–720.
- Zhang, J., Li, W., Xiang, T., Liu, Z., Laluk, K., Ding, X., Zou, Y., Gao, M., Zhang, X., Chen, S., Mengiste, T., Zhang, Y., and Zhou, J.-M. (2010). Receptor-like

## BIBLIOGRAPHY

---

- cytoplasmic kinases integrate signaling from multiple plant immune receptors and are targeted by a *Pseudomonas syringae* effector. *Cell Host and Microbe* 7(4), 290–301. ISSN: 19313128.
- Zhao, X., Li, G., and Liang, S. (2013). Several affinity tags commonly used in chromatographic purification. *Journal of Analytical Methods in Chemistry* (581093). ISSN: 20908873.
- Zheng, X.-y., Spivey, N. W., Zeng, W., Liu, P.-P., Fu, Z. Q., Klessig, D. F., He, S. Y., and Dong, X. (2012). Coronatine promotes *Pseudomonas syringae* virulence in plants by activating a signaling cascade that inhibits salicylic acid accumulation. *Cell Host Microbe* 11(6), 587–596. ISSN: 15378276.
- Zipfel, C., Robatzek, S., Navarro, L., Oakeley, E. J., Jones, J. D. G., Felix, G., and Boller, T. (2004). Bacterial disease resistance in *Arabidopsis* through flagellin perception. *Nature* 428(6984), 764–767. ISSN: 0028-0836.
- Zvereva, A. S. and Pooggin, M. M. (2012). Silencing and innate immunity in plant defense against viral and non-viral pathogens. *Viruses* 4(11), 2578–2597. ISSN: 19994915.